Proteasome Inhibition in Chronic Myeloid Leukaemia

Nicholas Benjamin Heaney

MBChB (Comm) BSc(Hons) MRCP DipRCPath

Submission for Degree of M.D.

The Faculty of Medicine

Division of Cancer Sciences and Molecular Pathology

University of Glasgow

February 2009

DECLARATION

This work represents original work carried out by the author and has not been submitted in any form to any other university.

Nicholas Heaney
February 2009

ACKNOWLEDGEMENTS

I am indebted to my supervisor Professor Holyoake for her help in directing this project and for providing guidance and assistance when obstacles were met. Invaluable technical support and advice was provided by Francesca Pellicano, Niove Jordanides, Ashley Hamilton, Heather Jorgensen and Jo Mountford. Professor Holyoake and the senior scientists working within the research team have created a working environment that is both motivational and inspiring. As a result of this I was truly able to enjoy my two years of academic research. This research would have not been possible without the generous sponsorship of Leukaemia Research, UK and the support of my wife and family.

CONTENTS

		page
1	**INTRODUCTION**	**18**
1.1	Classification	**18**
1.2	Epidemiology	**18**
1.3	Clinical manifestations	**18**
1.4	Pathogenesis	**19**
1.5	BCR-ABL and the malignant phenotype	**19**
1.5.1	Intracellular signalling pathways	**19**
1.5.1.1	Ras and PI3K pathways	**19**
1.5.1.2	JAK pathway	**22**
1.6	The haematopoietic stem cell in CML	**22**
1.6.1	The leukaemic stem cell	**22**
1.6.2	Advanced phase disease and self-renewal capacity	**24**
1.7	Current CML therapy	**25**
1.7.1	Imatinib	**25**
1.7.1.1	CML persistence despite imatinib therapy	**26**
1.7.1.2	Imatinib resistance mechanisms	**27**
1.7.1.2.1	BCR-ABL mutations	**27**
1.7.1.2.2	Resistance through mechanisms other than BCR-ABL mutation	**29**
1.7.1.2.2.1	Drug transport – efflux	**30**
1.7.1.2.2.1.1	P-glycoprotein	**31**
1.7.1.2.2.1.2	ABCG2	**31**
1.7.1.2.2.2	Drug transport – uptake	**31**
1.7.2	Second-generation TKI	**32**
1.7.2.1	Dasatinib	**32**
1.7.2.2	Nilotinib	**32**
1.7.2.3	Front line use of second generation tyrosine kinase inhibitors	**33**
1.7.2.4	Tyrosine kinase inhibitors in combination	**33**
1.7.2.5	Second generation tyrosine kinase inhibitors and the stem cell	**34**
1.8	The need for new approaches	**34**

1.9	The proteasome	**35**
1.9.1	Measuring proteasome activity	**37**
1.9.2	Proteasome inhibitors and cancer	**37**
1.9.3	Bortezomib	**38**
1.9.4	Proposed mechanism of proteasome inhibitors	**38**
1.9.4.1	The NFkB/IkB axis	**38**
1.9.4.2	Bortezomib and the cell cycle	**40**
1.9.4.3	Bortezomib and apoptosis	**42**
1.9.4.4	Bortezomib and reactive oxygen species generation	**44**
1.9.4.5	Bortezomib and autophagy	**44**
1.9.5	Current clinical use of bortezomib	**45**
1.9.5.1	Multiple myeloma	**45**
1.9.5.2	Mantle cell lymphoma	**46**
1.9.5.3	Other haematological malignancies	**46**
1.9.6	Pharmacodynamics of bortezomib	**47**
1.10	The proteasome in CML	**48**
1.10.1	Published use of proteasome inhibitors in CML	**48**
1.11	Rationale for this study	**49**
1.12	Stated hypotheses and aims	**50**
2	**METHODS**	**51**
2.1	Reagents and equipment	**51**
2.1.1	Reagents	**51**
2.1.2	Equipment	**54**
2.1.3	Antibodies for Western blotting and flow cytometry	**55**
2.2	Drugs	**56**
2.3	Cell lines and patient samples	**56**
2.3.1	Cell lines	**56**
2.3.2	Patient samples	**56**
2.4.	Viability and apoptosis assays	**57**
2.4.1	Assessment of viable cell counts	**57**
2.4.2	Apoptosis assays using flow cytometry	**57**
2.4.3	Intracellular caspase staining	**58**
2.4.4	Thymidine proliferation assay	**59**
2.4.5	CFSE staining	**59**
2.4.5.1	Background.	**59**
2.4.5.2	Day 0.	**60**

2.4.5.3	Day 1.	**60**
2.4.5.4	Day 3.	**60**
2.4.5.5	Calculation of cell numbers	**61**
2.5	Western blotting	**62**
2.5.1	Estimation of protein concentration	**62**
2.5.2.1	Preparation of sample lysates	**62**
2.5.2.2	SDS-PAGE electrophoresis	**62**
2.5.2.3	Electrophoretic transfer	**63**
2.5.2.4	Primary and secondary antibody incubation	**63**
2.6	Proteasome extraction and activity assay	**64**
2.7	Software and statistical analysis	**64**
2.7.1	Software used for data analysis	**64**
2.7.2	Analysis of data from synergism experiments	**65**
2.8	Culture media and other stock solutions	**68**
2.8.1	RPMI-1640 cell culture medium for culture of cell lines	**68**
2.8.2	DAMP solution for rehydration of stem cells	**68**
2.8.3	Serum free media for culture of stem cells	**68**
2.8.4	5-Growth factor cocktail used with SFM for stem cell culture	**68**
2.8.5	Protein lysis buffer for Western blot	**69**
2.8.6	Loading buffer for Western blot	**69**
2.8.7	Running buffer for Western blot	**69**
2.8.8	Transfer buffer for Western blot	**69**
2.8.9	10xTBS buffer for Western blot	**69**
2.8.10	TBS-T washing buffer for Western blot	**69**
2.8.11	ATP/DTT lysis buffer for proteasome activity assay	**70**
3	**RESULTS**	**71**
3.1	Bortezomib in BCR-ABL+ cell lines	**71**
3.1.1	Cell counting and flow cytometry	**71**
3.1.2	Bortezomib viability	**75**
3.1.3	Bortezomib wash-out	**76**
3.1.4	Detection of active caspase-3	**77**
3.1.5	Thymidine incorporation	**78**
3.2	Proteasome activity in BCR-ABL+ cell lines	**80**
3.2.1	Baseline proteasome activity in Ba/F3 mutants	**80**
3.2.2	Effect of bortezomib treatment on proteasome subunit	**81**

	activity	
3.3	Bortezomib reduces BCR-ABL activity in BCR-ABL+ cell lines	**83**
3.3.1	Effect of bortezomib treatment on BCR-ABL activity in K562 cells	**83**
3.4	Bortezomib in CML CD34+ patient samples	**84**
3.5	Bortezomib effects on proteasome and BCR-ABL activity in CML CD34+ patient samples	**89**
3.6	Bortezomib effects in CML and normal CD34+38- cells	**92**
3.7	Bortezomib is antiproliferative in CML CD34+ patient cells	**95**
3.8	Dasatinib and bortezomib act synergistically against CML CD34+ cells in vitro	**100**
4	**DISCUSSION**	**103**
4.1	Overview	**103**
4.2	Targeting BCR-ABL+ cell lines, including mutant forms	**103**
4.3	Targeting the CML stem cell	**107**
4.4	Relative non-selectivity of bortezomib	**110**
4.5	Combination of bortezomib with dasatinib	**112**
4.6	Potential future work	**113**
4.6.1	Extension of cell line data	**114**
4.6.2	Extension of patient sample data	**114**
4.6.3	Extension of stem cell data	**114**
4.6.4	Future clinical trials	**114**
5	**CONCLUSION**	**117**
6	**REFERENCES**	**118**

TABLES

Table 1.1	Characterisation of leukaemia initiating cells	**24**
Table 1.2	CML disease response definitions	**26**
Table 1.3	Comparative cellular proliferation assays of tyrosine kinase inhibitor treated BCR-ABL+Ba/F3 transfectants	**29**
Table 1.4	Strategies to target imatinib resistance and disease persistence	**35**
Table 1.5	Current clinical trials with bortezomib in myeloid malignancy	**46**
Table 2.1	Assessment of synergism by combination index	**67**
Table 3.1	Estimation of bortezomib LD_{50} by cell counting and flow cytometry in BCR-ABL+ cell lines	**75**
Table 3.2	CFSE data generated from 3 CML CD34+ samples analysed at 72h	**98**
Table 3.3	Combination indices for bortezomib and dasatinib used simultaneously in CML patient samples.	**102**
Table 4.1	Published data of BCR-ABL mutants	**106**
Table 4.2	Published effect of bortezomib on normal cells	**112**

FIGURES

Figure 1.1	RAS and RAF activation pathways	**21**
Figure 1.2	JAK activation pathway	**22**
Figure 1.3	Illustration of proteasome activity	**36**
Figure 1.4	Illustration of the NFkB/IkB axis	**39**
Figure 1.5	Illustration of the role of the cyclin – cyclin dependent kinase complex	**40**
Figure 2.1	Determination of cells undergoing apoptosis by flow cytometry with Annexin-V and 7-AAD staining	**58**
Figure 2.2	Gel “sandwich” used for electrophoretic transfer	**63**
Figure 2.3	Checker-square analysis of drug combinations	**66**
Figure 2.4	Illustration of Isobologram	**67**
Figure 3.1	Bortezomib exposure of K562 cells – viable cell counts	**72**
Figure 3.2	Bortezomib exposure of K562 cells – early and late apoptosis	**73**
Figure 3.3	Bortezomib exposure of BCR-ABL+ Ba/F3 cells – viable cell count and apoptosis	**74**
Figure 3.4	Investigation of the effects of storage and freeze-thawing of bortezomib	**76**
Figure 3.5	Effects of time limited exposure of K562 cells to bortezomib	**77**
Figure 3.6	Bortezomib exposure of BCR-ABL+ Ba/F3 cells – active caspase-3	**78**
Figure 3.7	Bortezomib exposure of K562 cells – thymidine incorporation	**79**
Figure 3.8	Proteasome subunit activity in BCR-ABL+ BaF3 and K562 cells	**80**
Figure 3.9	Proteasome subunit activity in BCR-ABL+ Ba/F3 cells	**81**
Figure 3.10	Bortezomib exposure of BCR-ABL+ Ba/F3 cells – proteasome activity	**82**
Figure 3.11	Bortezomib exposure of K562 cells – BCR-ABL activity	**84**
Figure 3.12	Bortezomib exposure of CD34+ CML patient samples – viable cell count and apoptosis	**86**
Figure 3.13	Bortezomib exposure of CD34+ CML patient samples – active caspases-3	**87**

Figure 3.14	Bortezomib exposure of CD34+ CML patient samples – PARP cleavage	**88**
Figure 3.15	Bortezomib exposure of CD34+ CML patient samples – ubiquinated protein and BCR-ABL activity	**90**
Figure 3.16	Bortezomib exposure of CD34+ CML patient samples – ubiquitin and $p57^{kip2}$	**91**
Figure 3.17	Bortezomib exposure of CD34+38- CML patient samples and normal controls – viable cell count and apoptosis	**93**
Figure 3.18	Bortezomib and dasatinib exposure of CD34+ CML patient samples – CFSE tracking of cell division	**96**
Figure 3.19	Bortezomib and dasatinib exposure of CD34+ CML patient samples – effect on different division peaks	**97**
Figure 3.20	Recovery of all CD34+ and undivided cells following bortezomib exposure of CML patient samples	**99**
Figure 3.21	Effect of bortezomib exposure on detectable CD34+ expression on CML patient samples	**99**
Figure 3.22	Dose-effect profile of bortezomib and dasatinib with CD34+ CML patient samples	**101**
Figure 3.23	Isobologram of fixed additive effects of bortezomib and dasatinib used in combination with CD34+ CML patient samples	**101**

PUBLICATIONS

Bortezomib induces apoptosis in quiescent chronic myeloid leukaemia stem cells and cells expressing T315I BCR-ABL mutation and synergises with dasatinib.
Heaney NB, Pellicano F, Crawford L, Kazmi SMA, Jorgensen HG, Irvine AE, Holyoake TL.

Submitted to *Blood* with ongoing experimental work to meet requested revisions prior to resubmission

A pilot study of continuous imatinib mesylate *vs*. pulsed imatinib with or without rHu-G-CSF in CML patients who have achieved a complete cytogenetic response (GIMI)
Drummond MW, Heaney N, Kaeda J, Nicolini FE, Clark RE, Wilson G, Shepherd P, Tighe J, McLintock L, Hughes T, Holyoake TL. *Leukaemia, In Press 2009.*

Complete molecular responses are achieved after reduced intensity stem cell transplantation and donor lymphocyte infusion in chronic myeloid leukemia.
Heaney NB, Copland M, Stewart K, Godden J, Parker AN, McQuaker IG, Smith GM, Crawley C, Shepherd P, Holyoake TL.
Blood. 2008 May 15;111(10):5252-5.

Therapeutic targets in chronic myeloid leukaemia.
Heaney NB, Holyoake TL.
Hematol Oncol. 2007 Jun;25(2):66-75.

What is new in chronic myeloid leukaemia?
Heaney NB, Holyoake TL.
Scott Med J. 2007 Feb;52(1):36-41.

LIST OF ABBREVIATIONS

Abbreviations are also defined at time of first use (including SUMMARY).

17-AAG	17-allylamino-17-demethoxygeldanamycin
5GF	5-growth factor
7-AAD	7-amino –actinomycin
ABC	ATP-binding cassette
AFU	Arbitrary fluorescence units
ALL	Acute lymphoblastic leukaemia
AML	Acute myeloid leukaemia
AP	Accelerated phase
APAF-1	Apoptosis protease activating factor-1
APEX	Assessment of proteasome inhibition for extending remissions
Ara-C	Cytosine arabinoside
BC	Blast crisis
BH	BCL-2 homology
BM	Bone marrow
Caspase	Cysteine protease cleaving after Asp enzyme
CCyR	Complete cytogenetic response
CFSE	Carboxy-fluorescein diacetate succinimidyl diester
CFU	Colony-forming units
CHR	Complete haematological response
CML	Chronic myeloid leukaemia
CP	Chronic phase
CT-L	Chymotrypsin-like
CyR	Cytogenetic response
D-PBS	Dulbecco’s phosphate buffered saline
E1	Ubiquitin activating enzyme
E2	Ubiquitin conjugating enzyme
E3	Ubiquitin protein-ligase enzyme
ERK	Extracellular signal-related kinase
FACS	Fluorescence activated cell sorting
FADD	FAS-associated death domain-containing protein
FCS	Foetal calf serum
FISH	Fluorescence in-situ hybridisation
GAP	GTPase-activating proteins
G-CSF	Granulocyte-colony stimulating factor
GDP	Guanosine diphosphate
GEF	Guanine nucleotide exchange factors
GMP	Granulocyte-macrophage progenitor
GRB-2	Growth factor bound-2
GTP	Guanosine triphosphate
h	Hour
HDAC	Histone deacetylase
hOCT1	Human organic cation transporter 1
HR	Haematological response
HSC	Haematopoietic stem cell
HSP	Heat shock protein
IAP	Inhibitor of apoptosis

IC_{50}	Concentration of drug required to inhibit proliferation of cells relative to untreated cells
IFNα	Interferon-alpha
IFNγ	Interferon-gamma
IKK	IkB kinase
IM	Imatinib
IRIS	International randomized study of interferon and STI571
JAK	Janus kinase
LD_{50}	Concentration required to reduce viable cell count by 50%
LTC-IC	Long term culture-initiating cell
m	Months
MAPK	Mitogen activated protein kinase
MAPKK	MAPK kinase
MAPKKK	MAPKK kinase
MDR	Multidrug resistance
MEK	MAPK/ERK kinase
MMolR	Major molecular response
MMP	Mitochondrial membrane permeabilisation
MNC	Mononuclear cells
MRD	Minimal residual disease
mTOR	Mammalian target of rapamycin
NOD/SCID	Non-obese diabetic, severe combined immunodeficiency
OCT	Organic cation transporter
PARP	Poly(ADP-ribose) polymerase
PB	Peripheral blood
PCyR	Partial cytogenetic response
PDK1	3-phosphoinositide-dependent protein kinase 1
PG	Postglutamyl peptide hydrolase like
Pgp	P-glycoprotein
PH	Pleckstrin homology
Ph+	Philadelphia chromosome
PI	Proteasome inhibitor
$PI(3,4)P_2$	Phosphatidylinositol (3,4) diphosphate
$PI(3,4,5)P_3$	Phosphatidylinositol (3,4) triphosphate
PI3K	Phosphatidylinositol 3-kinase
PINNACLE	Proteasome inhibition as innovative approach to relapsed mantle cell lymphoma a single agent evaluation
PIo	Propidium iodide
pRb	Retinoblastoma protein
ROS	Reactive oxygen species
RTK	Receptor tyrosine kinase
SAHA	Suberoylanilide hydroxamic acid
SFK	SRC-family kinase inhibitors
SFM	Serum free medium
SH2	SRC homology-2
SMAC	Second mitochondrial activator of caspase
SOS	Son of Sevenless
STAT	Signal transducers and activators of transcription
TKI	Tyrosine kinase inhibitor

T-L	Trypsin like
TNFα	Tumour necrosis factor-alpha
TRAIL	Tumour necrosis factor related apoptosis inducing ligand
y	Year

SUMMARY

Chronic myeloid leukaemia (CML) is a disorder of the haematopoietic stem cell (HSC) characterised by the presence of a characteristic chromosomal translocation which forms the Philadelphia chromosome. The disease is caused by BCR-ABL, a constitutively active tyrosine kinase and the protein product of the oncogene *BCR-ABL* which forms as a result of the chromosomal translocation.

The current recommended treatment for the majority of patients with chronic phase (CP) CML is the tyrosine kinase inhibitor (TKI) imatinib mesylate (IM). There is accumulating evidence that the majority of patients respond to this drug and achieve the therapeutic milestone of a complete cytogenetic response (CCyR). However TKI induce a state of minimal residual disease (MRD) in the majority with BCR-ABL transcripts detectable in peripheral blood (PB). The source of MRD in IM treated patients is presumed to be leukaemic HSC. These cells are relatively insensitive to all TKI. Furthermore the development of TKI-resistant BCR-ABL mutations is a cause of primary and secondary treatment failure. In particular the T315I BCR-ABL mutation is resistant to all available TKI and there is concern that selection pressure may result in this mutation becoming more prevalent.

The proteasome is an attractive target for cancer therapy and there has been expansion of the clinical use of bortezomib, to date the only licensed proteasome inhibitor (PI). There is published evidence that BCR-ABL expression is associated with increased proteasome activity, that primitive CML cells express higher levels of BCR-ABL than their more mature progeny and that BCR-ABL+ cell lines are susceptible to proteasome inhibition (1-4). We have extended this work to demonstrate that CD34 enriched samples taken at diagnosis from patients with CP CML have reduced proliferation and undergo apoptosis with bortezomib exposure. This effect was replicated in 7 different patient samples and the drug was consistent in its effect. The antiproliferative and apoptotic effects were associated with an accumulation of polyubiquitinated proteins consistent with inhibition of the proteasome. Despite these effects, bortezomib did not appear to influence BCR-ABL kinase activity as evident by pCrkl detection by Western blot. The concentration required to reduce the viable cell count by 50% (LD_{50}) in CD34+ CML cells was comparable to that quoted previously for CML blast crisis (BC) cell lines (10-15 and 32nM at 48 hours (h) (1, 3)), purified human multiple myeloma

cells from bone marrow (BM) (2.5-30nM at 48h (5)) and CD34 enriched human acute myeloid leukaemia (AML) cells (5-10nM at 7 days (d) (6)). Pharmacokinetic and pharmacodynamic data from treated patients would suggest that such concentrations are clinically achievable.

We used an established technique to isolate the CD34+38- cells from patient samples. This population contains the primitive and quiescent HSC which are resistant to current therapies. We demonstrate for the first time that these cells are sensitive to the apoptotic effects of bortezomib at comparable concentrations to those achieved *in vivo*. These data are in concordance with published observations of the sensitivity of CD34+38- AML cells to the PI MG132 (7). We extended the work to track cells through division using carboxy-fluorescein diacetate succinimidyl diester (CFSE) staining and flow cytometry. We demonstrate that proliferation of CD34+ CML cells is significantly affected by bortezomib exposure and at high concentrations the few surviving cells remain undivided. Recovery calculations were made and at concentrations of bortezomib comparable to the LD_{50} there is a depletion of CD34+ cells from all stages of division including the undivided state. This contrasts with dasatinib exposure, which may result in the accumulation of undivided cells.

Clinical trials with bortezomib have shown that reversible haematological toxicity (in particular severe thrombocytopaenia) is very common. We show that normal CD34+38- cells are susceptible to the apoptotic effects of bortezomib with LD_{50} values only slightly higher than those of the CML HSC. We could find no published data of the effects of bortezomib in this specific cell population. Other groups have used, as a control population, non-malignant CD34+ enriched cells (LD_{50} 11.3nM by assays of colony formation and <20nM by proliferation assays (6, 8)) and lymphocytes from PB (~5% apoptosis with 50nM by annexin-V staining (9)). The toxicity we demonstrate is concerning, however the reversible nature of the severe cytopaenias seen in patients may reflect an improved recovery of this population relative to malignant cells. It is noted that in Phase I dose escalation studies using more intensive regimes, the dose-limiting toxicity was haematological (10).

An established technique to ameliorate toxicity of chemotherapy is to use drug combinations. We speculated that TKI may provide additional benefits to bortezomib treatment in view of the presence of residual BCR-ABL kinase activity

in PI treated cells. We demonstrate that bortezomib and dasatinib are synergistic in inducing cell death using concentrations of both drugs that may be achieved *in vivo.*

We have also shown that bortezomib consistently induces apoptosis in cell lines expressing BCR-ABL mutations including T315I. This is associated with a reduction in chymotrypsin-like (CT-L) enzyme activity consistent with bortezomib effect. Interestingly we show for the first time that the proteasome subunit activity may vary amongst different BCR-ABL mutations and this is not thought to be due to different BCR-ABL protein levels.

In conclusion bortezomib is antiproliferative and induces apoptosis in CML CD34+ cells including the CD34+38- fraction, believed to be the source of residual disease in TKI treated patients. Potential toxicities associated with this drug may be bypassed by synergistic interactions with dasatinib. Bortezomib is also effective in the presence of TKI resistant BCR-ABL mutations. With these two key findings we believe that PI should play a future role in the treatment of patients failing current therapies.

1 INTRODUCTION

1.1 Classification

CML is classified by the World Health Organisation as a myeloproliferative disorder, one member of a group of conditions including essential thrombocythaemia, polycythaemia vera and chronic idiopathic myelofibrosis. The myeloproliferative diseases are clonal disorders of the HSC characterised by abnormal myeloid (i.e. granulocyte, erythroid and megakaryocytic) proliferation. CML (also termed chronic myelogenous or granulocytic leukaemia) has a characteristic molecular biology and is now more appropriately considered as a distinct entity.

1.2 Epidemiology

CML has an estimated incidence of 1-2 new cases per 100000 population per year (y) (11). Figures from Scotland (1980-2005) are in concordance with this, with an average of 60 new cases/y from a population of approximately 5 million. The incidence has changed little in Scotland over the decade 1994-2004. The median age affected is between 65y and 69y with a slight male predominance (cancer statistics accessed in January 2009 from the National Statistics section of the Information Services Division (ISD) Scotland, www.isdscotland.org and general population statistics from the General Register Office for Scotland, www.gro-scotland.gov.uk).

1.3 Clinical Manifestations

CML evolves through 3 clinical phases. The CP is characterised by leucocytosis and hepatosplenomegaly developing as a consequence of increased granulopoeisis and leukaemic infiltration. At diagnosis the majority of patients are in CP and are asymptomatic. The disease will then progress either directly to BC or through an intermediate accelerated phase (AP). AP is characterised by an increased number of primitive precursors in BM or PB. BC occurs when there is a failure of maturation of the malignant precursors, often accompanied by additional cytogenetic abnormalities and resulting in a disease resembling AML or acute lymphoblastic leukaemia (ALL). There have been significant advances in the treatment of CP disease and progression to advanced stage is seen less frequently. However, when it occurs the prognosis is poor and the median survival measured in months (m) (11).

1.4 Pathogenesis

CML arises as a consequence of a rare mutational event resulting in a reciprocal translocation between the long arms of chromosomes 9 and 22. The shortened chromosome 22 formed by this translocation is the Philadelphia chromosome (Ph+), named after the city in which it was discovered. The translocation creates the chimeric oncogene *BCR-ABL* with the protein product BCR-ABL, a tyrosine kinase with constitutive activity. BCR-ABL is responsible for the pathogenesis of CML as demonstrated by the transforming ability of BCR-ABL expression in cell lines and mice (12, 13). This oncoprotein is therefore the focus for investigations into the pathogenesis of CML and has provided a tangible target for therapy.

1.5 BCR-ABL and the malignant phenotype

BCR-ABL confers a survival advantage on cells by influencing signalling pathways which control proliferation and apoptosis. It may be the advantage is relatively subtle: BCR-ABL is detectable, transiently it is presumed, in a “normal” population (14, 15); and exposure to known triggers of CML, such as ionising radiation, have a disease latency of years (16). An outline of the signalling pathways affected by BCR-ABL provides insight into the mechanism by which the malignant phenotype may be established.

1.5.1 Intracellular signalling pathways

Enzyme-linked receptors provide a mechanism for cell signalling and play a role in proliferation, differentiation, apoptosis and migration. Of the different classes of enzyme-linked receptors, the most common have tyrosine kinase function (receptor tyrosine kinase, RTK) and include the RAS and phosphatidylinositol 3-kinase (PI3K) pathways (**Figure 1.1**). Others are associated with proteins which have tyrosine kinase activity and include the Janus kinase (JAK) pathways (**Figure 1.2**).

1.5.1.1. RAS and PI3K pathways

In outline, RTK binding results in autophosphorylation and so provides phosphotyrosine docking sites for intracellular proteins containing SRC-homology-2 (SH2) domains. Once bound, SH2-containing proteins may interact with other tyrosine phosphorylated proteins. This interaction may take place via additional binding domains, such as SH3 domains, on the signalling molecule.

RAS is a guanosine triphosphate (GTP)-binding protein associated with RTK (**Figure 1.1**). Through activation of RAS and downstream serine-threonine kinases the activity of gene regulatory proteins are influenced - including those responsible for cell proliferation. It has been demonstrated previously that BCR-ABL interacts directly with growth factor receptor bound-2 (GRB-2) and activates the RAS pathway (17). Furthermore, inhibition of tyrosine kinase activity abrogates the activation of RAS (18). Consistent with this, BCR-ABL+ cell lines have detectable levels of RAF activity and colony growth of CML cells appears to depend on this (19).

A further relevant and important signalling pathway activated through RTK involves PI3K activation (**Figure 1.1**). Through PI3K there is promotion of cell growth and survival through a pathway involving AKT (a serine-threonine kinase) with downstream targets which include mammalian target of rapamycin (mTOR). BCR-ABL interacts with and promotes activity of PI3K. Inhibition of PI3K in BCR-ABL+ cells will inhibit growth (20). AKT activity is also essential in BCR-ABL mediated leukaemogenesis seen *in vitro* as colony growth and *in vivo* in mouse transplantation models (21).

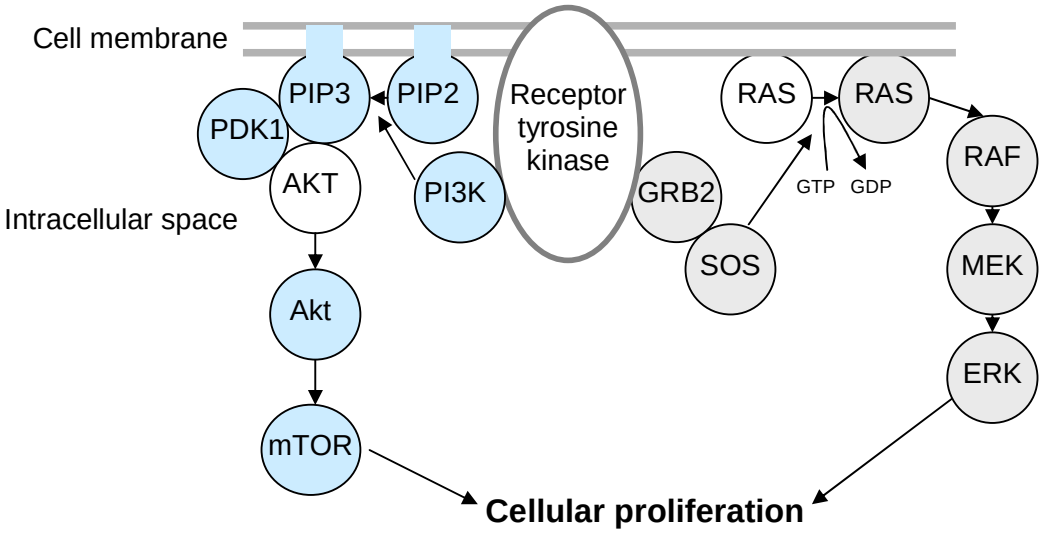

Figure 1.1. *RAS activation*. RAS exists in active (GTP-bound – activated by GEF) and inactive (GDP-bound – inactivated by GAP). RAS is linked to the RTK by adaptor proteins including GRB-2. GRB-2 contains an SH2 domain (so binding to the RTK) and two SH3 domains. Through the SH3 domains GRB-2 is associated with SOS proteins which function as a GEF (so activating RAS). Activated RAS recruits and activates MAPKKK (=RAF) which then activates MAPKK (=MEK) activating MAPK (=ERK). ERK then influences the activity of gene regulatory proteins and through this cellular proliferation. *PI3K activation*. PI3K catalyses the generation of PIP_2 and PIP_3. These phospholipids contain docking sites for PH-domain containing signalling proteins, enabling them to come in close proximity and so interact. An important example is PIP_3 dependent activation of AKT, a process requiring phosphorylation of AKT by PDK1. Once activated AKT phosphorylates many target proteins including mTOR, which serve to promote cell growth and survival.
Abbreviations in figure and legend– *RAS pathway* Guanosine triphosphate (GTP), Guanine nucleotide exchange factors (GEF), guanosine diphosphate (GDP), GTPase-activating proteins (GAP), receptor tyrosine kinase (RTK), growth factor receptor bound-2 (GRB-2), SRC-homology-3 (SH3), Son of Sevenless (SOS), mitogen activated protein kinase (MAPK), MAPK kinase (MAPKK), MAPKK kinase (MAPKKK), MAPK/ERK kinase (MEK), extracellular signal-related kinase (ERK) *PI3K pathway* Phosphatidylinositol 3-kinase (PI3K), phosphatidylinositol (3,4) diphosphate ($PI(3,4)P_2$), phosphatidylinositol (3,4) triphosphate ($PI(3,4,5)P_3$), pleckstrin homology (PH), 3-phosphoinositide-dependent protein kinase 1 (PDK1), mammalian target of rapamycin (mTOR).

1.5.1.2. JAK pathway

The Janus kinase (JAK) family are cytoplasmic tyrosine kinases activated following cytokine receptor binding (**Figure 1.2**). This activation proceeds through signal transducers and activators of transcription (STAT) proteins which directly regulate gene activity promoting expression of anti-apoptotic factors (including BCL-XL). STAT overexpression is seen in cancers including CML and it has been shown in BCR-ABL+ cells that STAT1/3/5 are phosphorylated and constitutively active (22-24). This activity may be abrogated by TKI (25, 26).

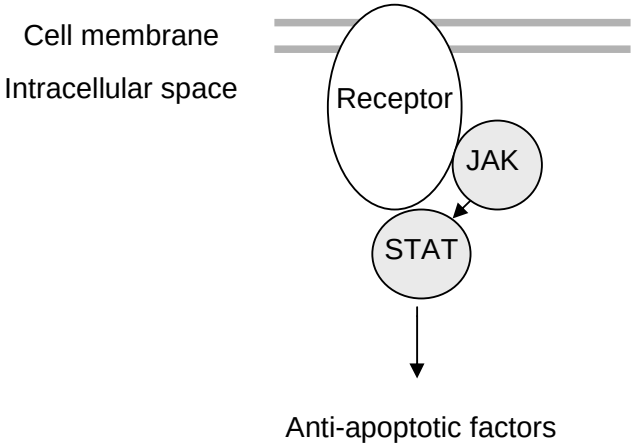

Figure 1.2 Activation of JAK results in activation of STAT proteins which directly regulate gene activity. STAT proteins contain an SH2 domain and may also be activated independently of JAK.
Abbreviations - Janus family kinase (JAK), signal transducers and activators of transcription (STAT), proteins.

1.6 The haematopoietic stem cell in CML

1.6.1 The leukaemic stem cell

The normal HSC performs characteristic stem cell functions of self-renewal, allowing perpetuation of haemopoiesis and the production of differentiated progeny, initially as lineage-restricted progenitors through to mature blood cells. These functions are regulated by soluble cytokines and interactions between cells and stroma. The term “HSC” describes a relatively heterogenous group of cells with varying self-renewal capacity and propensity to generate different lineages. In CML there is a population of leukaemic HSC characterised by the presence of the Philadelphia chromosome and *BCR-ABL* oncogene (Ph+HSC). Consistent with Ph+HSC precursors, BCR-ABL containing cells of all lineages (excluding mature T cells) are seen by different techniques, including: conventional cytogenetics (27, 28); glucose-6-phosphate dehydrogenase clonality (29); and fluorescence in-situ

hybridisation analysis (FISH) following fluorescence activated cell sorting (FACS) (30). The clinical consequence of the HSC basis is reflected in the manifestation of a broad range of disease subtypes associated with progression to BC CML.

The majority of normal HSC are quiescent, stabilised in cell cycle resting stage G0, with infrequent cell cycles every 1-3m (31, 32). The turnover of the Ph+HSC is deregulated with the majority of cells in cycle at any given time. These cells show autocrine IL-3 and granulocyte-colony stimulating factor (G-CSF) production and so may proliferate in the absence of exogenous growth factors (33). Despite this, it is estimated that approximately 0.5% of Ph+HSC remain quiescent and represent a more primitive Ph+HSC sub-population. These quiescent cells are capable of generating BCR-ABL+ progeny in immunocompromised (non-obese diabetic, severe combined immunodeficiency, NOD/SCID) mice, indicating that *in vivo* the quiescent state is reversible (34). In common with CML, both AML and ALL are thought to have a leukaemic HSC basis with cells identified capable of reconstituting disease following engraftment in NOD/SCID mice (35, 36). The diseased HSC is a key target for therapy - these cells may act as a reservoir of disease and through quiescence, self-renewal and increased proliferative potential be resistant to conventional therapy and remain capable of reconstituting the disease state.

Isolation of HSC relies on defining particular morphological and molecular characteristics. A combination of functional assays - to exploit HSC self-renewal and multi-lineage differentiation - and FACS have identified particular molecular characteristics of HSC in the normal and leukaemic state (**Table 1.1**). Colony formation is a functional assay. By this technique, cells are cultured in conditions to encourage proliferation and differentiation. The number of colonies formed will correlate to the number of colony-forming units (CFU) and hence indicate HSC number and function. A long term culture-initiating cell (LTC-IC) assay is a modification of this technique. Here a sample of cells containing primitive HSC is maintained for 5-8 weeks in culture on an established, irradiated, supportive stromal cell layer. The cells are then harvested and cultured in conditions to encourage colony formation. The formation of colonies will correlate to the persistence of primitive HSC throughout long-term culture. FACS when combined with functional assays has enabled identification of molecular characteristics particular to primitive HSC.

Table 1.1. Characterisation of leukaemia initiating cells

Cell type	Molecular characterisation	Proof of stem cell nature	Reference
normal	CD34+38-	Single-sorted cells give rise to sequential plated colonies	(37)
normal	CD34+38-33-	LTC-IC	(38)
AML	CD34+38-HLA-DR-CD71- (most cells capable of LTC-IC were CD34+38-)	LTC-IC NOD/SCID mice leukaemia initiating cells	(39)
AML	CD34+38-	SCID mice leukaemia initiating cells	(35)
AML	CD34+38-Hoechst 3342-*	CFU LTC-IC NOD/SCID leukaemia initiating cells	(40)
CML	CD34+38-	NOD/SCID mice leukaemia initiating cells	(41)

Normal cells are those from healthy donors. *Stem cells are believed to be particularly efficient at effluxing the dyes Hoechst 33342 and Rhodamine (termed "side population" due to appearance on FACS). Colony-forming units (CFU) and long term culture-initiating cell (LTC-IC) assays.

The selected studies seen in **Table 1.1** demonstrate that selection of CD34+38- cells will contain cells with the capacity to self renew and form multi-lineage colonies and so have key HSC characteristics. Furthermore, a high proportion of CD34+38- cells are in G0 and have a high proliferative potential (as measured by response to *in vitro* stimulation with growth factors) (42). This population may therefore have a role in studies to monitor therapeutic effects on the more primitive HSC.

1.6.2 Advanced phase disease and self-renewal capacity

CP disease is associated with myeloid lineage leucocytosis and this reflects the capacity of the Ph+HSC to differentiate to mature progeny. More advanced phases of the disease resemble acute leukaemia and are associated with accumulation of poorly differentiated cells. This is the consequence of a cumulative effect of different genetic insults to the Ph+HSC. These include BCR-ABL mediated

deficiencies in DNA repair, genomic surveillance, loss of tumour suppressor function and telomere shorting (reviewed (43)). Of interest is recent speculation that progression to advanced stages may be associated with the gain of self-renewal function in granulocyte-macrophage progenitor (GMP) cells. GMP are differentiated from HSC and would not normally have the capacity for self-renewal. However, a population of GMP cells selected from BC CML by FACS were capable of initiating leukaemia in mice (44) and BCR-ABL+ mouse GMP cells were capable of expanding *in vitro* (45). In both examples GMP self-renewal capacity was associated with activation of the β-catenin, a component of the WNT signalling pathway.

1.7 Current CML therapy

1.7.1 Imatinib

The current recommended first line therapy for patients with CP CML is IM (Glivec®, Novartis Pharma, Basel, Switzerland) (46), a rationally designed TKI which gained a UK license in 2001. IM underwent successful phase 1 dose-escalation studies (47, 48) and phase 2 trials (49) in patients with CML. This culminated in the phase 3 International Randomized study of Interferon and STI571 (IRIS) trial. In this untreated, newly-diagnosed patients with CP CML were randomised to receive either IM 400mg or interferon-alpha combined with low dose cytosine arabinoside (IFNα + Ara-C). The results showed IM as superior when considering haematological (HR) and cytogenetic responses (CyR), tolerability, or the likelihood of disease progression (50, 51). **Table 1.2** outlines accepted response criteria and definitions for CML clinical trials. Recent results of front line IM therapy for CP CML show complete HR (CHR) in 97% and CCyR in 82% (best observed responses). Disease progression was low but detectable in 0-2.8% patients/y (52). Other multi-centre experiences with IM have been published. De Lavallade *et al.* analysed response to IM in 204 patients with newly diagnosed CP CML and showed a cumulative 83% incidence of CCyR at 5y (by intention to treat analysis) (53). Lower CCyR rates (51% at 2y) have also been reported in a smaller population-based study (54). However, despite impressive responses it is accepted that two key problems with IM remain – disease persistence and IM resistance.

Table 1.2 CML disease response definitions

Haematological response	Cytogenetic response†		Molecular response‡	
*Complete**	*Complete*	Ph+0%	*Complete*	Undetectable
Plt <450x10^9/L	*Partial*	Ph+1-35%	*Major*	<0.10%
WC <10x10^9/L	*Minor*	Ph+36-65%		
normal differential	*Minimal*	Ph+66-95%		
spleen not palpable	*None*	Ph+>95%		

*Peripheral blood platelet count (Plt) and white cell count (WC) with normal differential implying a lack of immature granulocytes and <5% basophils. †Ph+ as % of total metaphases (at least 20) examined in bone marrow. ‡BCR-ABL to control gene ratio. Undetectable levels depend on sensitivity of assay. A major response may also be defined as a 3 log reduction from baseline.

1.7.1.1 CML persistence despite imatinib therapy

IM induces a state of MRD rather than cure. There is clinical evidence for this: the number sustaining a CCyR (66%) is far fewer than the number achieving this; BCR-ABL transcripts remain detectable in the majority of patients (55); and patients who discontinue IM are likely to suffer recrudescence of disease despite apparent disease control (56-59).

The source of MRD may be the Ph+HSC. This theory originates from a number of *in vitro* and *in vivo* studies. Graham *et al* cultured CD34+ enriched fresh leukapheresis products, taken at diagnosis from 5 patients, in the presence or absence of IM. Although IM induced death in dividing cells, there remained a population of viable, quiescent BCR-ABL+ CD34+ cells, surviving despite exposure to concentrations of IM higher than would be expected in treated patients. IM was also antiproliferative, with an increased proportion of cells found in the undivided state in the presence of IM and growth factors, as compared to when growth factors alone were present (60). Similar conclusions were reached by an independent group (Bhatia *et al.)* who used CFC and LTC-IC assays with primitive (CD34+38-) cells from patients newly diagnosed with CML (61). In addition, quiescent BCR-ABL+ CD34+ cells are insensitive to the effects of Ara-C, lonafarnib (farnesyl transferase inhibitor), LY294002 (PI3K inhibitor), 17-allylamino-17-demethoxygeldanamycin (17-AAG, a heat shock protein (HSP) 90 inhibitor) and arsenic, agents which cause apoptosis in the dividing cell population (62, 63). The clinical significance was confirmed by further work with CD34+

selected BM samples taken from 15 IM treated patients with a CCyR. Despite a confirmed response to IM in all, CFU and LTC-IC assays demonstrated that functional BCR-ABL+ progenitor cells remained. In addition, there was an increased frequency of BCR-ABL+ cells within the CD34+ cell fraction when compared to total BM mononuclear cells (MNC), indicating an enrichment of leukaemic cells within this population, consistent with earlier *in vitro* work (64). This work has been extended and presented recently. It has been shown that BCR-ABL+ primitive (CD34+38-) HSC are present in patients with CP CML in CCyR who have been treated with IM for 5y. Furthermore the BCR-ABL levels in this sub-population do not appear to decline during this time (65). The reversibility of the quiescent state which is consistent with Ph+HSC persistence has been demonstrated in a mouse model of CML. BM cells taken from mice with a CML-like disease, which were treated with and had responded to IM, were transplanted into irradiated recipients - all of which then developed disease (66).

1.7.1.2 Imatinib resistance mechanisms

Response criteria are used to define primary IM resistance and include a failure to achieve at least a partial CyR (PCyR) after 12m or a CCyR by 18m therapy (50). IRIS trial data show that 16% and 24% respectively do not achieve these targets. De Lavallade *et al.* showed a failure to achieve at least PCyR at 12m in 39% and Lucas *et al.* failure to achieve CCyR by 18m in 51% of treated newly diagnosed patients (53, 54). Secondary IM-resistance is indicated by a loss of previously achieved response and will affect approximately 16% of newly diagnosed patients in the first 3y of treatment (51). BCR-ABL kinase domain mutations and drug transport are considered important resistance mechanisms, though other mechanisms have been described, such as amplification of the *BCR-ABL* oncogene (seen in 6% of those with IM resistance (67)).

1.7.1.2.1 BCR-ABL mutations

Mutations of the BCR-ABL kinase domain are seen in 35-45% patients resistant to IM and so have generated particular interest as a cause for treatment failure (67-70). BCR-ABL mutations are more prevalent in advanced disease stages than in early CP and in the majority of patients (57-89%) are associated with acquired IM resistance (70, 71). Furthermore the detection of mutations may precede the development of resistance and is predictive of relapse. There is also evidence that BCR-ABL mutations may be seen in patients prior to initiation of IM therapy and so

may be a cause of primary resistance (72). Different mutations vary in their susceptibility to TKI as demonstrated by inhibition of proliferation of transfected BCR-ABL+Ba/F3 cell lines (**Table 1.3**). Of particular scientific significance is the T315I mutation. This is a phosphate-binding loop mutation found in all stages of CML and is associated with BCR-ABL resistance to all currently available TKI. The clinical significance is the subject of some debate. An analysis of 27 patients with T315I demonstrated that the 2y-survival (87% in CP patients) was similar to that of patients with no/other mutations (73). However disease phase is a well recognised indicator of prognosis and at the time of detection with T315I the majority of patients are in AP or BC (74).

Table 1.3 Comparative cellular proliferation assays of tyrosine kinase inhibitor treated BCR-ABL+Ba/F3 transfectants

	Imatinib		Nilotinib		Dasatinib	
	IC_{50} (nmol/L)	Fold change	IC_{50} (nmol/L)	Fold change	IC_{50} (nmol/L)	Fold change
T315I	>6400	>25	>2000	>154	>200	>250
Y253H	>6400	>25	450	35	1.3	2
E255V	>6400	>25	430	33	11.0	14
E255K	5200	20	200	15	5.6	7
Y253F	3475	13	125	10	1.4	2
M244V	2000	8	38	3	1.3	2
F359V	1825	7	175	13	2.2	3
V379I	1630	6	51	4	0.8	1
Q252H	1325	5	70	5	3.4	4
G250E	1350	5	48	4	1.8	2
F317L	1050	4	50	4	7.4	9
L387M	1000	4	49	4	2.0	3
M351T	880	3	15	1.2	1.1	1.4
H396P	850	3	41	3	0.6	0.8
F311L	480	4	23	2	1.3	2
WT	**260**	**1**	**13**	**1**	**0.80.**	**1**

Table adapted from reference (75). Cellular proliferation assessed at 72h drug incubation by a methane-thiosulfonate based assay. Fold change refers to wild type (WT) i.e. p210 BCR-ABL. Those mutants seen more commonly (85% of mutations) are highlighted ( ) (70). Rows highlighted ( ) are those mutants available to use in this project.

1.7.1.2.2 Resistance through mechanisms other than BCR-ABL mutation

1.7.1.2.2.1 Drug transport - Efflux

The ATP-binding cassette (ABC) transporter family form a large group of transmembrane proteins involved in many metabolic processes with the capacity to transport a variety of different substrates. There are 7 subfamilies (ABCA through to ABCG). Expression of these genes can be seen in normal and malignant cells. Members of the ABC family are important in the mechanism of

multidrug resistance (MDR) (reviewed in (76)). MDR is the simultaneous development of resistance to more than one therapeutic agent and can affect drugs with different mechanisms of action. Important genes encoding ABC transporters associated with MDR include: ABCB1, encoding P-glycoprotein (Pgp), also known as MDR1; ABCC1 with the protein product MRP1; and ABCG2 which is also named mitoxantrone-resistance protein or breast cancer resistance protein. Of these transporters ABCB1 and ABCG2 have been studied in CML, in particular for their role in IM transport. ABCC1 appears to play a less significant role and will not be discussed further (77).

1.7.1.2.2.1.1 P-glycoprotein

The importance of Pgp in a variety of tumour types has been established (reviewed in (76)) with the contribution to drug resistance in CML under investigation. BCR-ABL+ cell lines may acquire resistance through increased expression of Pgp if cultured *in vitro* in titrated concentrations of IM. This resistance may then be overcome through selective inhibition of this transporter using verapamil (78, 79). However these results have not directly translated in the clinical setting. Though Pgp inhibitors appeared to restore IM sensitivity *in vitro* to CML cells taken from the BM of 6 patients with IM-resistant BC CML – there was no evidence found for altered Pgp expression (79). However, Galimberti *et al* demonstrated that expression levels of ABCB1 in 33 IM treated patients distinguished those patients who progressed to advanced phases of the disease (80).

It may be that expression of Pgp is a crucial mechanism of IM resistance in a select group of patients; alternatively it may be one contributing factor influencing others. A novel approach targeting Pgp efflux as a presumed mechanism of IM resistance involves use of the HSP90 inhibitor 17-AAG. This compound disrupts the complex formed between HSP90 and BCR-ABL resulting in increased proteasomal degradation of BCR-ABL. 17-AAG has also been shown to inhibit Pgp activity, as shown by Rhodamine-123 efflux. This effect was demonstrated by Radujkovic *et al.* who also demonstrated synergy between IM and 17-AAG. This was seen in 2 IM-resistant cell lines, when the effects of reducing BCR-ABL levels and activity and apoptosis induction were considered. Synergism was not apparent in the IM-sensitive cell lines used for comparison. There was an additive effect on colony formation by PB MNC samples from 3 IM-sensitive patients in BC.

It was concluded that diminished Pgp activity may provide a mechanism for increasing intracellular concentrations of IM and so overcome IM resistance (81). This work is consistent with that of others, where evidence for an additive effect between 17-AAG and IM in BCR-ABL+ cell lines and CD34+ selected patient samples has been demonstrated. However, the quiescent Ph+HSC population are not sensitive to this combination (62).

1.7.1.2.2.1.2 ABCG2

ABCG2 is highly expressed in normal HSC though is downregulated with maturation. The function of high ABCG2 expression is not clear though it may provide a mechanism for drug resistance. IM interacts with ABCG2 and initial studies in BCR-ABL+ cell lines suggested that IM was a substrate for this transporter (82). More recent work on patient samples showed that in common with normal HSC, Ph+HSC express ABCG2 at high levels. IM inhibits the function of the transporter in Ph+HSC, shown by the accumulation of ABCG2 substrates (BODIPY-prazosin) and radiolabelled mitoxantrone. Co-exposure of an inhibitor of ABCG2 (fumitremorgin C) did not enhance the effect of IM on BODIPY-prazosin accumulation, or alter the intracellular accumulation of radiolabelled IM. This led to the conclusion that IM is an inhibitor of ABCG2 and not a substrate (83). Overexpression of this transporter should not therefore affect intracellular concentrations of IM or mediate resistance to this drug. Similar results were obtained by another group (84). Others have utilised BC CML and transfected cell lines and suggested that high levels of ABCG2 expression do mediate resistance to IM - though interpretation is complicated by evidence of IM induced downregulation of ABCG2 expression (85). The true answer to the question of ABCG2 involvement is of significance as this transporter may serve as a future target for drug and antibody therapy.

1.7.1.2.2.2 Drug transport - Uptake

IM is transported actively into cells by the human organic cation transporter 1 (hOCT1). This protein is a member of the solute carrier superfamily and organic cation transporter (OCT) subfamily. Treatment of CP CML samples with OCT-1 inhibitors (prazosin and procainamide) affects intracellular uptake and retention of IM (86). Furthermore, the concentration of IM retained within the cell correlates with kinase inhibition (derived from Crkl phosphorylation). This is of relevance clinically as the sensitivity of BCR-ABL kinase inhibition to IM correlates with

clinical outcome at 12 months (87). These results may not be translated directly to other TKI as nilotinib does not appear to be transported by OCT-1, presumably due to structural differences.

1.7.2 Second-generation TKI

1.7.2.1 Dasatinib

Dasatinib (Sprycel®, Bristol-Myers Squibb, New York, USA) was approved in 2007 for treatment of patients in Scotland with CP CML resistant to or intolerant of IM (www.scottishmedicines.org.uk). Dasatinib is one member of a family of dual ABL- and SRC-family kinase (SFK) inhibitors. SFK (in particular LYN and HCK) are downstream targets of BCR-ABL. However in IM-resistant patient samples and cell lines it has been shown that SFK may be active despite BCR-ABL inhibition and so support cell survival (88). Dasatinib binds the ATP-binding site of ABL in the inactive or active conformation – IM binds and stabilises only the inactive formation (89). In addition, dasatinib more potently inhibits BCR-ABL kinase activity than IM and effectively inhibits cell growth of cell lines expressing IM-resistant BCR-ABL mutations. However, it is not effective against the T315I mutation (90).

Clinical data from trials of dasatinib have been published. For those with CP CML and IM-resistance or intolerance best observed responses were 91% (CHR) and 49% (CCyR). Of interest is that 74% of these patients were IM-resistant and 40% had a confirmed BCR-ABL mutation (91). Recent extended follow-up from this trial has been presented and responses appear durable with 86% maintaining a CCyR once achieved (92). However, as with IM, BCR-ABL transcripts remain detectable in 37-56% of patients at 2y (93). Responses are also gained in patients with advanced stage CML. The phase 2 AP trial achieved a 24% CCyR in IM intolerant or resistant patients with responses seen in patients with a range of BCR-ABL mutations. However, as predicted by *in vitro* data, patients with T315I (or F317L) failed to respond (94).

1.7.2.2 Nilotinib

Nilotinib (Tasigna, AMN107, Novartis Pharma, Basel, Switzerland) was approved in 2008 for treatment of patients in Scotland with CP CML resistant to or intolerant of IM (www.scottishmedicines.org.uk). Nilotinib is a TKI designed on the molecular

framework of IM. Analysis of the crystal structure of nilotinib-ABL complexes show that like IM, the drug binds to the inactive conformation of ABL though with subtle alterations in structure allowing a better topographical fit. Pre-clinical data confirmed the *in vitro* efficacy of this drug in IM-sensitive and resistant cell lines with complementary *in vivo* data from a murine CML model (95). Clinical trials in CP CML with IM-intolerance or resistance have been published and show 74% and 31% achieve a CHR or CCyR respectively (96) (updated to 77 and 42% with 2y follow-up (97)). Responses appear durable with 84% of those with either CCyR or MCyR maintaining this. 42% of these patients had BCR-ABL mutations, however those with particular mutations including T315I, Y253F and E255V failed to respond. Few responses are seen in advanced phases of the disease, with 26% or 16% achieving a CHR or CCyR respectively (98).

1.7.2.3 Front line use of second generation tyrosine kinase inhibitors

Early phase 2 trial data suggests that use of the more potent TKI as first-line therapy may achieve more rapid response than IM. The rationale for this is based on analysis of the IRIS trial data which demonstrated that achievement of particular milestones – in particular CCyR at 12m and major molecular response (MMolR) at 18m – are associated with a low risk of disease progression (51). However despite impressive early responses (96/98% achieving CCyR with nilotinib/dasatinib) disease eradication is not achieved with detectable BCR-ABL transcripts in the majority (99, 100).

1.7.2.4 Tyrosine kinase inhibitors in combination

There is no significant cross resistance between nilotinib and dasatinib, with significant responses seen in a published series of patients with disease refractory to both IM and nilotinib therapy. Cytogenetic responses were seen in 31% of these patients, though the durability of response is not clear with limited follow up data so far available (101). Therefore there may be benefits to be gained from the combination of IM with either dasatinib or nilotinib as all 3 drugs appear to predispose to the development of different BCR-ABL mutation profiles (102). Synergism of IM and nilotinib has been demonstrated in a variety of cell lines and a murine model of CML, however predictably the T315I mutation remained resistant (103)

1.7.2.5 Second generation tyrosine kinase inhibitors and the stem cell

It is clear that currently available TKI are unable to treat CML where particular BCR-ABL mutations are found. There is also concern that the quiescent Ph+HSC population are insensitive to these drugs. It has been demonstrated *in vitro* using dasatinib that despite potent inhibition of BCR-ABL activity (using Crkl phosphorylation as a marker), a quiescent population of primitive Ph+HSC persist – despite the confirmed absence of BCR-ABL mutations (4). In a similar series of experiments tracking division of CD34+ CML cells in the presence of nilotinib, it was seen that quiescent Ph+HSC persist and may accumulate relative to untreated cells which will tend to divide and differentiate (104).

1.8 The need for new approaches

Within the leukaemic HSC population evidence is presented for a population of cells which are relatively insensitive to current TKI and characterised by phenotype (CD34+38-) and quiescence. This population will serve to sustain MRD, despite apparent adequate response to therapy. Patients will therefore remain on drug indefinitely for fear of disease recrudescence, and so with long-term therapy there is the theoretical risk that selection of resistant mutations (such as T315I) will occur. However it is accepted that longer term data from the IRIS trial supports the stance that MRD in the majority is of no consequence as once significant responses (MMolR) are obtained they appear durable with very few patients suffering disease progression. The only “curative” option remains haemopoietic stem cell transplantation, a procedure limited in application by donor availability and the toxicity of conditioning regimes. The success of TKI has led to a significant reduction in the popularity of transplantation for CML and it is now an option reserved in most UK centres for those with advanced stage disease (105).

A number of different strategies are being adopted to improve the treatment of CML and these are outlined in **Table 1.4** and have been reviewed (106). This introduction will focus on proteasome inhibition as a therapeutic strategy to target CML.

Table 1.4 Strategies to target imatinib resistance and disease persistence.

Target	mechanism	examples	reference
BCR-ABL			
Activity	newer tyrosine kinase inhibitors	dasatinib, nilotinib	Reviewed here
Stability	histone deacetylase inhibitors	LBH-589	(107)
	heat shock protein 90 inhibitors	geldanamycin 17-AAG	(107-110)
enhance IM effects	increased IM dose		(111-114)
	combination of IM with IFN-A	SPIRIT trial	(115)
	G-CSF scheduling	GIMI trial	(116)
	drug efflux inhibition	verapamil	(79, 81, 117, 118)
BCR-ABL location	nuclear trapping	leptomycin B	(119, 120)
alternative targets			
	proteasome inhibitors	bortezomib	Reviewed here
	farnesyl transferase inhibitors	lonafarnib, BMS-214662	(121)
	protein kinase C	bryostatin	(122)
	reactive oxygen species generation	adaphostin	(123, 124)
	hypusination inhibitors	ciclopirox	(125)
	aurora kinase inhibitors	MK-0457	(126-128)

1.9 The proteasome

The proteasome is an intracellular organelle which functions as a targeted mechanism for protein degradation. Through this it plays a vital role in cellular processes such as cell cycling, adhesion, proliferation and apoptosis – all of which may be deregulated in cancer. An outline of the mechanism of proteasome function is illustrated in **Figure 1.3**.

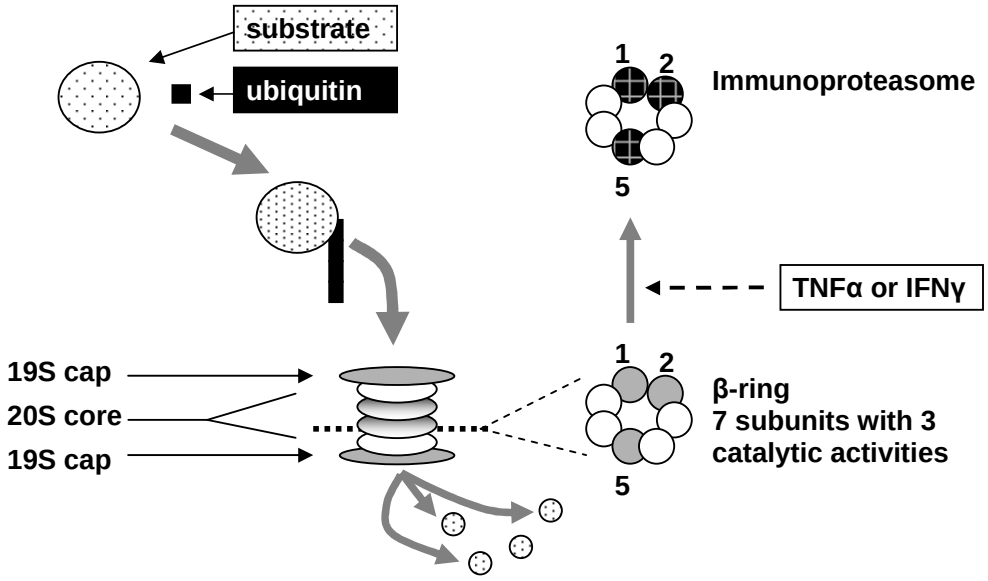

Figure 1.3 An illustration of proteasome activity.
TNFα (tumour necrosis factor-alpha) and IFNγ (interferon-gamma).

The 26S proteasome is formed from a 20S core with two 19S regulatory cap units. Proteins are targeted for proteasomal degradation by the attachment of ubiquitin - this process following a series of catalytic reactions. Ubiquitin activating enzyme (E1) first binds to and activates ubiquitin, which is then transferred to one of a group of ubiquitin conjugating enzymes (E2). Ubiquitin protein-ligase enzymes (E3) then catalyse the binding of E2-bound ubiquitin to the target protein. Through multiple reactions a polyubiquitin tag is formed on the substrate which enables recognition by a proteasome cap unit. There are around 1000 different E3 ubiquitin ligases in the human genome and this step provides substrate specificity to the process. Furthermore, deregulation of E3 ubiquitin ligase activity is seen in human cancer (129). Following recognition by the cap unit, the ubiquitinated substrate is presented to the catalytic sites within the 20S core. The core comprises 4 stacked rings. Each ring is divided into 7α (α-ring) or 7β (β-ring) subunits. The α-rings are associated with the cap units and act as gated channels. Catalytic activity occurs on the β-rings as 3 peptidase activities (CT-L, tryptic (T-L) and postglutamyl peptide hydrolytic (PG)) and each activity is associated with a specific beta subunit (β5, β2 and β1 respectively) (reviewed in (130)).

The substrate specificity of the β subunits is modified following stimulation with interferon-gamma or tumour necrosis factor-alpha and the designation of the subunits becomes β1i, β2i and β5i – the proteasome is then an immunoproteasome. This functional change enhances the ability of the cell to

present antigenic peptides via MHC class I. There is some evidence that the immunoproteasome activity may predominate in certain types of haematological malignancy (131). This change may be of significance when the measurement of proteasome activity is considered.

1.9.1 Measuring proteasome activity

Proteasome activity is conventionally measured by the turnover of fluorescent substrates for the 3 catalytic sites and results are expressed as released fluorescence units. Though widely adopted, it is recognised that there are limitations to this technique: cell lysis prior to analysis is required and it is not known how this will interfere with proteasome activity; immunoproteasome activity is not assessed by this method; and large numbers of cells ($>1x10^7$) are required. More recently, methods have been established using labelled compounds which act as PI and probe specific subunit activities in cell lysates (131) or live cells (132). This permits more detailed analysis of both proteasome and immunoproteasome activity using relatively small cell numbers. However, these are not commercially available. Activity may also be determined by indirect methods such as effects on pathways shown to be intimately associated with the proteasome for example the NFkB/IkB axis.

1.9.2 Proteasome inhibitors and cancer

Cancer cell lines have abnormally high levels of proteasome activity and expression (133) and have been shown to be relatively more sensitive to the effects of PI than their non-malignant counterparts. The first proteasome inhibitor to enter clinical trials was bortezomib (Velcade®, Janssen-Cilag International NV, Beerse, Belgium) and this remains the only PI approved for clinical use. It was licensed for use in Scotland in 2004 for patients with multiple myeloma who have received at least two prior therapies and who are refractory to alternative licensed treatments (www.scottishmedicines.org.uk). In addition bortezomib was licensed in the USA in 2006 for second-line use in patients with mantle cell lymphoma (www.fda.gov) and may be used in this disease in the UK within the context of a clinical trial (www.cancerhelp.org.uk). In the setting of two phase 1 clinical trials including Australia, Estonia and USA, NPI-0052 is a new PI under investigation for treatment of advanced malignancy including multiple myeloma. Carfilzomib (PR-171) is a further PI which has shown evidence for efficacy in multiple myeloma and

mantle cell lymphoma and which is available for use in these conditions in open clinical trials. (National Cancer Institute, www.cancer.gov).

1.9.3 Bortezomib

In 1999 the National Cancer Institute tested a selection of related boronic acid derivative PI for activity in a variety of cancer cell lines. Of these, bortezomib (formally PS-341) demonstrated particular efficacy based on potency of proteasome inhibition (using fluorescence-based assays) and ability to inhibit cancer cell growth. The prostate cancer cell line PC-3 was selected from this initial study for more detailed investigation. It was shown *in vitro* that the concentration required to kill 50% of PC-3 cells at 48 hours (h) was 20nM. This compound also inhibited growth of tumours in mice when used at a concentration of 1.0mg/kg with comparable and detectable levels of radiolabelled drug in the PB and BM (134). The activity of bortezomib is relatively selective for CT-L activity and this has been confirmed by fluorometric and subunit probe-based assays (131). Laboratory and clinical investigations have been extended by many other groups using tumour models and cell samples from patients with haematological and solid organ malignancies. It is from these studies that a mechanism of action has been proposed and pharmacodynamic and pharmacokinetic information has been established.

1.9.4 Proposed mechanism of proteasome inhibitors

The proteasome is found in all eukaryotic cells, both malignant and non-malignant. A PI must therefore exploit a difference in activity and/or reliance of the cell upon that activity if it is to be selective. The state of cancer is generally accepted to involve an imbalance between those factors driving proliferation and those promoting apoptosis. It is likely that PI “tilt the scales” from cell survival to apoptosis in malignant cells by a number if ways. A complete mechanism of action is not yet known fully and may vary between different cell types utilising abnormal proteasome activity in different ways.

1.9.4.1 The NFkB/IkB axis

NFkB is a transcription factor that serves to support cell survival. This is achieved by promoting expression of anti-apoptotic genes as well as those influencing inflammation, proliferation and differentiation. Regulation of NFkB activity is well described and is illustrated in **Figure 1.4**. NFkB exists as a cytoplasmic form

bound to an inhibitory molecule IkB. The principal pathway leading to NFkB activation is the phosphorylation of IkB by IkB kinase (IKK). IkB is ubiquitinated and degraded by the proteasome. NFkB may then enter the nucleus and bind to a specific consensus site within DNA. Furthermore, IkB transcription is activated by NFkB leading to loss of NFkB from the nucleus and enabling negative autoregulation of the pathway (reviewed in (135)). The structure of the proteins involved is more complex than has been illustrated. 'NFkB' is commonly used to describe a family of proteins which form homo- and heterodimers, the most well characterised form being p50/p65. The family of anchorin-domain containing inhibitory molecules binding NFkB and preventing nuclear translocation (termed 'IkB' in **Figure 1.4**) include IkBα, IkBβ, IkBγ, IkBαε, bcl-3, p105 and p100. IKK consists of IKKα, IKKβ, and IKKγ (together referred to as NFkB essential modulator subunits).

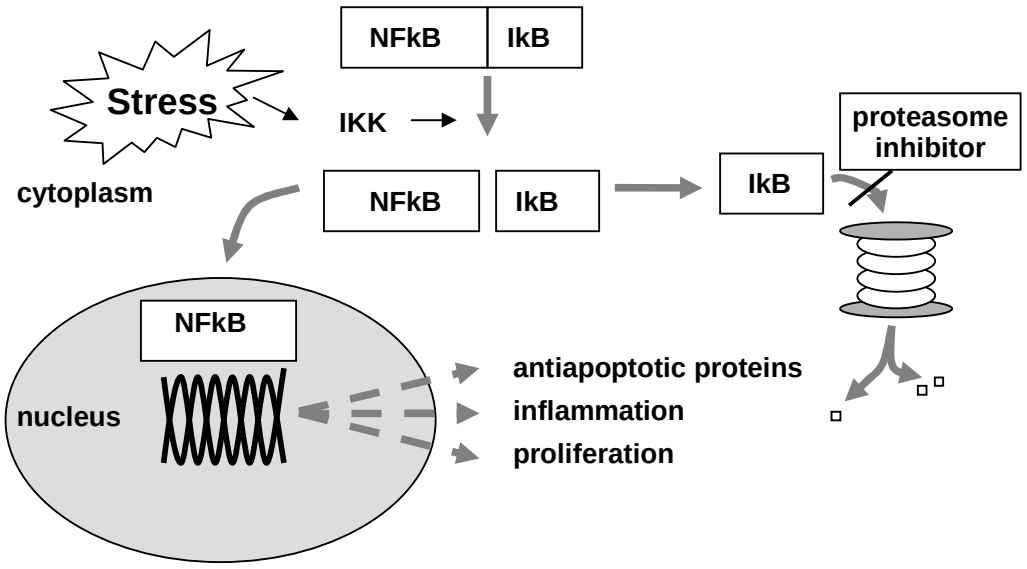

Figure 1.4 An illustration of the NFkB/IkB axis

When the role of this pathway in proliferation, apoptosis and inflammation is considered, it is not surprising that constitutive NFkB activity has been demonstrated in many malignancies, including CML (136-138). Relevant to CML is the finding that NFkB is required for tumour development and primary BM cell transformation by BCR-ABL+ cell lines (17) NFkB activation may occur downstream of BCR-ABL with suggested mechanisms involving BCR-ABL activation of serine-threonine kinases such as PKD2 (mediating activity through the IKK pathway) (137) and MEKK (139). BCR-ABL may also increase the degradation of IkB through an undefined mechanism independent of IKK (138). .

There is evidence for constitutive activation of NFkB in samples from patients with CML. PB and BM were taken from 17 patients with CML (15 CP, 2 myeloid BC) and analysed by electrophoretic mobility shift assays (EMSA) a standard measurement of nuclear NFkB activity. In both BC (but not in CP) a significant increase in activity was seen in comparison to healthy controls (140). These findings were confirmed in a separate study analysing PB from 8 patients with CML BC by EMSA. Here the activity was unaffected by exposure of patients to IM, which is surprising when considering the evidence for BCR-ABL mediated NFkB activation (138).

1.9.4.2 Bortezomib and the cell cycle

The cell cycle is a regulated and ordered process of growth and division. It is conventionally divided into 4 sequential phases: G1, a synthetic phase; S phase, during which DNA duplication occurs; G2, a second synthetic phase; and M phase, during which the cell undergoes mitosis. The progression through these phases is controlled by cyclin dependent kinases (CDK), which are expressed and degraded at various points of the cell cycle. Cyclins are regulatory proteins which form a complex with CDK and are necessary for kinase activity. An illustration of the cell cycle is shown (**Figure 1.5**) demonstrating the function of various cyclin-CDK complexes.

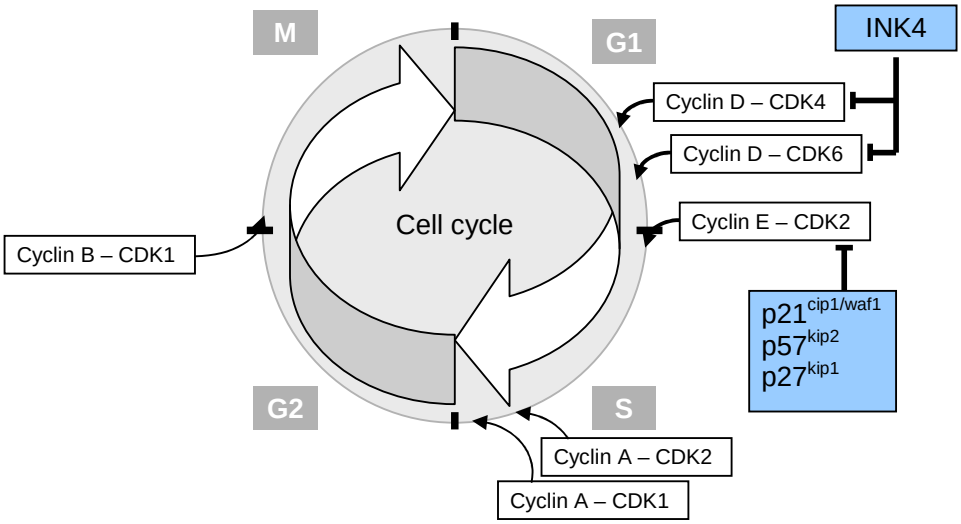

Figure 1.5 An illustration of the role of the cyclin - cyclin dependent kinase (CDK) complex (white text boxes) and CDK inhibitors (blue text boxes) in cell cycle progression through 4 key phases (grey text boxes) with corresponding check-points (black bars).

The retinoblastoma protein is (pRb) is of key importance for cell cycle initiation. pRb associates with E2F family of transcription factors and inhibits their activity. Phosphorylation of pRb leads to dissociation of the pRb-E2F complex. This phosphorylation is mediated by cyclin-CDK complexes (cyclin D–CDK3, cyclin D-CDK6 and cyclin E-CDK2). E2F transcription factors which have been released from inhibitory binding, promote the expression of genes necessary for progression from G1 to S phase. Transition through S phase requires the repression of E2F activity and this involves Cyclin A–CDK2 and CDK1. The phosphorylation inhibits the DNA binding of the E2F. Transition through G2 into M phase requires the activity of cyclin B–CDK1 complexes. A further level of control, in particular during the G1 and S phase, is provided by the cyclin dependent kinase inhibitors (CDKi). There are two families of CDKi - the Cip/Kip family ($p21^{cip1/waf1}$, $p57^{kip2}$ and $p27^{kip1}$) which inhibit the kinase activities of cyclin D-, E-, A- and B-CDK complexes, and the INK4 family which inhibit cyclin D-CDK4 and CDK6 complexes (141). Cell cycle transition is therefore mediated through loss of CDKi activity permitting progression and increased activity resulting in growth arrest. This may be illustrated by studies where $p27^{kip1}$ was over-expressed in human cells with consequent G1 arrest (142).

CDKi and the Cip/Kip family in particular are frequently deregulated in human malignancies and may be of prognostic value (143). It has been shown that BCR-ABL+ cell lines have reduced levels of $p27^{kip1}$ and this appears to be partially regulated by proteasomal degradation. A suggested mechanism involves BCR-ABL regulated expression of SKP2 - this then influences ubiquitination (as part of a multiple component complex with E3 ubiquitin ligase activity) and hence proteasomal degradation of the $p27^{kip1}$. It has recently been shown in cell lines that BCR-ABL induces phosphorylation of $p27^{kip1}$ at the Y88 position and so promotes ubiquitination and subsequent degradation - exploiting a mechanism for normal cell cycle progression into S-phase (144). Correspondingly it has been seen that BCR-ABL inhibition (with IM) in cell lines and CD34+ cells from patients with CML, results in $p27^{kip1}$ stabilisation and increased apoptosis (145). Furthermore, induced over-expression of $p27^{kip1}$ in BCR-ABL+ cell lines reduces proliferation rates, with accumulation in G1 phase and this renders cells insensitive to PI induced apoptosis. It is also speculated, though unproven, that increased $p27^{kip1}$ may be a mechanism for drug resistance in the quiescent stem cell population (146). The CDKi $p21^{cip1/waf1}$ and $p57^{kip2}$ and are related to $p27^{kip1}$ and presumed to share

similar activity. Treatment of BCR-ABL+ and lung cancer cell lines with bortezomib is associated with stabilisation of $p21^{cip1/waf1}$ and accumulation of cyclin B (147, 148). $p57^{kip2}$ is regulated in a similar manner to $p27^{kip1}$ through SKP2 ubiquitin ligase activity and proteasomal degradation (149). However, effects of bortezomib on $p57^{kip2}$ have not specifically been addressed in CML.

Bortezomib has established antiproliferative effects in cell lines and tumour cells from solid organ and haematological malignancies including BC CML. This has been demonstrated with accumulation of treated cells in G2-M phase (1, 9, 150). It is likely ineffective cell division is mediated by a failure of the normal cyclical degradation of CDK complexes and CDKi and it is presumed the increased proliferative potential of malignant cells renders them more susceptible to these effects than their non-malignant counterparts.

1.9.4.3 Bortezomib and apoptosis

Apoptosis describes a coordinated process by which cells die. Apoptosis is initiated in several ways and of most importance are the “extrinsic” and “intrinsic” pathways. Extrinsic apoptosis is precipitated by the binding of a ligand (e.g. TNF) to a cell surface death receptor (e.g. TNF –related apoptosis inducing ligand, TRAIL receptor). In intrinsic apoptosis, cell death follows a series of intracellular events. Both pathways result in the characteristic changes of cell shrinkage, chromatin condensation, nuclear fragmentation, blebbing and the exposure of phosphatidyl serine on the outer cell membrane. The latter is exploited in experimental techniques demonstrating cell death (**2.4.2**). Cysteine protease cleaving after Asp (‘caspase’) enzymes are important in apoptosis and are synthesised as an inactive pro-caspase requiring specific cleavage for activation. This cleavage is inhibited by inhibitor of apoptosis (IAP) proteins. In general “initiator” caspases (e.g. caspases-8,-9 and -10) activate “executioner” capases (e.g. caspase-3 (**2.4.3**) and -7) which then precipitate apoptosis.

The extrinsic pathway is stimulated by death receptor binding with consequent activation of caspases-8 and -10 through the adaptor molecule FAS-associated death domain-containing protein (FADD). In the intrinsic pathway the initiator is caspase-9, which is activated by formation of a complex with apoptosis protease activating factor-1 (APAF-1). This process requires cytochrome *c* release from the mitochondrion by membrane permeabilisation (MMP). With MMP, Cytochrome *c*

release is accompanied by second mitochondria-derived activator of caspase (SMAC) which binds and deactivates IAP (151). MMP is considered a critical phase of apoptosis and is influenced by the BCL-2 family of proteins, all members of which contain BCL-2 homology (BH) domains. They are either anti- or pro-apoptotic. Anti-apoptotic factors include BCL-2, BCL-XL and MCL-1. The pro-apoptotic members are subclassified as those with multiple BH domains (e.g. BAX, BAK) or only one (BH-3 only) domains (e.g. BIM, BID, BAD, NOXA and PUMA). Fundamental to MMP is the formation of molecular pores in the mitochondrial membrane and this is directly associated with the activation of BAX and BAK. BH3 only proteins indirectly contribute to this activity by either activation of BAX/BAK or by blocking the inhibitory activity of anti-apoptotic BCL-2 proteins.

Though the two pathways are described separately, there is recognised cross-activation. For example, TRAIL-stimulated caspase-8 activation mediates cleavage and activation of BID with resulting Cytochrome *c* release - hence linking the extrinsic and intrinsic pathways (152).

Bortezomib has been shown to affect the balance of pro- and antiapoptotic factors. A key member of the BH3-subgroup of pro-apoptotic factors is BIM. BCR-ABL may reduce BIM via ERK activity with resulting phosphorylation and proteasomal degradation. This influence on levels of BIM has been reversed with IM, nilotinib and PI exposure. Furthermore, siRNA reducing expression of BIM has been shown to rescue cells and the BH3-mimetic ABT-737 enhanced IM-induced cell death. These results have been generated from work with IM-sensitive and resistant cell lines and CML patient samples and have led to the suggestion that PI may be effective in combination with TKI (153-156). Other pro-apoptotic factors affected by bortezomib in various solid organ cell line models include NOXA (157, 158) and BIK (though at 100-500nM bortezomib) (159). Effects have been seen on anti-apoptotic factors with possible upregulation of BCL-2 though this has not been a consistent finding (159). Full activation of BIM, BAK and BAK requires loss of MCL-1 through proteasomal degradation. In CML cell lines MCL-1 has been demonstrated as constitutively active - when targeted with siRNA to reduce MCL-1 activity, cells undergo apoptosis. It is interesting to note in melanoma cells bortezomib treatment may enhance or stabilise MCL-1 by preventing breakdown (160). This observation is however consistent with the concept that PI shift the

balance towards apoptosis by influencing a number of factors rather than specific targeting of individual pathways.

1.9.4.4 Bortezomib and reactive oxygen species generation

Reactive oxygen species (ROS) are products of normal cellular processes and are involved in the initiation of apoptosis through stimulation of cytochrome *c* release. In the resting state ROS are stabilised through antioxidants such as glutathione. However following a disruption of the MMP there is an associated increased generation of ROS, saturating the antioxidant systems and resulting in the promotion of cell death ("bioenergetic crisis") (reviewed in (151)). Bortezomib treatment of non-small cell lung cancer cell lines at 50-100nM is associated with enhanced generation of ROS. Inhibition of this ROS generation (with the antioxidant Tiron) reduced ROS generation and apoptosis (161). In a similar manner 5nM bortezomib induced ROS generation in BCR-ABL+ Ba/F3 cells (p210 and T315I) with associated apoptosis which was partially reversed with antioxidant treatment (123).

Adaphostin is a member of the tyrophostin group of TKI. These compounds interfere with peptide binding, in contrast to IM which affects the kinase ATP binding site. Adaphostin is a derivative of AG957, a drug developed as an alternative to IM. Adaphostin has been shown to induce apoptosis and reduce BCR-ABL expression in cell lines. The mechanism of action may involve the generation of ROS. Recent work has produced results in cell lines suggesting synergism with adaphostin and bortezomib, presumably related to the response to oxidative injury (123). Minimal toxicity of adaphostin on normal human CD34+ cells was seen (124).

1.9.4.5 Bortezomib and autophagy

Autophagy is a pathway to cell death that is distinct from apoptosis. It is a process through which portions of the cytoplasm are enveloped and bound within the cell and then the contents digested by lysosomal enzymes. This enables elimination of abnormal intracellular proteins or damaged organelles. The process may be progressive with resultant destruction of the entire cell (reviewed in (151)). Of relevance to the proteasome is that the pathway is an additional mechanism for protein degradation, though it involves aggregation of the abnormal proteins (aggresome) and requires histone deacetylase (HDAC) activity. Studies have

shown that targeting of both the proteasome (with bortezomib) and the aggresome pathway (by tubacin a HDAC inhibitor) in multiple myeloma PB and BM cells results in synergistic accumulation of polyubiquitinated proteins and apoptosis even in the presence of supportive stromal cells (162). Bortezomib also was synergistic with LBH589 (a HDAC inhibitor) in multiple myeloma BM and PB cells though here evidence was presented for the role of inhibition of aggresome migration through tubulin deacetylase inhibition preventing autophagy (103). There is relevance here to CML as it has been demonstrated that TKI induce autophagy in BCR-ABL+ cells. This may be a protective response as concomitant exposure of cells to drugs which inhibit autophagy enhanced TKI induced cell death (163, 164). Suberoylanilide hydroxamic acid (SAHA, Vorinostat) is a HDAC inhibitor which is currently under investigation in clinical trials for haematological and non-haematological malignancies, including BC CML. The mechanism of action includes both induction of apoptosis and autophagy, demonstrated by caspase-3 activation and characteristic morphological changes seen under electron microscopy of HeLA cells (165). Treatment of BCR-ABL+ cell lines and patient BM samples, including those expressing T315I, with SAHA resulted in apoptosis that was independent of BCR-ABL activity. Apoptosis was enhanced when SAHA was used in combination with drugs known to target autophagy, which include chloroquine.

1.9.5 Current clinical use of bortezomib

1.9.5.1 Multiple myeloma

Particular biological features of multiple myeloma (a malignant disorder of plasma cells) justified *in vitro* experiments exposing cell lines and BM cells from patients with this condition to bortezomib. In multiple myeloma IL-6 promotes growth and survival of the tumour cells and secretion of IL-6 is dependent on NFkB activity (166, 167) – as described (**1.8.1.2.1**) NFkB activity and proteasomal function are intricately connected. With bortezomib treatment, selective apoptosis and significant inhibition of cell growth was seen in comparison to normal PB MNC. Phase 1 clinical trials demonstrated particular efficacy in plasma cell dyscrasias (168) and phase 2 (169, 170) trials in multiple myeloma the safety and efficacy of a 1.3mg/m^2 dosing regime with additive benefits seen when bortezomib was combined with dexamethasone. These findings formed the basis of the randomised phase 3 APEX (Assessment of Proteasome Inhibition for Extending

Remissions) trial which compared bortezomib monotherapy with high-dose dexamethasone in patients with relapsed multiple myeloma (171). Bortezomib was associated with higher response rates, a longer time to disease progression and improved survival. Data from these clinical trials led to the acceptance by the Scottish Medicines Consortium for restricted use of bortezomib in multiple myeloma as described (**1.8**).

1.9.5.2 Mantle cell lymphoma

The USA licensing for bortezomib in relapsed or progressive mantle cell lymphoma is based on supportive data generated from the phase 2 PINNACLE (Proteasome Inhibition as an Innovative Approach to Relapsed Mantle Cell Lymphoma a Single Agent Evaluation) trial. Here a similar dosing schedule to that of the APEX trial was seen to be safe and effective with approximately one-third of patients achieving a reduction in tumour burden (172). No submission has been made for a UK license for use in this setting though the drug is available for use as part of a clinical trial (www.cancerhelp.org.uk).

1.9.5.3 Other haematological malignancies

There are currently (December 2008) 194 open and recruiting trials using bortezomib for treatment of cancer patients. 10 trials involve treatment of patients with AML and of these 1 will accept patients with BC CML. All involve bortezomib as combination therapy.

Table 1.5 Current clinical trials with bortezomib in myeloid malignancy

Disease	Trial phase	Additional therapies	Trial number
AML	1/2	mitoxantrone + etoposide	NCT00410423
AML	1/2	fludarabine + idarubicin + G-CSF	NCT00651781
AML	2	tipifarnib	NCT00510939
AML	2	idarubicin + ara-C or etoposide + ara-C	NCT00666588
AML	2	daunorubicin and ara-C	NCT00742625
AML and CML-BC	1	tipifarnib	NCT00383474
AML	1	idarubicin	NCT00382954
AML	1	azacytidine	NCT00624936
AML	Not stated	melphalan	NCT00789256
AML	1	decitabine	NCT00703300

1.9.6 Pharmacodynamics of bortezomib

A number of clinical trials with bortezomib in solid organ (renal, colon, lung, breast, prostate, neuroendocrine and hepatocellular cancers) and haematological (both lymphoid and myeloid) malignancies have published and the particular pharmacokinetic features of this drug are described. Following intravenous administration in a phase 1 trial the plasma bortezomib concentration followed a biphasic elimination profile, with an initial half life <30 minutes. The plasma concentration of bortezomib varied from a peak of 1.5-7.5ng/mL at 1h and did not clearly correlate with proteasome inhibition measured in PB. The conclusion drawn was that plasma levels of drug may not a reliable method for predicting or measuring drug effect (173). Millennium Pharmaceuticals provide data indicating a wide range of peak plasma concentrations (109-1300ng/mL) with the caveat "the pharmacokinetics of Velcade® as a single agent have not been fully characterised" (www.velcade.info). Myeloma patients (n=23) were specifically assessed for pharmacokinetic and pharmacodynamic data. Patients were treated with 1.3mg/m^2 (standard dose) following a standard schedule and at day 11 of cycle 3 peak levels of 114.9±98.3ng/mL (299nM) and area under the curve at 48h of 85.2±18.7ng.h/mL (approximately equivalent to 5.3±1.2nM continuous exposure) were recorded (174). The majority of published trials rely on a standardised fluorometric method to determine a CT-L:T-L ratio and from this derive data on achieved levels of proteasome inhibition in PB cells (175). From

animal data >80% proteasome inhibition is predictive of significant morbidity and mortality (134, 176), this data was extrapolated to clinical trials to predict a maximum tolerated dose of 1.96mg/m^2 (177). The current recommended dose is 1.3mg/m^2 twice weekly for 2 weeks followed by a 10 day rest period. This approximates 70-83% maximal proteasome inhibition at 1h (168, 173, 174). Following peak levels of inhibition at 1h approximately 50% and <20% of peak activity are seen at 24 and 72 hours (h) respectively with levels returning to baseline prior to day 4 (i.e. next dose) (168, 178-180). Data to indicate drug effects in tumour and BM tissue are conflicting. In a murine model of MM the levels of proteasome inhibition achieved in the tumour was approximately half that of the blood (176), however data from a phase I trial in prostate cancer showed levels in blood and tumour were equivalent. Proteasome inhibition achieved in the BM was assessed in 2 patients in this trial and the levels were approximately half that seen in the blood (173).

1.10 The proteasome in CML

There is evidence that the proteasome may provide a relevant therapeutic target in CML. BCR-ABL+ cells have significantly higher levels of proteasome activity relative to comparable BCR-ABL- cells (as measured by turnover of fluorescent substrate for CT-L activity). Furthermore, relatively high activity in 6 diagnostic BM samples from patients with CML has been demonstrated (2). This is consistent with data from other malignancies.

1.10.1 Published use of proteasome inhibitors in CML

A number of *in vitro* studies of PI, including bortezomib, in CML have been published. These will be reviewed in detail in the **Discussion** chapter. Despite promising *in vitro* effects, there is little *in vivo* data. A phase 2 study has been published in abstract form, where bortezomib was used as monotherapy in 7 IM-refractory or intolerant patients. Data suggest *in vitro* and *in vivo* effects from analysis of apoptosis of patient derived mononuclear cell samples. No cytogenetic responses were seen and no survival data were presented (181).

1.11 Rationale for this study

There is promising published data and a logical rationale for the use of PI in CML. Targeting the proteasome may offer a solution to the two key problems with TKI therapy: that of IM resistance, commonly in the form of BCR-ABL mutations; and the relative insensitivity of the stem cell to TKI. Cell line studies have demonstrated that IM-resistant cells are susceptible to bortezomib (1) though particular effects on viability and proteasome activity in cells with specific BCR-ABL+ mutations have not been presented. Little work has been published on the effects of bortezomib on the Ph+HSC though 2 groups have published CFU data (3, 8). Assays that have demonstrated TKI effects on the quiescent Ph+HSC population include CFSE tracking of cell division and FACS to obtain the CD34+38- population. This has not investigated in CML with bortezomib. The current clinical trial profile of bortezomib serves to demonstrate that PI are effective agents in combination with established therapies. There is preliminary published data with conflicting results in BCR-ABL+ cell lines with bortezomib in combination with IM (1, 155). Dasatinib is a more potent TKI than IM though has not been assessed in combination with bortezomib. Combination of these agents would establish whether potent inhibition of BCR-ABL and proteasome activity could result in synergistic effects on cell viability. This may be particularly relevant in the Ph+HSC as BCR-ABL activity has been shown to be relatively high in this population (4). These questions provide the basis of the novel work performed in this project which aims to enhance knowledge in this field and may provide the basis for a clinical trial.

1.12 Stated hypotheses and aims

The hypothesis as stated in the grant proposal:

“Increased BCR-ABL expression in CML stem cells may lead to increased proteasome activity, therefore, simultaneous inhibition of both BCR-ABL tyrosine kinase and proteasome activity might induce CML stem cell specific apoptosis and this combined treatment could be clinically translated in the immediate future.”

The individual aims are stated as follows:

1 Effect of PI on viability and proliferation in BCR-ABL+ cell lines including those resistant to TKI
2 Proteasome activity in BCR-ABL+ cell lines
3 Effect of PI on BCR-ABL activity in BCR-ABL+ cell lines
4 Effect of PI on viability and proliferation of CML patient samples
5 Effect of PI on BCR-ABL activity in CML patient samples
6 Proteasome activity of CML patient samples
7 Effect of PI on primitive cells from CML patient samples
8 Effect of PI on non-CML patient samples
9 The potential synergistic effect of PI and TKI on viability and proliferation of BCR-ABL+ cell lines and CML patient samples.

2. METHODS

2.1 Reagents and Equipment

2.1.1 Reagents

Reagent	Company and address
2-mercaptoethanol	Invitrogen, UK
7-amino-actinomycin D (7-AAD, Via-Probe™ solution)	BD Biosciences
Adenosine triphosphate (ATP)	Sigma-Aldrich, UK
Annexin V-FITC	BD Biosciences
Beta-mercaptoethanol	Sigma-Aldrich, UK
Bortezomib	Janssen-Cilag International NV, Beerse, Belgium
Bovine Serum Albumin/Insulin/Transferrin (BIT) 9500	StemCell Technologies Inc., USA
BSA™ Protein Assay Kit	Pierce, Rockford, USA
Carboxy-fluorescein diacetate succinimidyl diester (CFSE)	Invitrogen, UK
Dasatinib	Bristol-Myers Squibb, Princeton, USA
Demecolcine (Colcemid®, N-Deacetyl-N-methylcolchicine)	Sigma-Aldrich, UK
Dimethyl sulphoxide (DMSO)	Sigma-Aldrich, UK
Dithiothreitol (DTT)	Sigma-Aldrich, UK
DNase I	StemCell Technologies Inc., USA
Dulbecco's Phosphate Buffered Saline (D-PBS)	Sigma-Aldrich, UK
ECL+™ Chemiluminescence solution	GE Healthcare UK Ltd.
FACSFlow™	BD Biosciences, San Jose, CA
Fetal calf serum (FCS)	Invitrogen, UK
FIX and PERM kit	Caltag laboratories, Burlingame, CA
Full range Rainbow® recombinant protein	Amersham Biosciences,

molecular weight marker (12-225x$10^3$$M_r$)	Buckinghamshire, UK
Granulocyte-Colony Stimulating Factor	Chugai Pharma Europe, UK
Human Serum Albumin 20%	Scottish National Blood Transfusion Service
Imatinib	Novartis Pharma, Basel, Switzerland
Isove's modified Dulbecco's media (IMDM)	Sigma-Aldrich, UK
Laemmli sample buffer	Bio-Rad Laboratories, Hercules, CA
L-Glutamine	Invitrogen, UK
Low density lipoprotein	Sigma-Aldrich, UK
Magnesium Chloride	Sigma-Aldrich, UK
MG132	Calbiochem®, Merck, Darmstadt, Germany
$MgCl_2$	Sigma-Aldrich, UK
Non-fat dried milk	Morrisons supermarket, UK
Nonidet® P-40	Roche Diagnostics, Mannheim, Germany
PE-conjugated rabbit anti-active caspase-3.	BD Biosciences
Penicillin/Streptomycin	Invitrogen, UK
Propidium iodide	BD Biosciences
Re-Blot^{TM} Plus Antibody Stripping Solution	Upstate, Temecula, USA
Recombinant human Flt-3 ligand	StemCell Technologies Inc., USA
Recombinant human IL-3	StemCell Technologies Inc., USA
Recombinant human IL-6	StemCell Technologies Inc., USA
Recombinant human Stem Cell Factor	StemCell Technologies Inc., USA
Recombinant murine IL-3	Peprotech, NJ, USA
RPMI-1640 media	Sigma-Aldrich, UK
10xTG buffer Tris (25mM pH 8.3)/Glycine (192mM)	Bio-Rad Laboratories Ltd., UK
10xTGS buffer Tris (100mM pH8.3)/Glycine (100mM)/SDS (0.1%)	Bio-Rad Laboratories Ltd., UK

Tris-HCl	Sigma-Aldrich, UK
Trisodium citrate	Sigma-Aldrich, UK
Trypan blue	Sigma-Aldrich, UK
Tween®-20 (polyethylene glycol sorbitan monolaurate)	Sigma
Z-ARR-AMC	Calbiochem
Z-LLE-AMC	Calbiochem
Z-Succ-LLVY-AMC	Calbiochem

2.1.2 Equipment

Equipment	Use	Company
Branson 200 Ultrasonic cleaner	Sonication of proteasome activity lysates	Kell-Strom, Wethersfield, USA
Cimarec® hot plate	Adhesion of MeltiLex® and FIltermat A prior to scintillation counting	Barnstead International, Thermo Fisher Scientific, Iowa USA
Criterion® Blotter Filter paper	Western blot	Bio-Rad Laboratories Ltd., UK
Epson Perfection 4490 Photo Scanner	Western blot	Epson UK Ltd.
FACSAria	Cell sorting	BD Biosciences, San Jose, CA
FACSCaliber	Flow cytometry	
Gilson Pipetman Single channel Pipettes	Pipetting	Gilson, Inc., Middleton, USA
Haemocytometer	Cell counting	Hawksey, UK
Kodak X-OMAT 1000	Development of photographic film	Carestream Health Inc., Rochester, NY, USA
MicroBeta FilterMate-96 Harvester	Cell harvesting prior to analysis with scintillation counter	PerkinElmer Life and Analytical Sciences, Milano, Italy
MicroBeta Trilux beta-scintillation counter	Cell line proliferation	
Mini-PROTEAN® 3 cell	SDS-PAGE	Bio-Rad Laboratories Ltd., UK
Multiscan EX photometer	Protein concentration estimation	Thermo Fisher Scientific
Nitrocellulose membrane	Western blot	Bio-Rad Laboratories Ltd., UK
PowerPac300	Electrophoresis and Semi-dry transfer in Western blot	Bio-Rad Laboratories Ltd., UK
Spectramax M5	Proteasome Activity Assay	Molecular Devices
Thermoshaker	95C incubation in Western blot	Schutron, Reutlingen, Germany
Trans-Blot® SD Cell	Semi-dry transfer in Western blot	Bio-Rad Laboratories Ltd., UK

2.1.3 Antibodies for Western blotting and Flow Cytometry

Antibody	Use	Company
Anti poly (ADP-ribose) polymerase (PARP), (rabbit)	Western blot	Cell Signaling Technology, Inc. Danvers, USA
Anti active caspase-3	Flow cytometry	BD Biosciences, San Jose, CA
Anti rabbit IgG, HRP-linked	Western blot	Cell Signaling Technology, Inc. Danvers, USA
Anti mouse IgG, HRP-linked	Western blot	Cell Signaling Technology, Inc. Danvers, USA
Anti ubiquitin (P4D1) (mouse)	Western blot	Cell Signaling Technology, Inc. Danvers, USA
Anti phosphorylated Crkl (rabbit)	Western blot	Cell Signaling Technology, Inc. Danvers, USA
Anti $p27^{kip1}$ (rabbit)	Western blot	Cell Signaling Technology, Inc. Danvers, USA
Anti pan-actin (rabbit)	Western blot	Cell Signaling Technology, Inc. Danvers, USA
Anti CD34-APC	Flow cytometry	BD Biosciences, San Jose, CA
Anti CD38-FITC	Flow cytometry	BD Biosciences, San Jose, CA
Annexin V-FITC	Flow cytometry	BD Biosciences, San Jose, CA

2.2 Drugs

The drugs were stored as aliquots as follows: dasatinib as 10mg/mL (2.05mM - based on molecular weight 488.01) in dimethyl sulphoxide (DMSO) at -20˚C; imatinib mesylate as 59mg/mL (100mM based on molecular weight 589.7) in sterile distilled water at 4˚C; MG132 as 48mg/mL (100mM based on molecular weight 475.6) in sterile D-PBS at -20˚C; and bortezomib as 1mg/mL (2.6mM based on molecular weight 384.24) in sterile 0.9%NaCl at -20˚C.

2.3 Cell lines and patient samples

2.3.1 Cell lines

Three cell lines were used. K562 cells are a BCR-ABL+ immortilised human cell line derived from a patient with BC CML (182, 183). HL60 are a human promyelocytic leukaemia cell line (BCR-ABL-). Ba/F3 cells are a mouse pro-B cell line. Wild-type (WT) Ba/F3 are BCR-ABL- and dependent on IL-3 for growth. Ba/F3 cells transfected with BCR-ABL (BCR-ABL+ Ba/F3) grow independently of IL-3. Used here were Ba/F3 transfected with p210 (unmutated, Ba/F3-p210) or with mutated BCR-ABL (BaF/3-T315I, Ba/F3-H396P and BaF3-M351T).

All cells were cultured in suspension (humidified incubator at 37˚C and 5%CO_2) in RPMI-1640 media supplemented as shown (RPMI-1640 cell culture media **2.8.1**). WT-Ba/F3 required addition of IL-3 at 10ng/mL. All cells were counted every 2-3 days and resuspended in fresh media at a concentration of approximately $2x10^5$cells/mL.

2.3.2 Patient samples

Patient samples were leukapheresis products taken at time of diagnosis with CP CML, with informed consent and approval of the NHS Greater Glasgow Institutional Review Board. The CD34+ population was enriched using CliniMACS (Miltenyi Biotech, Auburn, CA) according to standard protocols, prior to storage as aliquots at -150ºC. For particular experiments CML CD34+ samples were stained with CD34-APC and CD38-FITC and sorted using a FACSAria to obtain the CD34+38- population, which represent primitive HSC.

Prior to use, patient samples were rehydrated in 10mL DAMP solution (**2.8.2** incubated at 37ºC prior to use) added drop-wise to the cell solution. The solution

was washed in DAMP solution three times (1000rpm for 10 minutes). Following the third wash the pellet was suspended in 10mL of serum free medium (SFM **2.8.3**) with a 5 growth factor cocktail (+5GF **2.8.4**) in a 25mL tissue culture flask. SFM+5GF was used for all CML and non-CML samples except where stated SFM-5GF. The cells were maintained overnight in a humidified incubator at 37ºC and 5% CO_2. The cells were counted and assessed for viability by trypan blue exclusion prior to use.

2.4 Viability and apoptosis assays

2.4.1 Assessment of viable cell counts

Cells were counted by vital dye exclusion. An equal volume of a 0.8mM Trypan blue solution was added to an aliquot of the sample under investigation. The cell count was then performed by light-microscopy using a haemocytometer under x40 magnification. The viable cell count was the number of cells which had maintained membrane integrity with exclusion of dye. All counts were performed as a minimum in duplicate.

2.4.2 Apoptosis assays using flow cytometry

Cells were assessed for the presence of early and late apoptosis using annexin V-FITC and 7-amino-actinomycin D (7-AAD). One of the early changes of apoptosis is the translocation of phosphatidyl serine from the inner to outer cell membrane leaflet. As a consequence of this translocation phosphatidyl serine is then available for binding by Annexin-V. Cells will continue to bind Annexin-V even once membrane integrity is breached and the cell has died. The vital dye 7-AAD will only bind cells where the membrane integrity is lost (as with Trypan blue and propidium iodide, PIo). 7-AAD was used in conjunction with Annexin-V to distinguish cells in early and late apoptosis (Annexin-V+ 7-AAD- versus Annexin-V+ 7-AAD+) (**Figure 2.1**).

Cells were cultured in appropriate media and exposed to drug prior to analysis at the stated times. For the drug wash-out experiments, cells were cultured in drug-containing media which was replaced with drug-free media (two washes in D-PBS with a 5 minute 1200rpm spin) at stated times with all aliquots analysed at 72h. For the apoptosis assay, samples were spun (1200rpm for 5 minutes) then resuspended in 100µL binding buffer (10mM Hepes/NaOH (pH7.4), 140mM NaCl,

2.5mM $CaCl_2$) and incubated in the dark, at room temperature, with the fluorescent-labelled antibody for 15 minutes (5µL annexin-V and 10µL Via-Probe solution/1x10^5cells). 400µL of binding buffer was added to each sample and then analysed immediately. The use of non-viable, unlabelled and single-labelled controls provided appropriate compensation between channels prior to analysis of the experimental arms. Annexin-V was labelled with FITC and so analysed in FL1, 7-AAD was detected in FL3. The viable cell count was derived from the cell count by trypan blue exclusion and light microscopy. It was assumed that this count represented the total 7-AAD negative population (by flow cytometry). The ratio of cells staining both negative for annexin-V and 7-AAD compared to all 7-AAD negative cells could then be applied to the trypan blue cell count (assumed equal to all 7-AAD negative cells) to get a more accurate "viable cell count by flow cytometry" which would then take account of cells in early apoptosis. The percentage of cells in early and late apoptosis was used to give a total percentage apoptosis.

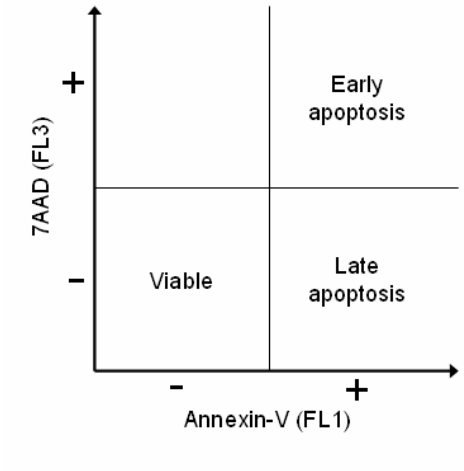

Figure 2.1 Determination of cells undergoing apoptosis by flow cytometry with Annexin-V and 7-AAD staining

2.4.3 Intracellular caspase staining

A key regulator activated during the early stages of apoptosis is caspase-3. The presence of this enzyme is an accepted marker for cells undergoing apoptosis. The mAb recognises the active form in human and mouse cells. Here we used a monoclonal rabbit antibody (mAb) conjugated to PE which recognises the active form of caspase-3 in mouse and human cells.

This technique required flow cytometry to assess binding of the labelled antibody to intracellular antigens and was performed using the FIX and PERM kit. Cells

were spun (1200rpm for 5 mins) and the pellet resuspended in 100µL of Reagant A (a formaldehyde-containing commercial solution for cell fixation) and then incubated at room temperature for 15 mins. The cells were then washed in D-PBS as before and the pellet resuspended in 100µL of Reagant B (commercial cell permeabilisation solution). 10µL of PE-labelled anti-caspase-3 antibody was added and the samples incubated in the dark for 60 mins. Prior to flow cytometry the samples were washed twice in D-PBS (each spin 1200rpm for 5 mins). For each experiment an unstained and isotype control was used to set analysis parameters.

2.4.4 Thymidine proliferation assay

This assay was to assess proliferation of cell lines in the presence of drug. It was assumed that incorporation of ^{3}H-thymidine was proportional to the rate of proliferation at the time of analysis. Cells seeded at $2.5x10^{5}$/mL in a 96-well plate and exposed to relevant concentrations of drug. On the day of analysis a 0.2µCi/mL solution of ^{3}H-Thymidine in RPMI-1640 cell culture media was added to each sample. Following 4h incubation cells were harvested onto a printed glassfibre filtermat (Filtermat A), which was then sealed with a melt-on scintillator sheet (MeltiLex® A) at 95℃ and placed in a sample bag prior to analysis with a beta-scintillation counter. Each experiment was performed as a minimum in triplicate.

2.4.5 CFSE staining

2.4.5.1 Background

This technique has an established role in tracking cells as they undergo division (184) and was applied to total CD34+ patient samples to assess the effects of drug treatment. CFSE crosses freely into cells where endogenous esterases remove acetate groups rendering CFSE membrane-impermeable and highly fluorescent. In addition, the succinimidyl group forms stable covalent bonds with intracellular proteins. In effect the molecule is “trapped” within the cell and divided equally between daughter cells with each cell division. This stepwise reduction in cell fluorescence was visualised by flow cytometry (FL1 channel) enabling estimation of the number of divisions a sample of cells has undergone. The protocol described here was adhered to.

2.4.5.2 Day 0

CD34+ CML patient samples were taken from liquid nitrogen storage and rehydrated by drop-wise addition over 10mins of 10mL of an ice-cold solution of 2% FCS in D-PBS (FCS/PBS). The cells were then washed twice (1000rpm for 10mins) in 10mL 2% FCS/PBS, resuspended in 5mL of 2% FCS/PBS, transferred to a sterile 50mL tube and counted by dye exclusion (as described above). 2 aliquots of $0.5x10^6$cells were removed and made up to 1mL (for day 1 analysis) and 2mL (day 3 analysis) with SFM+5GF (CFSE-). The remaining cell solution was made up to 5mL with 2% FCS/PBS. CFSE (stored as aliquots of 5mM in DMSO at -20ºC) was added to this sample to give a final concentration of 1µM. Once CFSE was added the sample (CFSE+) underwent 10mins timed incubation in a water bath at 37ºC. 50mL of ice-cold 20% FCS/PBS (quenching solution) was added and the cells spun and then washed in 2% FCS/PBS (both 1000rpm for 10mins). The cells were then resuspended in 10mL of SFM+5GF in a 25mL sterile flask. CFSE+ and CFSE- samples were incubated overnight at 37℃ and 5% CO_2.

2.4.5.3 Day 1

Sufficient SFM+5GF was added to the CFSE+ cells to give a final concentration $2.5x10^5$cells/mL. 500µL samples were added to a 48-well plate and exposed to the relevant experimental conditions. For each experiment 2 samples were treated with 100ng/mL demecolcine (Colcemid®, stored as a 25ng/mL stock solution at 4ºC). Demecolcine arrests the cell cycle in metaphase by depolymerising microtubles and was used to determine the position of the undivided population by flow cytometry at day 3. In addition, 3 unstained and 3 CFSE-stained controls were used. All experimental samples were incubated for 72h at 37℃ and 5% CO_2.

2.4.5.4 Day 3

Each sample was well mixed and a cell count performed. The samples were transferred to a FACS tube with an additional rinse of each well (2% FCS/PBS) to minimise wastage. The cells were spun (1200rpm for 5mins) and the supernatant discarded. To determine CD34+ cells, 5µL CD34-PE antibody was added to each pellet (excluding controls) the samples mixed and left at room-temperature for 15mins. The samples were then washed twice with 2% FCS/PBS (1200rpm for 5mins). To determine viable cells, 2µL propidium iodide (PIo) in 2mL 2% FCS/PBS was added to each sample (excluding controls). Viable cell membranes are impermeable to PIo however this dye will bind the DNA of on viable cells with

disrupted membranes and once bound displays enhanced fluorescence. The were cells then spun (1200rpm for 5mins), the supernatant discarded to remove unbound PIo and the pellet resuspended in a small volume of FACSFlow^{TM} (a commercial PBS/azide solution) and then analysed by flow cytometry. The controls (CFSE+ with PIo, CFSE+ with PIo and CD34-PE, CFSE- with PIo and CFSE- with PIo and CD34-PE) enabled appropriate detection of the live cells on forward (FSC) and side-scatter (SSC) with adequate compensation between the channels FL1 (detecting CFSE), FL2 (PE) and FL3 (PIo).

2.4.5.5 Calculation of cell numbers

The number of viable cells was estimated by trypan blue cell count at days 0, 1 and 3. At day 3 a gate was created on the forward and side-scatter plots to include cells and exclude cell debris. The focus of analysis was then limited further by gating only on viable (PIo-) and CD34+ cells. From this population, undivided cells were assumed to be those with CFSE fluorescence of an intensity comparable to the Colcemid® control (PIo-CD34+CFSE^{MAX}). A region was set around this peak to include all cells with comparable CFSE staining. Subsequent division peaks were set by calculating regions where the mean CFSE fluorescence intensity was approximate half that of the preceding region. For assessment of the CD34+ percentage for each division peak only PIo- cells were included. For assessment of the percentage of cells in each division viable (PIo exclusion) cells both CD34+ and CD34- were included. Calculation of the cell recovery was a method for determining how many of the seeding population of cells (presumed to be undivided) could be accounted for at day 3 – a formula was applied (**Equation 2.1**) where *R*=recovery number n_0= number of undivided cells, n_1=number of cells in division 1, n_2=number of cells in division 2, n_3=number of cells in division 3 and so on.

$$R = n_0 + \frac{n_1}{2} + \frac{n_2}{3} + \frac{n_3}{4} \ldots\ldots \qquad \textbf{Equation 2.1}$$

The recovery number was then compared (as a percentage) to the known input number to calculate a *recovery percentage*. The percentages could then be compared to the no drug control arm. The day 3 recovery of viable undivided cells (CD34+PIo-CFSE^{MAX}) was also compared between the experimental arms.

2.5 Western Blotting

2.5.1 Estimation of protein concentration

The BSA™ Protein Assay Kit was used. This method exploited the colour change associated with the reduction of copper ions by protein in alkaline conditions. The colour change was detected as absorption at 550nm by photometer. Standards of known protein concentration were made from dilutions (5µg/mL to 1500µg/mL) of bovine serum albumin in water. These were loaded as duplicate 25µL samples in a 96-well plate. Aliquots of the sample under analysis were added, in duplicate, as a 1:5 dilution in water (5µL sample and 20µL water). To each well was added 200µL of a mixture of the alkaline BCA™ Solution A (50 parts) and the copper-containing BCA™ Solution B (1 part). The plate was incubated for 30mins at 37℃ and loaded on a photometer with light absorbance measured using a 550nm filter. The software (Ascent v2.6) plotted a derived linear-plot of protein-concentration to absorbance and provided estimation of the protein concentration of the diluted sample.

2.5.2.1 Preparation of sample lysates

Following 2 washes in ice-cold D-PBS (1200rpm for 5 mins), samples were re-suspended in ice-cold 150µL lysis buffer (50mM Tris pH7.5, 150mM NaCl, 5mM EDTA, 1% Nonidet® P-40 substitute **2.8.5**) containing a protease inhibitor cocktail (1 “Complete” Protease Inhibitor Cocktail tablet per 10mL lysis buffer). Following 10 minutes incubation on ice samples were spun (14000rpm for 10 minutes at 4˚C) and the supernatant removed for analysis, including estimation of protein concentration as described above. Samples were stored at -80℃.

2.5.2.2 SDS-PAGE electrophoresis

10mcg of the protein lysate was made up to 10µL with H_2O and mixed with an equal volume of loading buffer (**2.8.6**). The samples were incubated at 95℃ for 5 minutes, returned to ice then immediately loaded onto a 4-15% sodium dodecyl sulphate gradient gel immersed in running buffer (**2.8.7**). The samples were separated at 120V for 90mins using the Mini-PROTEAN® 3 cell system. For each gel a molecular weight Rainbow® marker sample was run.

2.5.2.3 Electrophoretic transfer

A semi-dry transfer method was followed, using a Bio-Rad Trans-blot® SD cell. The gel "sandwich" was made as shown in **Figure 2.2** and run at 10V for 30mins:

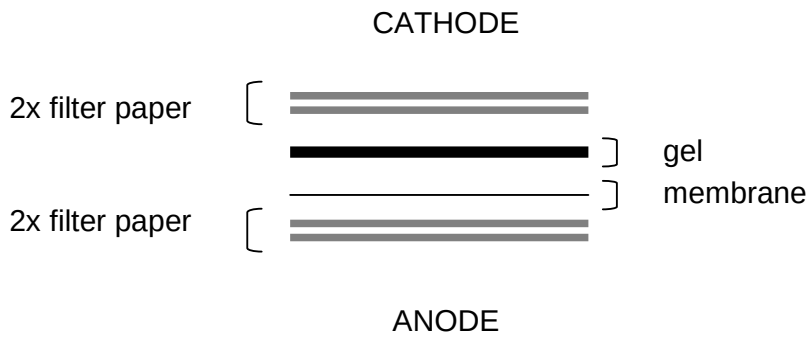

Figure 2.2 Gel "sandwich" used for electrophoretic transfer

The nitrocellulose membrane and filter papers were soaked in transfer buffer (**2.8.8**) prior to use. To prevent non-specific protein interactions with nitrocellulose, the membrane was incubated for 1h at room temperature with 5% milk in TBS-T (**2.8.9/10**) buffer (blocking solution). This and all subsequent washes and antibody incubations were performed with gentle agitation on a mixer platform

2.5.2.4 Primary and secondary antibody incubation

Following exposure to the blocking solution, which was discarded, the membrane was incubated overnight (4ºC) with the primary antibody of interest (1:1000 dilution in 10mL TBS-T with 1% milk). The following morning, the membrane was washed 4 times with TBS-T. Each wash was 15mins on a mixer platform with sufficient buffer to completely cover the membrane. Membranes were then labelled with the appropriate horseradish peroxidase-labelled secondary antibody (1:3000 dilution in TBS-T with 1% milk) and incubated at room temperature for 1h. After a further series of 4 washes of 15mins in TBS-T and a short incubation (2-5mins) with an ECL+^{TM} chemiluminescence solution, the images were developed onto photographic film. The membranes were then stripped of bound antibody using Re-Blot^{TM} solution (15mins incubation at room temperature). Prior to probing with different primary antibodies the membrane was twice washed for 5mins with 5% milk in TBS-T.

2.6 Proteasome extraction and activity assay

This followed an established method for preparing cell lysates with preserved proteasome activity. The lysates were then incubated with individual fluorogenic substrates for each of the 3 enzymic activities of the proteasome. The release of the fluorescent substrate was detected by the fluorimeter and enzymic activity compared between different experimental conditions.

Cells ($1x10^7$) were washed in D-PBS and resuspended in fresh 1mL ATP/DTT lysis buffer. After 10 minutes incubation on ice, the cells were sonicated and then spun for 10 minutes at 13000rpm. The supernatant was collected and protein concentration calculated (as described in **2.5.1**). Samples were either analysed immediately or mixed with 20% glycerol and stored at -80ºC. The fluorogenic substrates N-Succ-LLVY-AMC, Z-ARR-AMC and Z-LLE-AMC (used to measure CT-L, T-L and PGH-L activities respectively) were stored protected from light, at -20ºC as 10mM stock solutions in DMSO. The assay was carried out in ATP/DTT lysis buffer (**2.8.11**) containing 50µg of the protein extract, 5mM EDTA and 50µM fluorogenic substrate in an opaque-walled 96-well plate. Analysis by a dual-monochromator, multi-detection microplate reader immediately followed addition of the fluorescent substrate. Activity was represented by the release of fluorescent substrate at excitation and emission wavelengths of 380nm and 460nm respectively (manufacturer's recommendations). Readings were taken every 5mins for 35mins and expressed as arbitrary fluorescence units (AFU). The equation of the linear rise in AFU per unit time was used to determine the rate of fluorescence release (AFU/min).

2.7 Software and Statistical Analysis

2.7.1 Software used for data analysis

GraphPad Prism® (version 4, California USA) was used to draw graphs, charts, calculate descriptive statistics, predict dose-response curves and perform statistical analysis. The concentration of drug shown to achieve a 50% reduction in viable cell count was termed LD_{50}. This figure was estimated from the dose response curves predicted using Prism® software. Flow cytometry data was analysed by CellQuest Pro software (BD Bioscience). Fluorimetry data was analysed by both SpectraMax® Pro 5 (derivation of numerical data) and Microsoft Excel® software (analysis of numerical data).

2.7.2 Analysis of data from synergism experiments

To assess synergism, dose-response data generated from drugs used individually and in combination were analysed with CalcuSyn® (Version 2.0 Biosoft, Cambridge, UK). The underlying mathematical model is described in detail by Chou (185) and is outlined here. For this analysis a number of calculations were performed by the software (**Equations 2.2-2.4**). Prior to input of data, the viable cell count (as a percentage of untreated control) was converted to an effect (**Equation 2.2**) where f_a is the fraction affected and VCC% the viable cell count expressed as a percentage of untreated cells.

$$f_a = 1 - \frac{VCC\%}{100} \qquad \textbf{Equation 2.2}$$

The *median-effect equation* (**equation 2.3**) forms the basis of the Calcusyn® software analysis, where D was the dose of a drug, f_a the fraction affected by D (percentage inhibition/100), f_u the fraction unaffected ($1\text{-}f_a$) and D_m the median effect dose (=LD_{50} as used here).

$$\frac{f_a}{f_u} = \left(\frac{D}{D_m}\right)^m \qquad \textbf{Equation 2.3}$$

The logarithm of **equation 2.3** formed the *median-effect plot* (**equation 2.4**) which converted the dose-effect curve to a straight line where m was the slope and D_m the anti-log of the x-intercept.

$$\log\frac{f_a}{f_u} = m\log(D) - m\log(D_m) \qquad \textbf{Equation 2.4}$$

The data was then assessed for conformity by generation of an r-value (where r>0.95 was accepted). For the combination of two drugs a fixed ratio of concentrations was applied and this is illustrated in **Figure 2.4**.

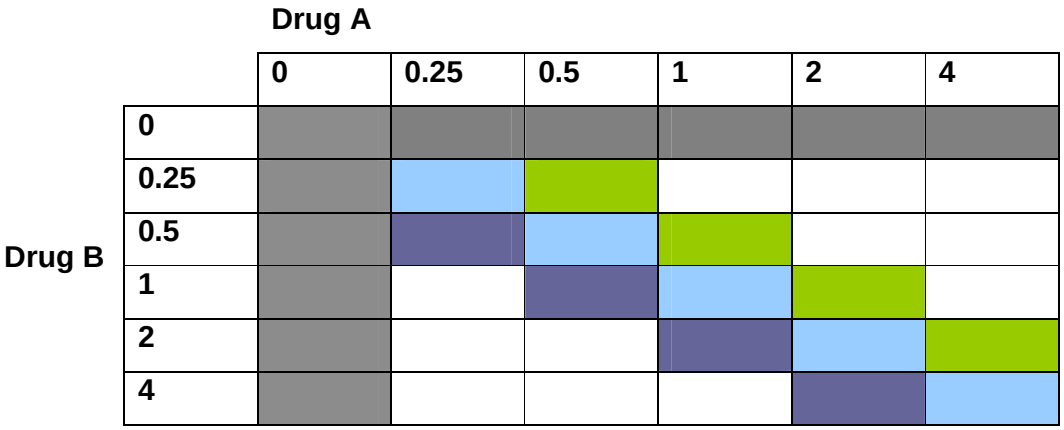

Figure 2.3 Checker-square analysis of drug combinations. Drugs were analysed for effect individually ( ) and then in combination at fixed ratios (, ,). It is this data that was analysed using Calcusyn®. The numbers shown indicate multiples of the drug concentration required to achieve a 50% effect.

This data was then analysed within the software by **equation 2.5** where $(D_x)_1$ was the concentration of Drug 1 causing x% inhibition, $(D_x)_2$ the concentration of Drug 2 with x% inhibition and $(D)_1+(D)_2$ the concentration of Drug A and B with the same (x) degree of inhibition.

$$CI = \frac{(D)_1}{(D_X)_1} + \frac{(D)_2}{(D_X)_2} \qquad \textbf{Equation 2.5}$$

Therefore a ratio is derived (Combination Index, CI) where >1 indicates antagonism, <1 synergism and 1 an additive effect. The degree of synergism corresponds to the CI as shown in **Table 2.1**.

Table 2.1 Assessment of synergism by combination index

CI range	description	Graded symbols
<0.1	Very strong synergism	+++++
0.-0.3	Strong synergism	++++
0.3-0.7	synergism	+++
0.7-0.85	Moderate synergism	++
0.85-0.9	Slight synergism	+
0.9-1.1	Nearly additive	±
1.1-1.2	Slight antagonism	-
1.2-1.45	Moderate antagonism	--
1.45-3.3	antagonism	---
3.3-10	Strong antagonism	----
>10	Very strong antagonism	-----

Table adapted from Chou TC (185)

Data are also displayed as a conventional isobologram (**Figure 2.4**) where selected linear additive effects are plotted on a graph of (Drug A, Drug B). Experimental data was then shown and compared to these linear plots as synergistic (below the line), additive (on the line) or antagonistic (above the line).

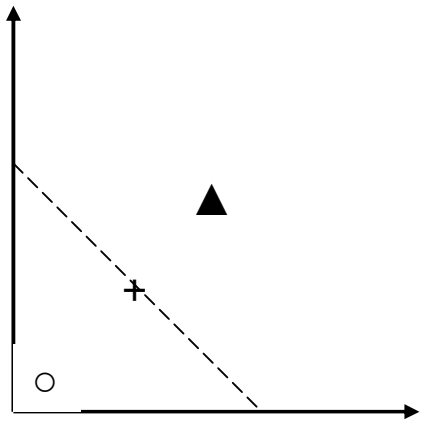

Figure 2.4 Illustration of isobologram. The broken line indicates additive effect (for example LD_{50}) when considering two drugs (Drug A, Drug B)**.** Experimental data may reveal ○ synergistic, x additive or ▲ antagonistic effects in combination.

2.8 Culture media and other stock solutions

2.8.1 RPMI-1640 Cell Culture Medium for culture of cell lines

	Final concentration
Penicillin/Streptomycin	$1x10^5$units/L and 100mg/L
Glutamine	2mM
Foetal calf serum	10%
Made up in 440mL RPMI 1640	

2.8.2 DAMP solution for rehydration of stem cells

	Final Concentration
DNase I	10000units/L
Magnesium Chloride	2.5mM
Trisodium citrate	16mM
Human Serum Albumin 20%	1%
Made up in 418.75mL D-PBS	

2.8.3 Serum Free Medium for culture of stem cells

	Final concentration
Bovine Serum Albumin/Insulin/ Transferrin (BIT9500)	
L-Glutamine	2mM
Penicillin/Streptomycin	$1x10^5$units/L and 100mg/L
2-Mercaptoethanol	0.1mM
Low density lipoprotein	0.8µg/mL
Made up in 97.25mL Isove's modified Dulbecco's media (IMDM)	

2.8.4 5-Growth Factor Cocktail used with SFM for stem cell culture

	Final concentration
IL-3	20ng/mL
IL-6	20ng/mL
Flt3	100ng/mL
Stem cell factor	100ng/mL
Granulocyte-Colony Stimulating Factor	20ng/mL

2.8.5 Protein lysis buffer for Western blot

	Final concentration*
Tris pH7.5	50mM
Sodium chloride	150mM
EDTA	5mM
Nonidet® P-40 substitute	1%

*Made in ddH_20

2.8.6 Loading buffer for Western blot

	Volume per mL
Laemmli sample buffer	950µL
B-mercaptoethanol	50µL

2.8.7 Running buffer for Western blot

	Volume per L
10xTGS buffer	100mL
ddH_20	900mL

2.8.8 Transfer buffer for Western blot

	Volume per L
10xTG buffer	100mL
Methanol	200mL
ddH_20	700mL

2.8.9 10xTBS buffer for Western blot

	Final concentration*
Tris-HCl, pH 8	0.1M
NaCl	1.5M

*Made in ddH_20

2.8.10 TBS-T Washing buffer for Western blot

	Volume per L
10xTBS	100mL
ddH_20	900mL
Tween®-20	1mL

2.8.11 ATP/DTT lysis buffer for proteasome activity assay

	Final Concentration*
Tris-HCl, pH7.8	10mM
DTT†	0.5mM
ATP†	5mM
$MgCl_2$	5mM

*Made in ddH_20 †Aliquots of DTT and ATP were stored at 4ºC and -20ºC respectively and added immediately prior to use.

3. RESULTS

Aim 1 Effect of PI on viability and proliferation in BCR-ABL+ cell lines including those resistant to TKI.

The initial investigation of the effects of bortezomib exposure on BCR-ABL+ cells focussed on the proliferation and viability of cell line models for CML. Those used were K562 and BCR-ABL+Ba/F3 cells. K562 cells are an immortilised human cell line derived from a patient with CML BC and are an established model for monitoring drug effects (182). Ba/F3 cells are murine, IL-3 dependent haematopoietic cells which may be reliably transfected with BCR-ABL thus rendering their growth IL-3 independent. BCR-ABL+ Ba/F3 cells are an established model for monitoring the effects of TKI (90). To achieve this aim it was also considered important to ensure that the effects of the drug were not influenced by the storage conditions used.

3.1. Bortezomib is antiproliferative and induces apoptosis in BCR-ABL+ cell lines

3.1.1 Cell counting and Flow cytometry

BCR-ABL+ cell lines (K562 and Ba/F3-p210) were maintained in RPMI-1640 cell culture media and exposed to concentrations of bortezomib (1 to 40nM) for set time periods (24, 48 and 72h). For these initial experiments, dose-response curves for drug effect were established in K562 by cell counting at 24, 48 and 72h with vital dye exclusion. The cells were cultured in cell culture media containing bortezomib added at the start of the experiment with no additional dosing or drug wash-out. It was seen that an increase in bortezomib concentration was associated with a decrease in viable cell count (**Figure 3.1**). Estimated LD_{50} for K562 were 6.4nM (24h) 5.6nM (48h) and 11.2nM (72h) (**Table 3.1**).

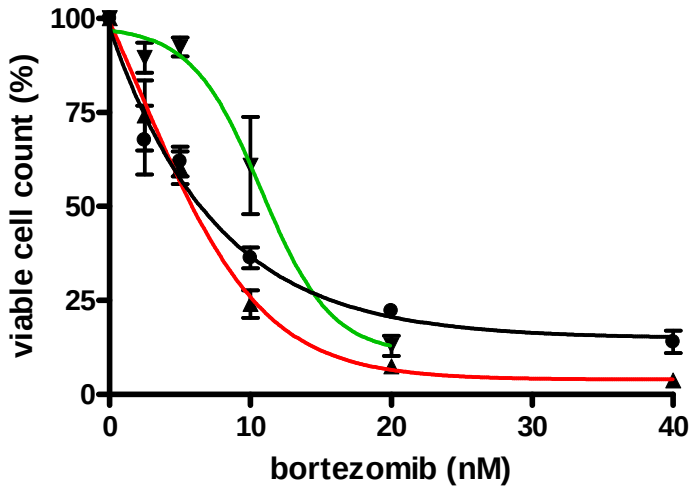

Figure 3.1. K562 cells were exposed to bortezomib for 24h (—●), 48h (—▲) and 72h (—▼) with the viable cell count expressed as a percentage of untreated cells. Points and error bars indicate mean±SEM and adjoining lines demonstrate dose-response curves of best fit.

K562 cells were then examined at 24, 48 and 72h of bortezomib exposure for early/late apoptosis by flow cytometry (as described in **2.4.2**). It was shown that with increasing concentration of bortezomib there was an increase in the percentage of cells staining positive for annexin-V alone (early apoptosis) and both annexin-V and 7-AAD (late apoptosis).

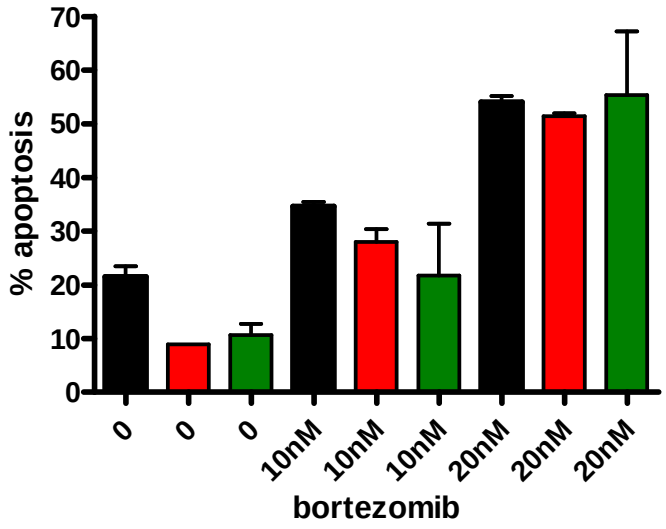

A

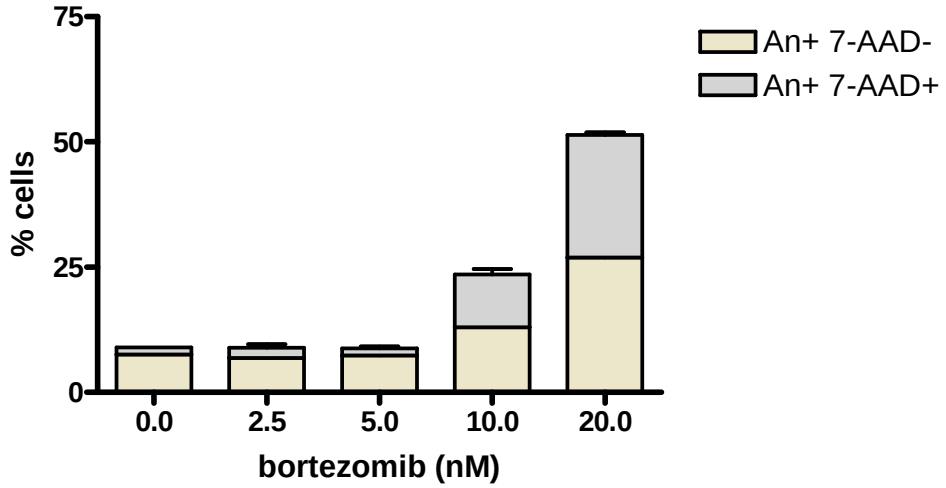

B

Figure 3.2. (A) K562 cells were exposed to bortezomib and then analysed by flow cytometry to determine the total % cells undergoing apoptosis. Results from 24h (■) 48h (■) and 72h (■) drug exposure are shown. (B) K562 cells exposed to bortezomib for 48h and analysed as in (A) then displayed to show the % cells in either early or late apoptosis. Error bars indicate mean±SEM. Annexin-V (An), detection/no detection of bound fluorophore by flow cytometry (+/-).

A combination of vital dye exclusion and flow cytometry (as described in **2.4.2**) was used to compare the effect of bortezomib on Ba/F3 p210 with Ba/F3 BCR-ABL mutants (Ba/F3-M351T Ba/F3-H396P and Ba/F3-T315I) (**Figure 3.3**). LD_{50} results were similar between the 4 BCR-ABL+ Ba/F3 transfectants (**Table 3.1**) though there was a trend for the mutant forms to be slightly less sensitive than Ba/F3-p210.

A

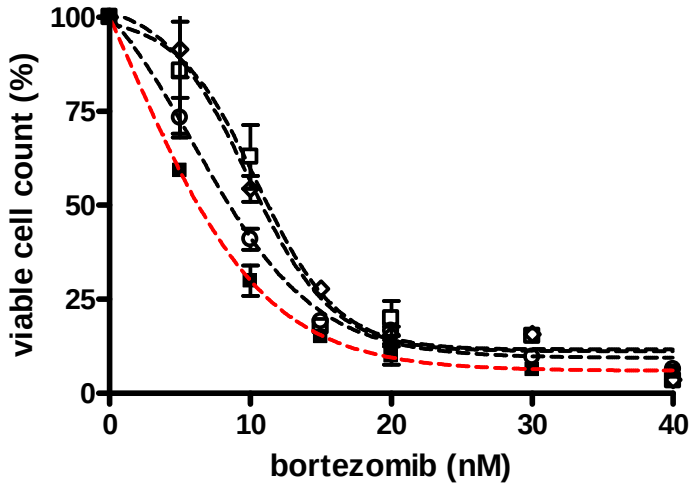

B

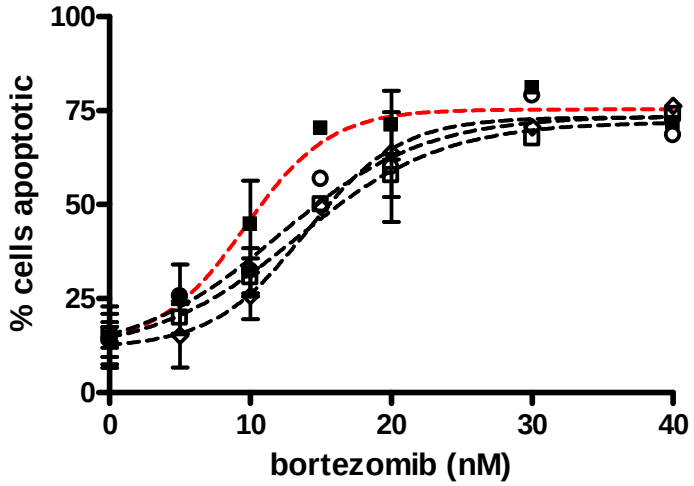

Figure 3.3. BCR-ABL+ Ba/F3 cells were exposed to bortezomib for 24h and then analysed by cell counting and flow cytometry to determine (A) the reduction in viable cell count (as a % of untreated cells) and (B) the increase in the % of cells in early and late apoptosis. Points and error bars in both (A) and (B) indicate mean±SEM and adjoining lines demonstrate dose-response curves of best fit. Ba/F3-p210 (--■--) BaF3-M351T (--□--) Ba/F3-H396P (--◊--) Ba/F3-T315I (--○--).

Table 3.1. Estimation of bortezomib LD50 by cell counting and flow cytometry in BCR-ABL+ cell lines

Cell type	Exposure time	LD_{50} (nM)	Figure
K562	24h	6.4	3.1
	48h	5.6	
	72h	11.2	
Ba/F3-p210	All 24h	6.3	3.3(A)
Ba/F3-H396P		10.8	
Ba/F3-M351T		11.3	
Ba/F3-T315I		8.5	

3.1.2 Bortezomib stability

It is the recommendation of Janssen-Cilag International that bortezomib is administered to patients immediately following reconstitution in sterile 9mg/mL NaCl for injection (bortezomib Summary of Product Characteristics August 2008). Independent studies have shown the drug to be stable up to 42d after once reconstituted in this way and stored at 4-5℃ or room temperature (23℃) (186, 187). Here we used aliquots of reconstituted bortezomib stored initially at 4℃ for <24h and then as aliquots at -20ºC. Other researchers have reconstituted and stored bortezomib in a variety of ways. These include reconstitution and storage in DMSO (-20℃(1, 5, 9), -80℃ (188) or no temperature stated (123)), Me_2SO (no temperature stated), PBS (-20℃ (3) or no temperature stated) (159, 161) and 9mg/mL NaCl (-70℃ (88) or no temperature stated (8)). To ensure that the method of storage that we adopted did not influence the drug effect we assessed the ability of fresh and stored bortezomib to induce cell death in K562 cells (**Figure 3.4**). This experiment was performed only twice and so sufficient data to perform meaningful statistical analysis were not generated – however, it was considered that these data provided reassurance our storage method was appropriate and consistent with other workers in this field.

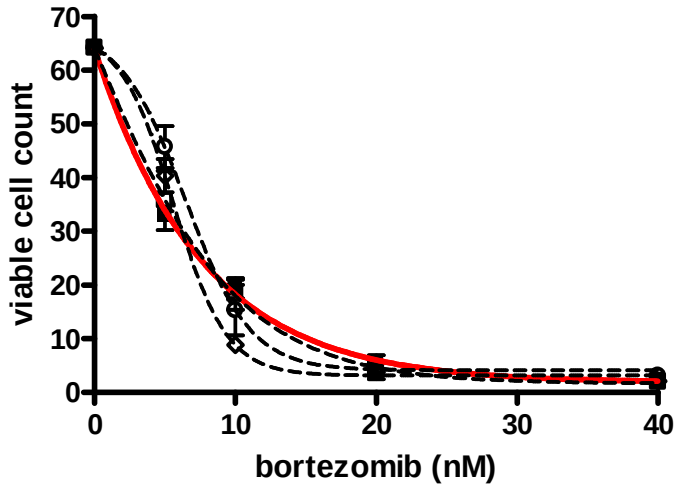

Figure 3.4. An investigation of the effects of storage and freeze-thawing of bortezomib in K562 cells. Viable cell count is x10^4/mL. Points and error bars indicate mean±SEM with adjoining line of best fit. Conditions compared were bortezomib used within 24h of reconstitution (-■-), 24h storage at -20℃ (-◊-), 2m storage at -20℃ (-○-) and 3m storage at 4℃ (-□-).

3.1.3 Bortezomib wash-out

Bortezomib is a reversible proteasome inhibitor. Data generated from *in vivo* exposure indicates that peak plasma levels may be acheived in the PB at 1h following administration with associated maximal proteasome inhibition (discussed in section **1.9.6**). The exposure time required to achieve irreversible cell death may therefore be short. To investigate this drug wash-out experiments were performed with K562 cells as described in **2.4.2**. Cells were exposed to drug containing medium for the stated times with the final analysis at 72h (**Figure 3.5**). The data show that in our *in vitro* system between 12 and 24h exposure is required to induce significant cell death, hence a minimum of 24h exposure was used in our experiments. The limited effect of short exposure times may reflect the reversible nature of proteasome inhibition with bortezomib. In addition, drug containing medium was incubated in cell culture conditions (37ºC with 5% CO_2) for up to 72h prior to treatment of K562 cells. This caused no apparent reduction in efficacy for inducing cell death (data not shown here). This was interpreted as an indication that viable drug may be present in the cell culture media for up to 72h. However, metabolism of bortezomib by exposed K562 cells is not assessed by this method.

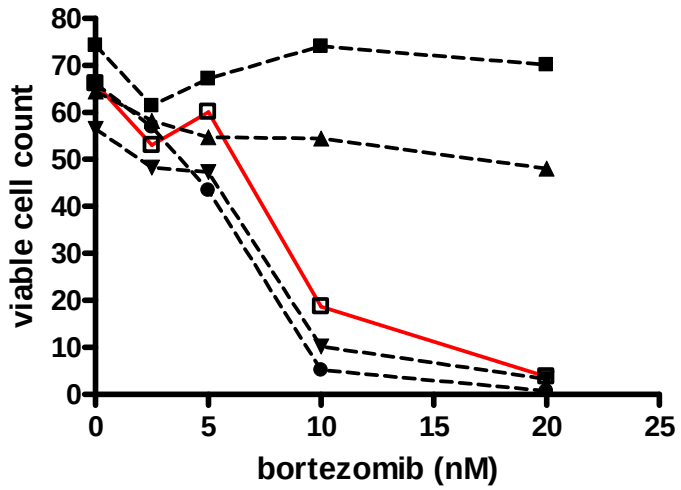

Figure 3.5. Effects of time limited exposure to bortezomib in K562 cells. All cells analysed by cell counting and flow cytometry at 72h after exposure to bortezomib containing media for set times from initiation of experiment. No wash out (-□-), wash out at 1h (-■-), 6h (-▲-), 24h (-▼-) and 48h (-●-) exposure. Viable cell count is $x10^4$cells/mL. Points indicate mean values for experiment with adjoining lines.

3.1.4 Detection of active Caspase-3

Active caspase-3 is a key regulator and a recognised marker of cells undergoing apoptosis. Cell viability experiments with annexin-V and 7-AAD staining provided an indication that bortezomib induced apoptosis in BCR-ABL+ cell lines. Demonstration of the presence of active caspase-3 was considered important to verify this by an alternative experimental technique. BCR-ABL+ Ba/F3 cells were treated with 20nM bortezomib for 24h, a viable cell count taken and then cells treated as described in **2.4.3** to determine the presence of active caspase-3 (**Figure 3.6**). For all BCR-ABL mutants a significant change in detectable active caspase-3 was shown when compared to the untreated control populations, though there was no statistically significant difference between the 4 transfectants in either viable cell count or % of cells with active caspase-3. These findings confirm that bortezomib induces apoptosis irrespective of BCR-ABL mutation status and is consistent with published work in other cancer cell lines (3, 9, 148).

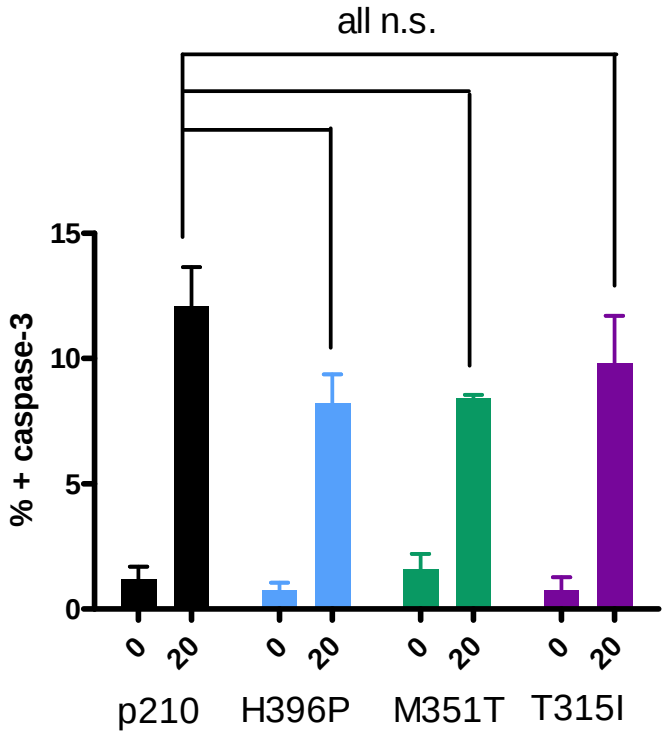

Figure 3.6. Percentage of BCR-ABL+ Ba/F3 cells with active caspases-3 detectable by flow cytometry. A comparison is made between untreated cells (0) and those exposed to 20nM bortezomib (20) for 24h. There was no significant difference (n.s.) between Ba/F3-p210 and the mutated BCR-ABL forms following drug exposure.

3.1.5 Thymidine incorporation

There is published data produced by various methods which show that bortezomib is antiproliferative in cancer cell lines (1, 6, 9). IM, dasatinib and nilotinib have a significant antiproliferative effect in BCR-ABL+ cells and this is likely to be relevant in their efficacy for treating CML a disease characterised by uncontrolled cell proliferation. A method by which incorporation of ^{3}H-thymidine is measured was utilised to establish whether bortezomib influenced cell proliferation. K562 and BCR-ABL+ Ba/F3 cells were cultured with defined concentrations of bortezomib. It was seen that drug exposure was associated with reduced incorporation of ^{3}H-thymidine, consistent with reduced proliferation when compared to the untreated cells. Using this method (**2.4.4**) and at 48h drug exposure the concentration required to inhibit proliferation by 50% in comparison to untreated cells (IC_{50}) was estimated at 8.4nM (K562) and 8.7nM (Ba/F3-M351T). As a consequence of technical problems with the cell harvester this assay became increasingly unreliable during the course of the project and so was used only in the preliminary experiments.

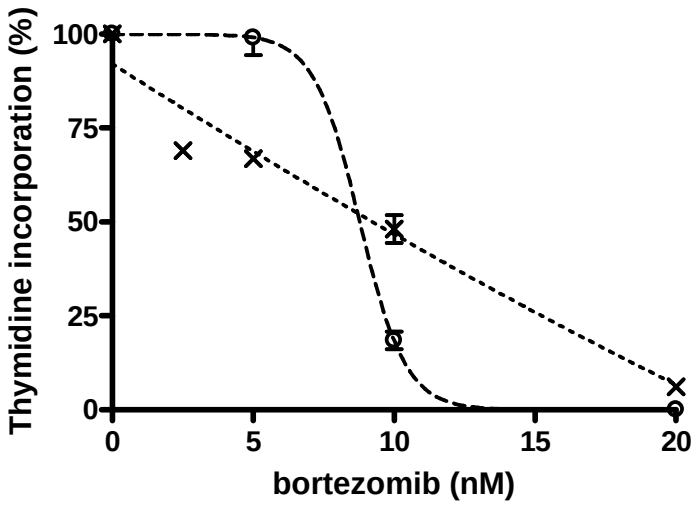

Figure 3.7. A reduction in proliferation with K562 cells (··X··) and Ba/F3–M351T (--○--) cells exposed to bortezomib for 48h as measured by incorporation of ^{3}H-thymidine. Points and error bars indicate mean±SEM with line of best fit.

Aim 2 Proteasome activity in BCR-ABL+ cell lines

It has been demonstrated that cancer cells have abnormally high levels of proteasome expression and activity (133). Furthermore, there is evidence from cell line work and samples from patients with CML that the presence of BCR-ABL is associated with increased proteasome activity, as measured using a fluorescent substrate based assay (2). We aimed to demonstrate detectable proteasome activity in the BCR-ABL+ cell lines which are susceptible to the apoptotic and antiproliferative effects of bortezomib and to assess the impact on this activity of exposure to PI.

3.2 Proteasome activity is detectable in BCR-ABL+ cell lines and in Ba/F3 cells, is variable between different BCR-ABL mutations and is inhibited by bortezomib.

3.2.1 Baseline proteasome activity in Ba/F3 mutants

A fluorescence based assay (**2.6**) was used to measure the proteasome activity of Ba/F3 cells. A linear rise in AFU was seen, consistent with AMC release representing proteasome subunit enzyme activity (**Figure 3.8** and **3.9**). Interestingly, the basal proteasome activity appeared to vary between the Ba/F3 BCR-ABL+ mutants when considering PG and CT-L activity. Statistical significance was achieved in PG activity ($p<0.01$ (H396P), $p=0.013$ (M351T)) and CT-L activity ($p=0.047$ (T315I), $p=0.045$ (H396P), $p=0.038$ (M351T)).

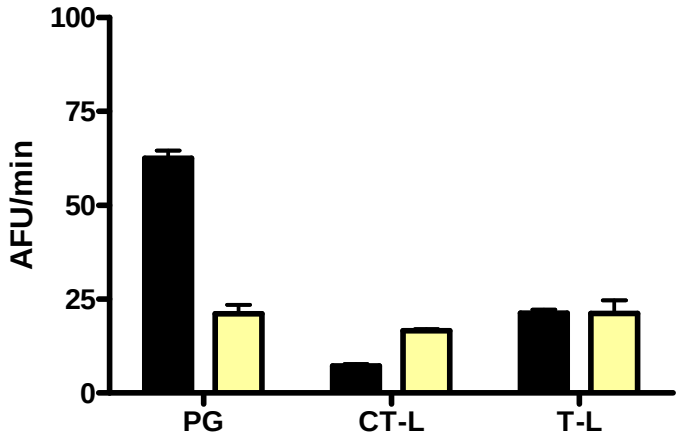

Figure 3.8 Detectable proteasome subunit activity in Ba/F3-p210 (■) and K562 (■) cells expressed in AFU/min (mean±SEM). PG (post-glutamyl hydrolyzing), CT-L (chymotrypsin-like) and T-L (trypsin-like) activities are represented.

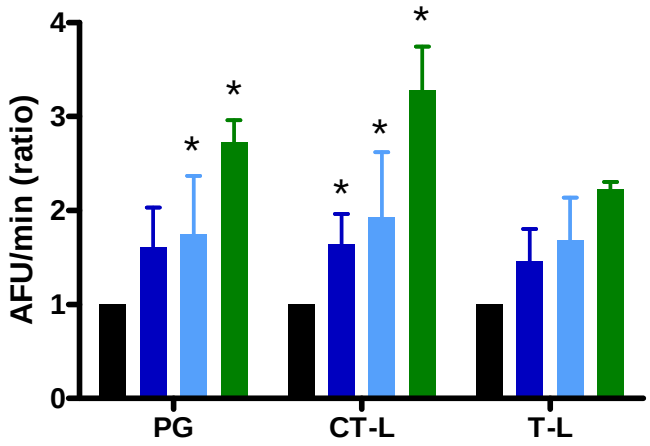

Figure 3.9 Proteasome activity in Ba/F3-T315I (■), Ba/F3-H396P (■) and Ba/F3-M351T (■) expressed in AFU/min (mean±SEM) as a ratio compared to Ba/F3-p210. PG (post-glutamyl hydrolyzing), CT-L (chymotrypsin-like) and T-L (trypsin-like) activities are represented. * indicates statistical significance.

3.2.2 Effect of bortezomib treatment on proteasome subunit activity

Ba/F3 cells were cultured in the presence of 20nM bortezomib for 24h and proteasome subunit activity assessed (as described **3.2.1**). This concentration was chosen to induce significant apoptosis and impair proliferation. The effect of bortezomib of the subunit activities in the different BCR-ABL+ Ba/F3 cell types was similar and so data from the 4 types was pooled and is shown in **Figure 3.10**. Significant residual proteasome subunit activity remained despite significant effects on viability (**figure 3.3**). This has been seen by others in HeLa cells where high concentrations of bortezomib (500nM) were required to achieve >90% inhibition of CT-L activity (189). Of interest is that bortezomib inhibited all 3 subunit activities, despite the purported CT-L selectivity of this drug. These results we show are in concordance with published data with bortezomib treatment of cell lines (10-500nM) and using a similar technique reveals inhibition of T-L (10->90%) and PG (20-90%) activities(186, 189).

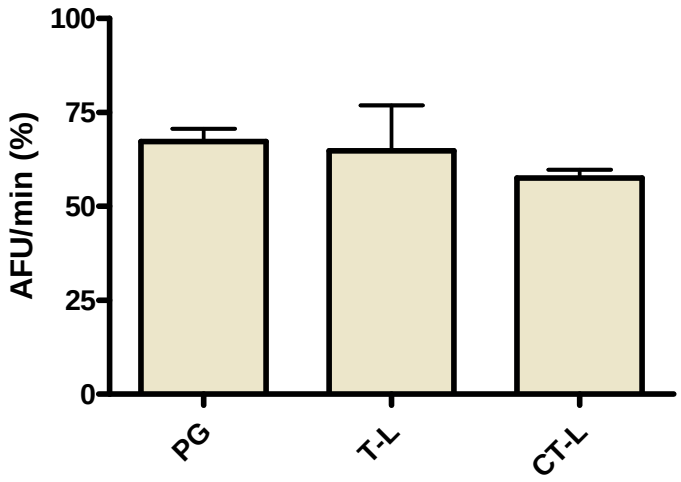

Figure 3.10 Effect of bortezomib 20nM on proteasome subunit activity in BCR-ABL+ Ba/F3 cells. Results shown represent % AFU/min in comparison to untreated cells (of same cell type). Pooled data is shown from Ba/F3-p210, -H396P, -M351T and -T315I cells and expressed as mean±SEM.

Aim 3 Effect of PI on BCR-ABL activity in BCR-ABL+ cell lines

Bortezomib has antiproliferative and apoptotic effects in BCR-ABL+ cells and this activity is associated with a reduction in proteasome activity. The deregulated tyrosine kinase activity of BCR-ABL is associated with the malignant phenotype and characterised by increased proliferation and cell survival (described in section **1.5**). The effect of proteasome inhibition on BCR-ABL activity is therefore of interest. There is also particular relevance to the later aim of establishing whether there is potential benefit in combining bortezomib with TKI.

3.3 Bortezomib reduces BCR-ABL activity in BCR-ABL+ cell lines

3.3.1 Effect of bortezomib treatment on BCR-ABL activity in K562 cells

K562 cells were exposed to bortezomib (2.5 to 20nM) or dasatinib (150nM) for 24h and then lysates prepared for Western blot analysis (**2.4.2**). Following SDS-PAGE electrophoresis and electrophoretic transfer onto a nitrocellulose membrane, the samples were probed with anti-pCrkl and anti-pan-actin. Crkl is an adaptor protein which plays an important role in BCR-ABL mediated signal transduction. The detection of pCrkl is an established method for demonstrating BCR-ABL activity. Crkl is tyrosine phosphorylated by BCR-ABL (190) and this phosphorylation correlates well with the level of BCR-ABL expression (191). Furthermore, the reduction in pCrkl as a consequence of BCR-ABL inhibition has been demonstrated with TKI therapy in CD34+ CML cells (192). By this technique we demonstrated that in K562 cells bortezomib exposure appeared to be associated with a decrease in BCR-ABL activity. BCR-ABL activity was effectively reduced with exposure to 150nM dasatinib for 24h for comparison (**Figure 3.11**).

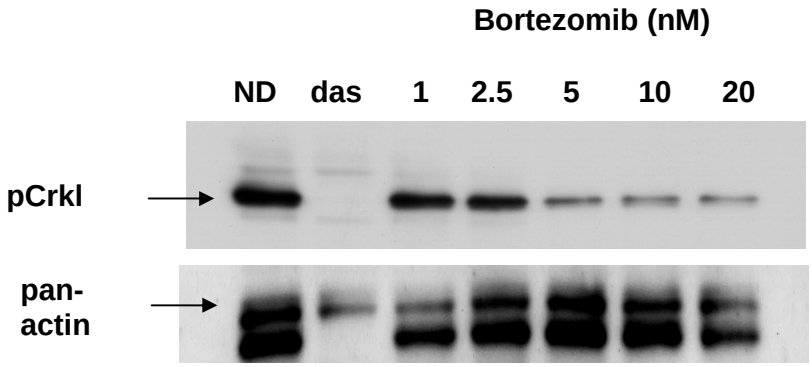

Figure 3.11. Treatment of K562 cells for 48h. Membrane probed with anti-pCrkl and anti-pan actin. Additional second band in lower membrane is due to residual anti-pCrkl binding as a consequence of inadequate membrane stripping of an avid antibody. Dasatinib 150nM (das) in comparison to stated nM concentrations of bortezomib. Densitometry (expressed as % of ND control and relative to actin loading) das 24% bortezomib 1nM 109% 2.5nM 81% 5nM 21% 10nM 22% 20nM 20%.

Aim 4 Effect of PI on viability and proliferation of CML patient samples including the quiescent subpopulation

Cell line work established that bortezomib was antiproliferative and induced apoptosis in BCR-ABL+ cell lines with an associated decrease in BCR-ABL and proteasome activity. By use of similar techniques, this work was extended to investigate effects on BCR-ABL+ CD34+ cells taken at diagnosis from patients with CP CML.

3.4 Bortezomib is antiproliferative and induces apoptosis in CML CD34+ patient samples

CML CD34+ cells were cultured in SFM+5GF in the presence and absence of bortezomib. At each time point the viable cell count and percentage of apoptotic cells were calculated (as described **2.4.1** and **2.4.2**). The effect of bortezomib did not vary significantly between different patient samples as is seen in data generated from initial experiments (**Figure 3.12A**) and the results were therefore pooled with mean±SEM established and dose-response curves predicted (**Figure 3.12B**). The LD_{50} was 8.8±0.7nM (n=5) at 24h, 7.6±0.4nM (n=3) at 48h and 5.7±1.6nM (n=7) at 72h. The effect of bortezomib on the expansion of the CML CD34+ cell population in SFM+5GF can be seen in **Figure 3.12C**.

CML CD34+ (n=1) were also analysed for the effects of bortezomib on cell viability in SFM-5GF with the LD_{50} 7.89±1.07nM (24h), 3.54±1.41 (48h) and 4.13±0.18nM (72h).

Figure 3.12 (**A**) A comparison of the effect of 24h bortezomib exposure on the viable cell count of 3 different CD34+ CML patient samples cultured in SFM+5GF. CML217 (■), CML218 (■) and CML228 (□). Based on estimations from the curves of best fit the LD_{50} was 8.4nM (CML217), 9.2nM (CML218) and 10.4nM (CML228). (**B**) The effect of 24h bortezomib exposure on the viable cell count and % cells undergoing apoptosis in 5 different CD34+ CML samples cultured in SFM+5GF. □ viable cell count and ▲ % cells undergoing apoptosis with broken lines indicating predicted curves of best fit. (**C**) CD34+ CML samples (n=3) were seeded at $2.5x10^5$cells/mL and then analysed for viable cell count and apoptosis at 24, 48 and 72h. Points indicate untreated cells (-□-), 4nM, (-▲-), 8nM (-▼-) and 16nM (-●-) bortezomib with adjoining lines.

A

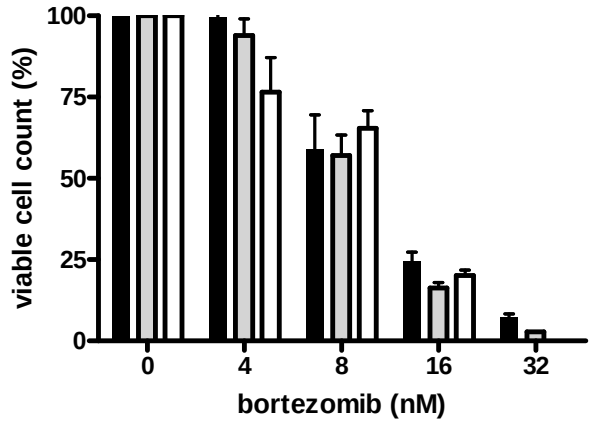

B

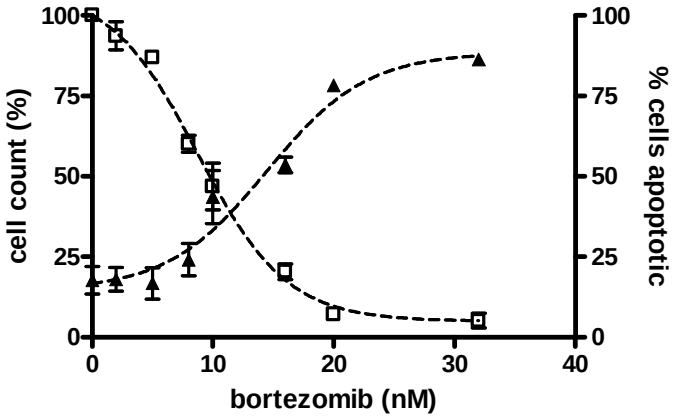

C

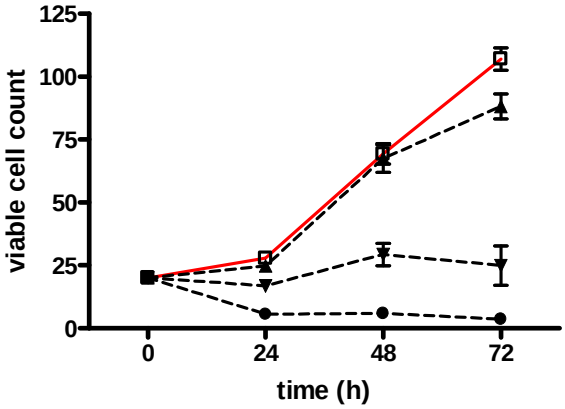

Figure 3.12

Total CD34+ from 4 patients were taken and examined in duplicate on 3 separate occasions for the presence of intracellular active caspase-3 when cultured with 10 and 20nM bortezomib. It was seen that there was a significantly reduced viable cell count in all these 3 samples with the addition of bortezomib at these

concentrations, or dasatinib 150nM. There was a trend to an increase in detectable intracellular activated caspase-3 when exposed to bortezomib (reaching statistical significance with 20nM) – this was not the case with the dasatinib treated samples (**Figure 3.13**).

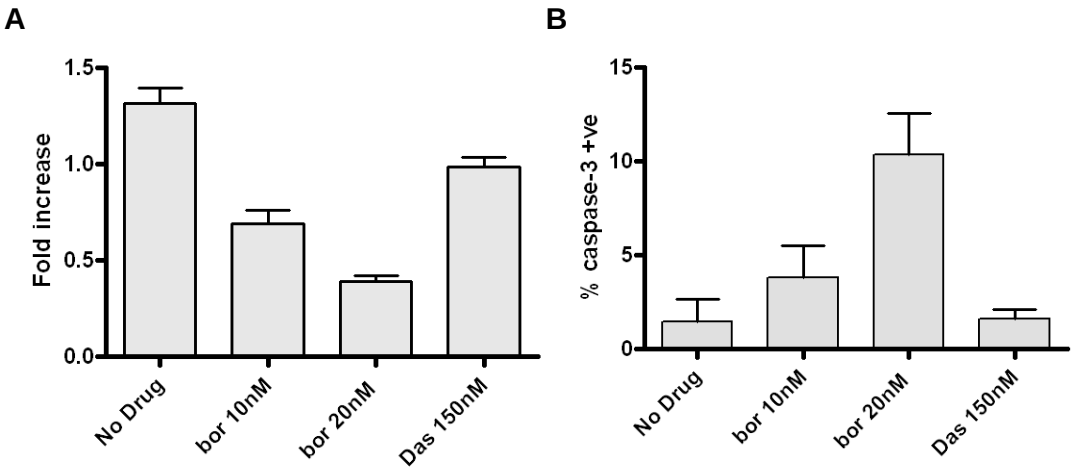

Figure 3.13. (A) Total CD34+ cells (n=4) cultured for 24h in SFM+5GF with viable cell counts taken and then the fold increase in population compared between untreated cells (no drug) and those treated with bortezomib (10nM or 20nM) and dasatinib 150nM. (**B**)These samples were then analysed by flow cytometry to assess the % cells with detectable active caspase-3.

An important substrate of caspase-3 is poly(ADP-ribose) polymerase (PARP). This protein plays a role in DNA repair and is cleaved to detectable fragments by caspases. The detection of these fragments is therefore a useful marker for caspase activity and apoptosis. Here we showed the cleavage of PARP in cell lysates following incubation of CML CD34+ cells for 24h with bortezomib (**Figure 3.14**). The PARP antibody used detects full-length PARP (116kDa) and the large (89kDa) cleavage fragment. Dasatinib 150nM did not induce significant apoptosis at this time point.

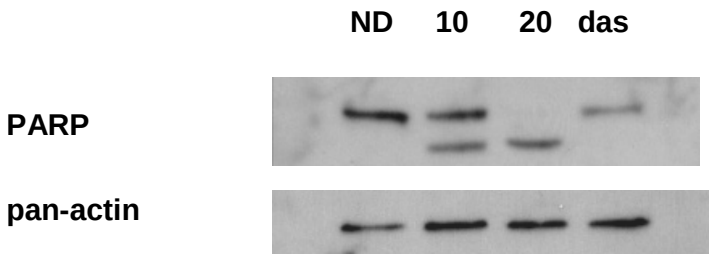

Figure 3.14. CML CD34+ cells treated with 10 or 20nM of bortezomib or 150nM dasatinib (das) and compared to untreated (ND) cells. All cells were cultured in SFM+5GF for 24h prior to preparation of cell lysates for Western blotting. The upper band represents full length PARP and the lower the 89kDa cleavage fragment. Membranes were probed with anti pan-actin to assess protein loading.

Aim 5 Effect of PI on BCR-ABL activity in CML patient samples
Aim 6 Proteasome activity in CML patient samples

These aims are considered together. Western blotting using a variety of different primary antibody incubations enabled both questions to be considered simultaneously in these experiments.

3.5 Bortezomib inhibits proteasome activity but does not affect BCR-ABL activity in CML CD34+ patient samples

The fluorescent substrate assay was not suitable for use in patient samples due to the large number of cells required ($1x10^7$) to provide the required 50-100µg lysate per replicate. Preliminary experiments using fewer K562 and Ba/F3 cells (0.1-$0.5x10^7$cells) were unsuccessful in yielding consistent, detectable proteasome activity. Therefore, indirect measures of proteasomal inhibition were investigated. Substrates are targeted for proteasomal degradation by the attachment of ubiquitin units in the form of a polyubiquitin chain. Therefore, the accumulation of polyubiquitinated proteins, shown here by Western blot, is an accepted marker of proteasome inhibition. This method was applied to CML CD34+ cells following 24h exposure to bortezomib (**Figure 3.15A**). This effect was not seen with dasatinib 150nM (**Figure 3.16**). We used the presence of the adaptor protein pCrkl as a specific marker of BCR-ABL kinase activity as described in **3.1.3**. The detection of pCrkl by Western blot following 24 and 48h bortezomib and 24h dasatinib treatment is seen in **Figure 3.15B**. Despite significant effects on cell viability there was minimal effect on BCR-ABL activity with either 10nM bortezomib (97±23%) or 20nM bortezomib (73±5%) in contrast to dasatinib 150nM (23±10%) - results from 24h drug exposure, expressed as densitometry readings (n=2) using the ratio of pCrkl:actin bands shown as a percentage of the untreated sample (mean±SD).

A

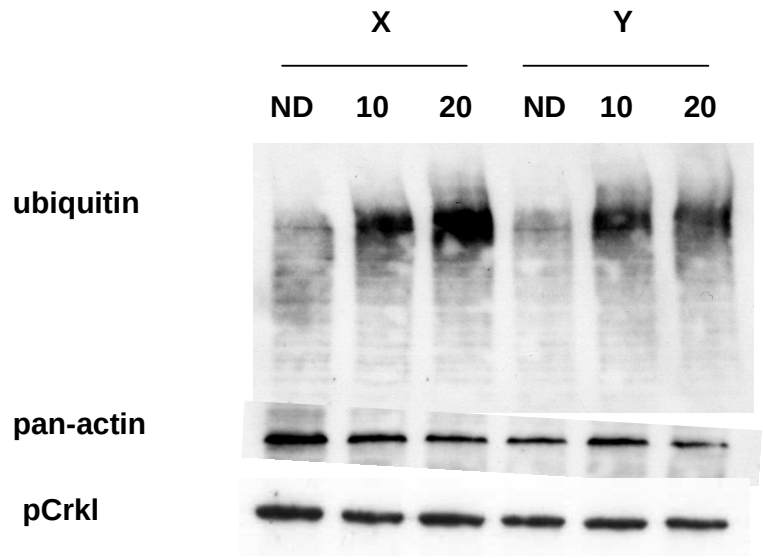

B

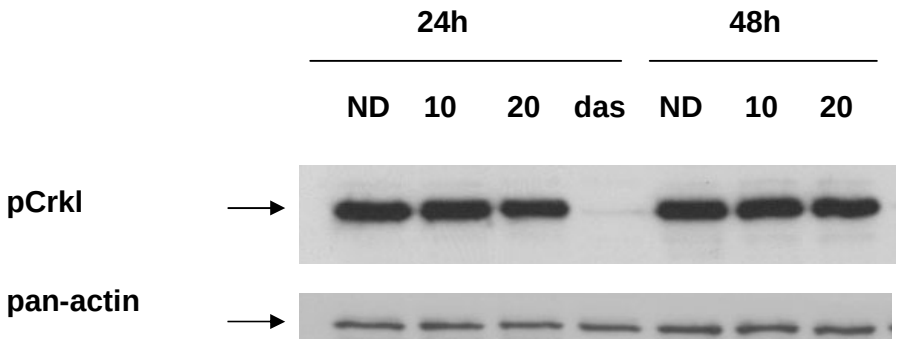

Figure 3.15 (**A**) Separate CML CD34+ samples (X, Y) were treated for 24h with bortezomib 10 or 20nM (10, 20) and compared with an untreated control (ND). Accumulation of poly-ubiquitinated proteins of varying molecular weights was seen. Protein loading was assessed using anti-actin antibody. Residual BCR-ABL activity represented by the pCrkl band can be seen in all samples. (**B**) A representative CML CD34+ sample treated with bortezomib 10 or 20nM (10, 20) or dasatinib 150nM (das) for 24h and 48h and compared with untreated control (ND). The presence of the pCrkl band demonstrates the significant residual BCR-ABL kinase activity in PI treated samples compared with the abrogated activity in the das treated sample.

The cyclin dependent kinase inhibitor $p57^{kip2}$ was also selected as a marker of proteasome inhibition. As described in the introduction, the CDKi $p27^{kip1}$ and $p57^{kip2}$ are substrates for the proteasome and accumulation with PI exposure in cell lines has been demonstrated. We used an anti-$p27^{kip1}$ antibody which has dual specificity for $p27^{kip1}$ and $p57^{kip2}$. We failed to demonstrate a clear band at the

expected molecular weight for $p27^{kip1}$ despite varying the quantity of lysate (10-20µg per well) and by use of a 15% gel. However a clear band was seen consistent with the 57kDa protein $p57^{kip2}$ with relatively increased protein levels detected in those cells treated with 20nM bortezomib, consistent with proteasome inhibition (**Figure 3.16**).

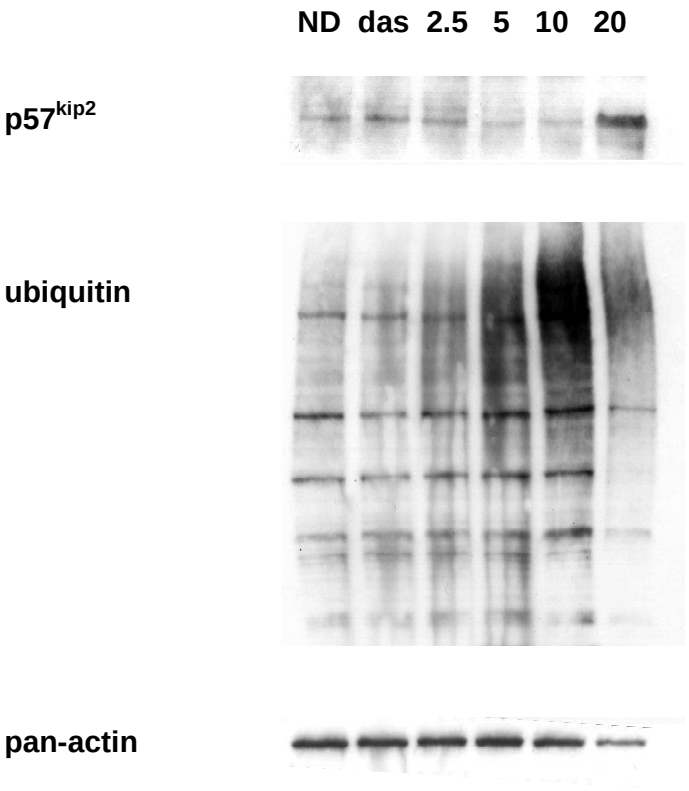

Figure 3.16 CML CD34+ cells cultured in SFM+5GF and treated with dasatinib 150nM (das) or bortezomib at stated concentrations (2.5nM to 20nM) for 24h and compared with untreated cells (ND). Lysates were prepared for Western blot and membranes probed with anti-p27kip1, anti-ubiquitin and anti-pan-actin.

Aim 7 Effect of PI on primitive cells from CML patient samples
Aim 8 Effect of PI on non-CML patient samples

Patients with CML on TKI harbour a primitive population of cells, enriched within the CD34+38- fraction, which are resistant to TKI exposure. We aimed to establish whether these cells were sensitive to the effects of bortezomib and if so, whether there was any difference in sensitivity in comparison to a similar sub-population of cells derived from patients without CML. Proliferation assays using CFSE staining were also performed to achieve Aim 7. By these means it was possible to determine drug effects within distinct subpopulations separated by division number and therefore allowed assessment of the effect of bortezomib on quiescent cells.

3.6 Bortezomib induces apoptosis in the CML CD34+38- population, though with minimal selectivity for leukaemic stem cells

Previous work has demonstrated the relative insensitivity of early haematopoietic progenitor cells to TKI therapy. We used a process of cell sorting to isolate the CD34+38- fraction of the CD34+ CML patient samples. It is within this population that primitive progenitor cells are enriched as has been shown in both the normal marrow (37) and leukaemia (41, 42). CD34+38- cells were enriched from 3 CML CD34+ patient samples. Samples were cultured in SFM+5GF with bortezomib and viable cell counts taken at 24h of drug exposure (**Figure 3.17A**). Results were compared to untreated controls. The LD_{50} at 24h was 8.93±1.42nM. This was similar to the LD_{50} of the unsorted CML CD34+ cells (section **3.4**). To illustrate this consistent effect on different cell populations, CML CD34+38- and CML CD34+38+ cells (n=3) were exposed to bortezomib for 24h and effects compared (**Figure 3.17B**). CD34+38+ enriched cells represent a relatively more mature and proliferating population of CML cells. LD_{50} values of 8.18±0.64nM for CD34+38+ cells were obtained and this was not significantly different from the CD34+38- population.

Similar experiments were performed in duplicate using 2 non-CML samples. At 24h drug exposure, the LD_{50} was 10.18±1.85nM (**Figure 3.17C**), which was not significantly higher than for CML CD34+38- cells.

A

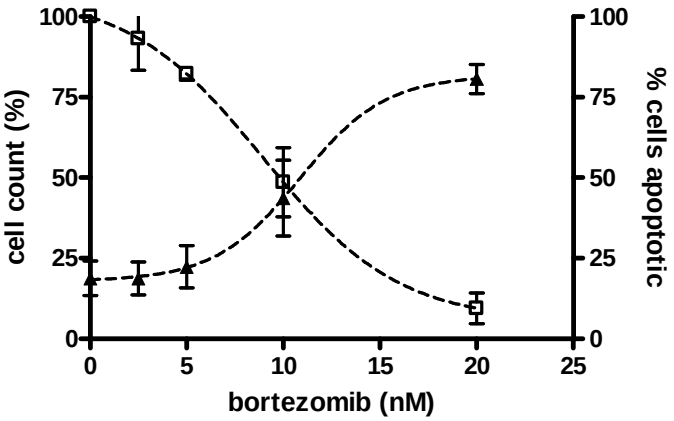

B

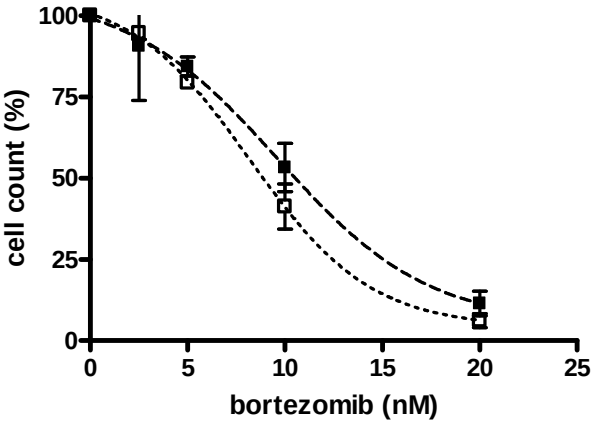

C

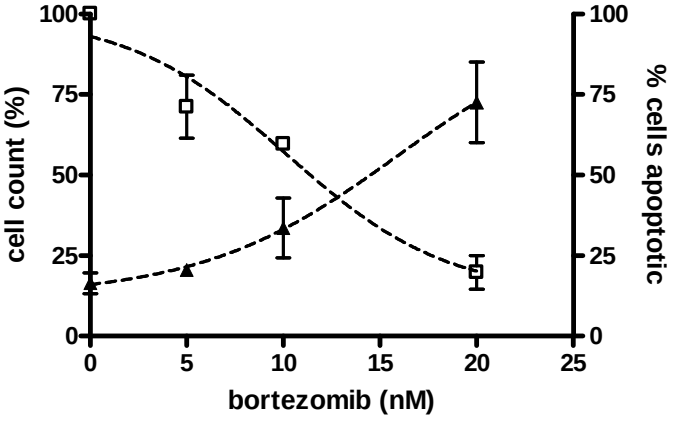

Figure 3.17

Figure 3.17 (**A**) CD34+38- (n=3) cells were cultured in SFM+5GF and analysed at 24h. The viable cell count (□) is expressed as a percentage of untreated (cell count %). The percentage of cells staining positive for 7-AAD (▲) is expressed on the y–axis (% cells apoptotic). (**B**) The effect of bortezomib on CD34+38-(■) and CD34+38+ cells (□) (n=3) was compared. The viable cell count is expressed as in (**A**). (**C**) CD34+38- (n=2) cells from non-CML samples were cultured in SFM+5GF and analysed at 24h. The viable cell count (□) and % cells apoptotic (▲) are derived as in (A). All results represent mean±SEM with predicted dose-response curves.

3.7 Bortezomib is antiproliferative in CML CD34+ patient cells

The effect of bortezomib on differentiation and division of CD34+ CML patient samples cultured in SFM+5GF was assessed with CFSE and flow cytometry (**2.4.5**). A comparison of the effect of dasatinib 150nM or bortezomib 20nM with untreated cells is shown in **Figure 3.18A**. Here 3 control groups were used: CFSE-, showing no fluorescence on the CFSE-channel (FL1-H); CFSE+ cells exposed to demecolcine to arrest cell division (undivided, $CFSE^{MAX}$); and CFSE+ cells exposed to no drug (untreated). In the analysis only viable cells (based on exclusion of PIo) were examined. For each sample a similar number of events ($1x10^4$) from each sample were counted therefore cell numbers ("Counts" in figures **3.18A** and **B**) do not reflect the total number of residual viable cells for each condition. This data is examined in later figures. With 72h culture, untreated viable cells underwent up to 6 divisions, however cells exposed to greater than 5nM of bortezomib underwent fewer divisions (**Figure 3.18B**). Exposure to 2.5nM bortezomib over-lay that of untreated cells (not shown). The majority of cells exposed to 20nM bortezomib, the maximum dose used in these experiments, failed to divide and the histogram (CFSE staining intensity, cell number) was seen to overlay the peak intensity of the demecolcine undivided control (**Figure 3.18A** and **B**). Consistent with published data, cells exposed to 150nM dasatinib underwent fewer divisions when compared to the untreated controls (reference (4) and **Figure 3.18A**). Mean data generated from 2 different CD34+ CML samples were analysed in **Figure 3.19** and demonstrate the percentage of viable cells in each division peak.

A

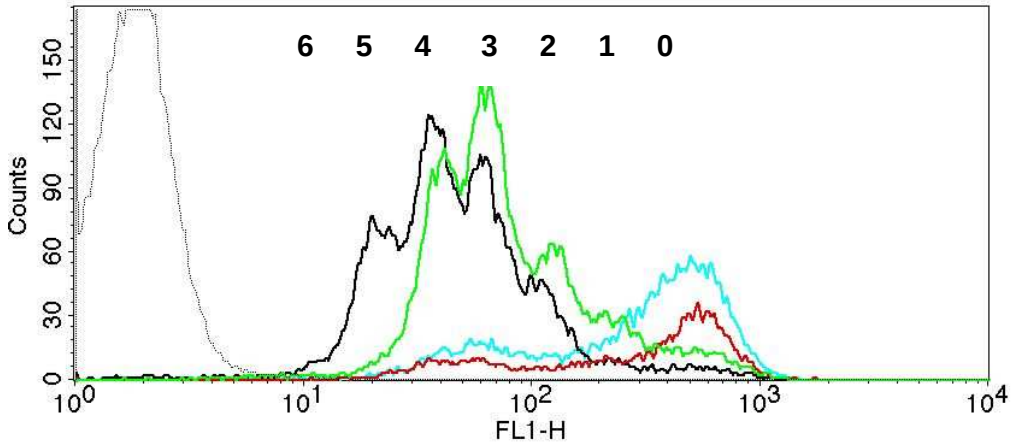

B

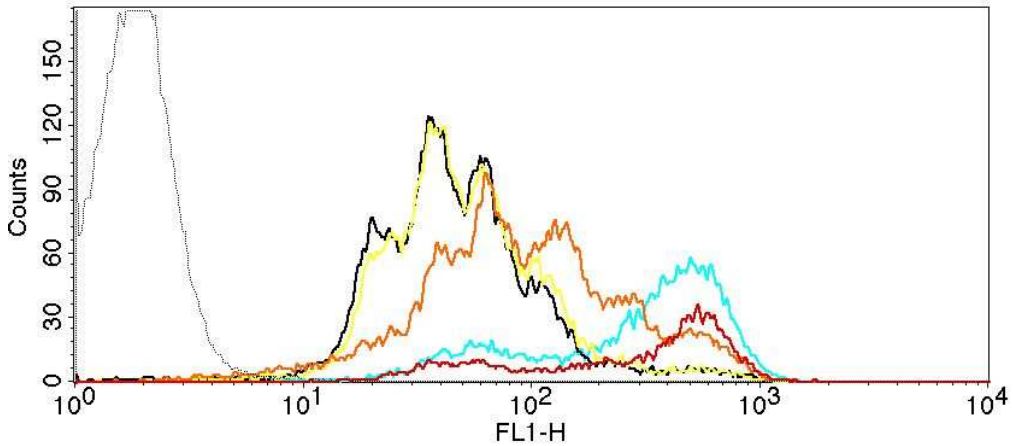

Figure 3.18. Representative plots from CD34+ CML patient sample cultured for 72h in SFM+5GF following CFSE exposure. (**A**) — CFSE-, — demecolcine, — untreated, — dasatinib 150nM and — bortezomib 20nM. (**B**) — CFSE-, — demecolcine, — untreated, — bortezomib 5nM, — bortezomib 10nM and — bortezomib 20nM. In (**A**) and (**B**) FL1-H (x-axis) indicates fluorescence intensity of CFSE staining and Counts (y-axis) the number of viable cells (based on PIo staining). The numbers above graph (**A**) indicate number of cell divisions each population has progressed through.

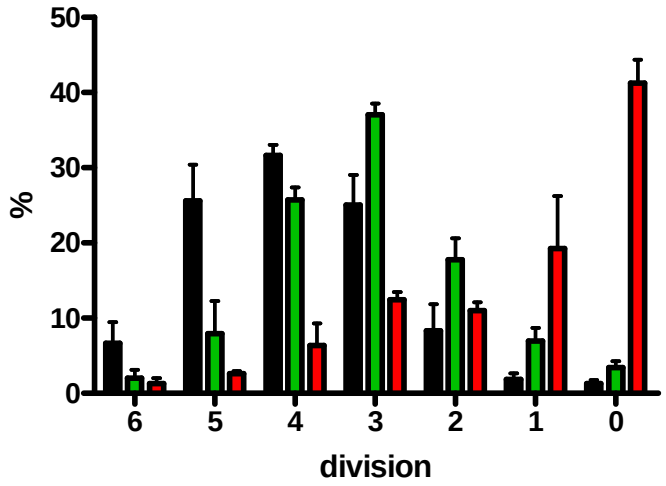

Figure 3.19 CFSE stained cells cultured for 72h in SFM+5GF with no drug (■) dasatinib 150nM (■) or bortezomib 20nM (■). The percentage (not total number) of viable cells in each sample from each division peak is seen from undivided (0 – right) to 6 (left) divisions. Error bars indicate mean±SEM.

The number of cells at each division in the different treatment groups was assessed as described in **2.4.5.4** with data shown in **Table 3.2**. Expansion of the CFSE+ cell population in SFM+5GF and the absence of drug was similar to that published previously (mean 3.77 versus 3.8 (60)). The percentage recovery indicates that fewer cells were surviving in the bortezomib and dasatinib treated arms relative to untreated cells – though the percentage recovery considered low in the untreated arm, presumably a result of commitment to death in cells counted as viable at day 1. Of interest is that the apparent antiproliferative effect of both bortezomib 20nM and dasatinib 150nM results in relatively more viable quiescent cells being detected in the sample after 72h culture (**Table 3.2**). The effect of bortezomib 10nM does not consistently produce this effect (**Figure 3.20**).

Table 3.2. CFSE data generated from 3 CML CD34+ samples analysed at 72h.

drug	Total CD34+ cells		undivided CD34+ cells		
	recovery (%)	recovery relative to ND (%)	viable cells (%)	recovery of input (%)	recovery relative to ND (%)
ND	58.05	100	0.74	11.99	100
B10	9.25	15.93	4.79	3.59	30
B20	3.65	6.28	3.96	1.58	13.2
DAS	29.69	51.15	3.05	18	150.1
ND	33.05	100	0.83	3.32	100
B5	26.39	79.5	1.35	4.3	115.1
B10	11.08	33.52	7.66	3.82	110.2
B20	11.94	36.14	44.35	3.66	290.4
DAS	24.89	75.33	2.56	9.64	124.1
ND	36.17	100	1.73	5.2	100
B5	30	82.93	1.79	4.24	81.5
B10	11.82	32.67	6.7	3.19	61.3
B20	10.73	29.66	38.07	7.25	139.4
DAS	15.19	41.99	4.25	3.19	61.3

Results from 3 different samples are shown CML232 ( ), CML194 ( ) and CML166 ( ). All samples were cultured for 72h in SFM+5GF with (bortezomib (B) at 5, 10 or 20nM or dasatinib (DAS) 150nM) or without (ND) drug exposure. Recovery refers to a calculation based on the viable cell count and the percentage of cells in each division peak (from CFSE staining) which estimated the original number of undivided cells from which these populations must have arisen. For total CD34+ and undivided CD34+ (i.e. $CFSE^{MAX}$) a comparison was made to the untreated (ND) control (relative to ND columns). The percentage of viable cells which are undivided is also shown.

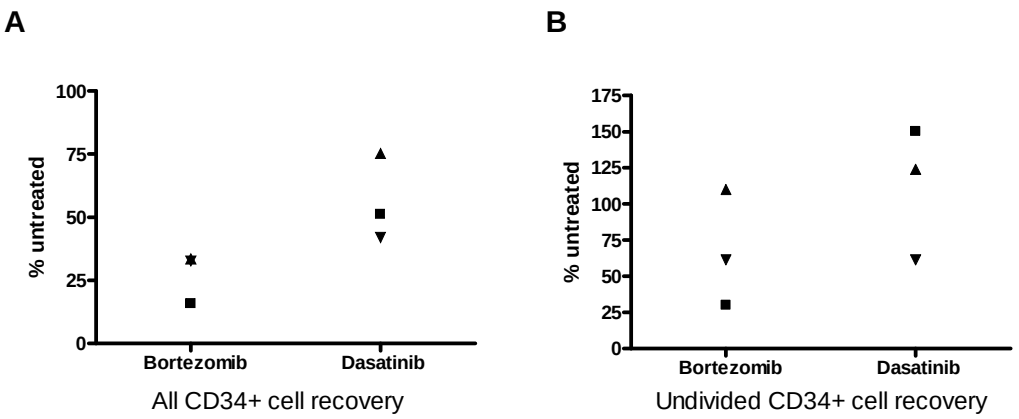

Figure 3.20. (**A**) Recovery of all CD34+ cells and (**B**) undivided ($CFSE^{MAX}$) CD34+ CML cells displayed as a percentage of the untreated control with comparison between bortezomib 10nM and Dasatinib 150nM. For both graphs, CML194 (▲) CML166 (▼) and CML 232 (■).

With evidence of cell division (by CFSE staining intensity) there was an associated reduction in the percentage of CD34+ cells consistent with the loss of CD34 expression associated with myeloid maturation (**Figure 3.21**). In dasatinib treated cells there was a trend for the surviving cells at each division peak to have relatively less CD34+ expression. This is in contrast to bortezomib treated cells where the opposite was seen. In the context of the results seen in **Table 3.2** it appears that surviving cells have undergone fewer divisions and are of a less mature phenotype. This phenomenon has been noted by others using CD34+CML cells cultured in SFM-5GF (60).

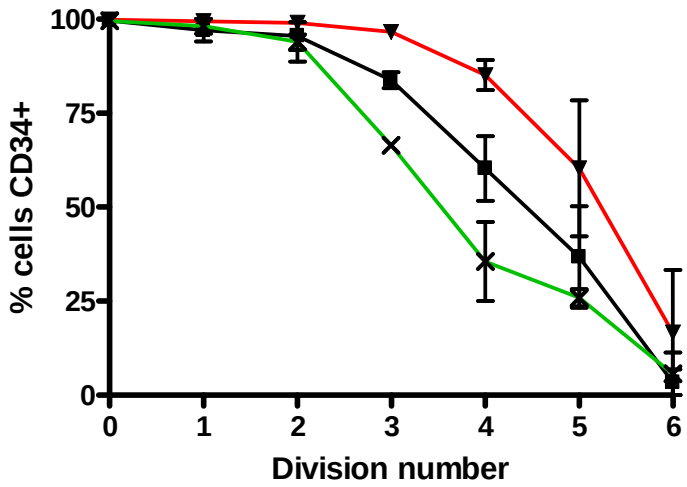

Figure 3.21 CD34+ CML samples (n=2) exposed to CFSE and cultured in SFM+5GF for 72h. Division number represents the number of divisions each cell population has undergone and is based on CFSE staining intensity, % cells CD34+ is the % of viable CD34+ cells (based on PI staining) of that CFSE intensity. -■- untreated, -×- dasatinib 150nM and -▼- bortezomib 20nM. Points indicate mean±SD with adjoining lines.

Aim 9 The potential synergistic effect of PI and TKI on viability and proliferation of BCR-ABL+ cell lines and CML patient samples

The current trend in the clinical use of bortezomib is for use in combination with other therapies. This is particularly appealing in the setting of this project as the results of Aim 8 indicate toxicity to normal cells. Combination therapies are established as a mechanism of increasing toxicity to abnormal cells, through targeting multiple pathways or different elements of similar pathways with the associated benefit of potentially achieving similar effects with reduced individual drug exposure. We aimed to investigate the novel combination of bortezomib with a TKI. Dasatinib was selected as a model TKI due to the high levels of BCR-ABL inhibition that are recorded with clinically achievable doses.

3.8 Dasatinib and bortezomib act synergistically against CML CD34+ cells

Calcusyn® is a software package designed to estimate synergy between 2 drugs used together at a fixed ratio of concentrations. The sigmoidal dose-effect curve is converted through a logarithmic derivation to a linear graph (**Equation 2.2** and **2.3**). Data derived from individual drugs can then be compared to the drug combination (which is considered as a 3rd drug) by the CI (**Equation 2.4**) which is a measure of synergy/antagonism.

CML CD34+ cells (n=3) were cultured in SFM+5GF and exposed simultaneously to a combination of bortezomib:dasatinib at different fixed ratios (2.5:1 to 10:1) . Cell counts and flow cytometry were performed at 72h to assess the effects on cell viability. This time point was chosen as preliminary experiments demonstrated that earlier time points underestimated cell death induced by dasatinib. The data were analysed using Calcusyn®. **Figure 3.22** illustrates a dose-effect profile of bortezomib, dasatinib and the drug combination (2.5:1).

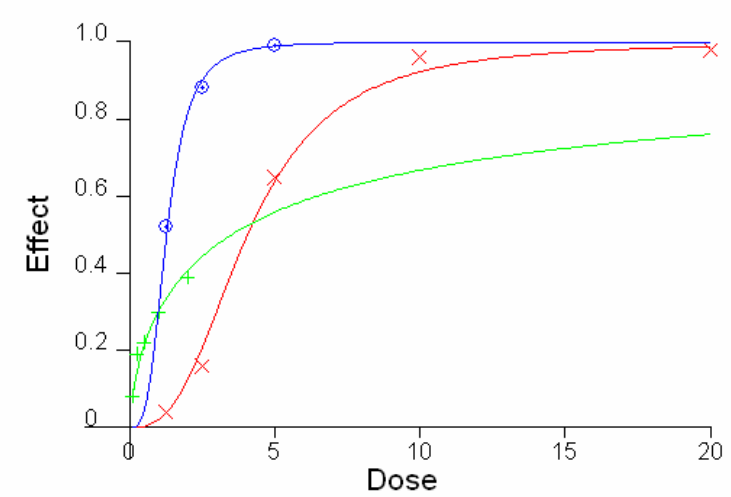

Figure 3.22 Dose effect profile for dasatinib (—), bortezomib (—) and 2.5:1 combination (—). Effect (x-axis) is f_a as calculated in **Equation 2.3** and Dose (y-axis) the concentration of drug (nM) and expressed as bortezomib concentration in the drug combination.

This data may also be viewed as an isobologram where the linear profile of defined effects (LD_{50}, LD_{75} and LD_{90}) is seen with the corresponding data from the drug combination experiments (**Figure 3.23**). Data fell consistently below the line of effect and so indicated synergy.

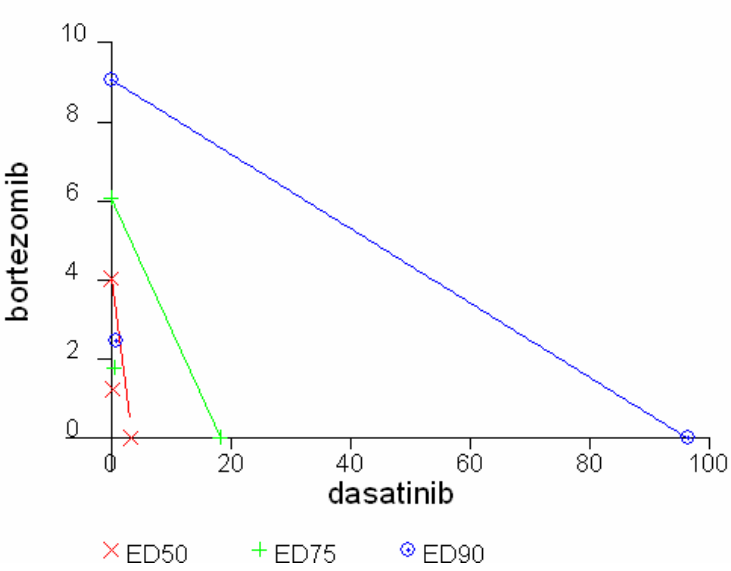

Figure 3.23 Isobologram of fixed additive effects at LD_{50} (—), LD_{75} (—) and LD_{90} (—). Experimental data from ratio of 2:5:1 is shown corresponding to these effects (**X**, **X** and **X**) respectively.

Synergy was demonstrated in these samples at both drug ratios and at end points including LD_{50}, LD_{75} and LD_{90} (**Table 3.3**).

Table 3.3 Combination indices for bortezomib and dasatinib used simultaneously in CML patient samples.

Ratio	Combination index			r-values
	LD_{50}	LD_{75}	LD_{90}	
2.5:1	0.67±0.16	0.54±0.16	0.53±0.21	0.85-0.99
5:1	0.78±0.12	0.66±0.13	0.64±0.16	0.90-0.98
10:1*	0.87±0.25	0.75±0.22	0.69±0.22	0.93-0.94

Ratio described as bortezomib:dasatinib, synergism ( ), moderate synergism ( ) and slight synergism ( ) as defined by Chou TC (185).
*For 10:1 n=2, for 2.5:1 and 5:1 n=3.

4. DISCUSSION

4.1. Overview

The current recommended treatment for the majority of patients with CP CML is IM. There is accumulating evidence that the majority of patients respond to this drug and achieve the therapeutic milestone of a CCyR. However TKI induce a state of MRD and many patients continue to have detectable BCR-ABL transcripts. In addition, MRD may persist in those with undetectable BCR-ABL transcripts, with the "undetectable" results a reflection of the limitation of the assay rather than true CML eradication. There may be a subpopulation of patients treated with IM with undetectable BCR-ABL transcripts who have achieved disease eradication. This question was addressed in the Stop Imatinib (STIM) study, with preliminary results presented recently. Here it was seen that 15 of 34 patients with undetectable BCR-ABL who had discontinued IM for ≥6m showed no evidence of disease relapse. Of these 5 patients had received IM therapy alone. However follow-up is relatively short and the recommendation remains that patients should be treated indefinitely (98).

For the majority if IM treated patients, the source of MRD is presumed to be the population of Ph+HSC. These cells are relatively insensitive to TKI. Furthermore the development of TKI-resistant BCR-ABL mutations is a cause of primary and secondary treatment failure. In particular T315I is resistant to all available TKI and there is concern that selection pressure may result in this mutation becoming more prevalent. The proteasome is an attractive target for cancer therapy and there has been expansion of the clinical use of bortezomib, to date the only licensed PI. In this study we provide evidence that this drug has potential as a therapy to target cells expressing BCR-ABL including T315I mutated forms. There is also evidence that the Ph+HSC may be susceptible to the apoptotic effect of this drug. Concerns over the relatively non-selective action of bortezomib may potentially be overcome by use in combination with TKI. This would be in line with the majority of clinical studies of bortezomib where it is now seldom used as monotherapy.

4.2 Targeting BCR-ABL+ cell lines, including mutant forms

We demonstrate that BCR-ABL+ cell lines (K562 and Ba/F3-p210) are subject to reduced proliferation and increased apoptosis when exposed to bortezomib for greater than 12h (**Figure 3.5**). Different techniques were used to establish an LD_{50}

in K562 and included cell counting by vital dye exclusion (LD_{50} 5.6nM at 48h **Figure 3.1**), cell counting combined with flow cytometry with annexin-V and 7-AAD staining (LD_{50} 6nM at 48h **Figure 3.2**) and ^{3}H-thymidine proliferation assays (IC_{50} 8.4 **Figure 3.7**). Ba/F3 cells transduced and expressing p210 and mutated BCR-ABL were assessed following bortezomib exposure with cell counting and flow cytometry. An LD_{50} of between 6.3 and 11.3nM at 24h was established, with no significant difference between p210 and the 3 different BCR-ABL mutants (H396P, M351T and T315I). These cells were assessed at this early time point as drug wash-out experiments indicated that longer exposure was probably not necessary. We confirmed by flow cytometry for activated caspase-3 that apoptosis was induced by bortezomib in Ba/F3 cells (**Figure 3.6**) a result predicted by the movement of cell populations through the annexin-V and 7-AAD quadrants with continuous drug exposure.

These results may be compared to published work previously demonstrating that BCR-ABL+ cell lines are susceptible to the antiproliferative and antiapoptotic effects of PI. Servida *et al.* exposed a range of cell lines to the PI bortezomib and Z-Ile-Glu(OtBu)-Ala-Leucinal (PSI) – though in this study the LD_{50} for bortezomib in IM-sensitive K562 was 110nM at 48h (by PIo staining and flow cytometry) (8). These results are at variance with others using flow cytometry and annexin-V staining and showing an LD_{50} of 32nM with bortezomib in K562 at 48h (3). A separate group examined KBM-5 and -7 (as with K562 both lines derived from human BC CML) which were either IM sensitive or IM resistant. Assays of cell proliferation demonstrated an IC_{50} between 10-15nM at 48h with identical dose-response curves between the IM-resistant and sensitive cells lines. This inhibition was correlated with accumulation of cells in G2M phase, induction of caspase-3 and an inhibition of NFkB activity by EMSA (1).

It is difficult to explain why our results with K562 are at variance with Servida *et al.* as a similar technique was adopted. It is unlikely to be due to storage artefact of bortezomib as we have demonstrated that freeze-thawing does not appear to enhance the potency of drug effect in the assays used. In addition in all cases the bortezomib was obtained directly from the manufacturers.

Our results add evidence to those published previously that IM-resistance does not appear to influence bortezomib sensitivity. What is added by our work is that

specific mutations of BCR-ABL are equally sensitive to apoptosis, including the T315I mutation. This is clearly of clinical relevance as there is no current licensed therapy available for these patients other than conventional treatments such as hydroxycarbamide or busulphan which will achieve only haematological responses. Haematopoietic stem cell transplantation is a further option though is limited by the toxicity of conditioning regimes – of particular concern in CML which is predominantly a disease of the elderly. The results with bortezomib can be compared to those generated with the aurora kinase inhibitor MK-0457 (VX680) and homoharringtonine (HHT). The aurora kinases are key regulators of mitosis and abnormal activity is associated with a number of malignancies including leukaemia. Aurora kinase inhibitors block cell-cycle progression and induce apoptosis in BCR-ABL+ cell lines, including the T315I mutant (126, 128). A series of 3 patients with the T315I mutation and treated with MK-0457 showed promising early evidence of clinical responses (127)., however clinical trials were subsequently stopped due to unacceptable levels of toxicity. HHT is a cephalotaxus alkaloid which has previously been shown to have antiproliferative effects and induce caspase-3 dependent apoptosis in IM-sensitive and resistant BCR-ABL+ cell lines (193). Prior to the introduction of IM, HHT was used in a clinical trial for patients with CP CML with 72% CHR and 15% CCyR achieved (194). More recently HHT has been used in 17 patients with IM-resistant CML in all disease phases. Conventional responses were obtained only in the small number of CP patients treated and none were sustained (195). However, of particular interest is emerging data that HHT may have a preferential effect on the T315I mutant. This comes from 2 clinical trials where patients with IM-resistant CML and the confirmed presence of the T315I mutation have been treated with HHT. In both trials a rapid fall in T315I BCR-ABL transcripts was reported with associated haematological and cytogenetic responses (99, 196).

In addition we performed baseline proteasome activity assays in the K562 and Ba/F3 cells and were surprised to document differences in both PG and CT-L activity between the Ba/F3 mutants. This reached statistical significance in Ba/F3 T315I, Ba/F3-H396P and Ba/F3-M351T for CT-L activity and Ba/F3-H396P and Ba/F3-M351T for PG activity. This did not translate into differences in susceptibility as shown, though there was a trend for the BCR-ABL mutants to be slightly less susceptible. Multiple replicates would be required to determine any subtle differences – which may not be of clinical consequence. However such data would

be interesting and comparable to the apparent enhanced susceptibility of T315I mutations to HHT (196). Our findings may also augment data published in this field comparing the biology of different BCR-ABL mutants, in particular mutations are present in IM-naïve patients which may confer a survival advantage to cells (197). There are published data demonstrating that BCR-ABL mutants may have differing oncogenicity (by transformation of mouse BM cells) and ABL-kinase activity (by global phosphotyrosine assays) with selected data demonstrated in **Table 4.1**. However, there are no data published comparing the proteasome activity of the mutants.

Table 4.1 Published data of BCR-ABL mutants

BCR-ABL mutant	Transforming potential	Kinase activity	Reference
T315I	=/↑	↓	(198, 199)
H396P	↓	↓	(198)
M351T	↓	↓	(199)

Activity relative to p210 BCR-ABL with ↓ increased and ↑ decreased activity.

With bortezomib treatment we demonstrate the expected inhibition of CT-L activity. Data for the Ba/F3 mutants was pooled as little differences were seen between the mutants at the concentration tested (20nM). We also demonstrated some reduction in PG and T-L activity. This has been demonstrated by others using this technique with bortezomib which is reported to be a relatively selective CT-L PI. (186). This may reflect a limitation of the assay for determining specific proteasomal subunit activity or illustrate the theory that protein degredation is reliant on all active sites and so inhibition of CT-L activity may impair protein degradation through other routes (189). We did not assay proteasome activity to determine a dose response curve. This has been done previously both *in vitro* and data has been generated from clinical trials. There appears to be a maximally tolerated threshold effect at around 80% inhibition where toxicity is significantly limiting (177). This may reflect the non-selective nature of proteasome inhibition and there may be an exposure level at which all cells will be unable to function and so undergo apoptosis. It is reassuring to see that the concentration used here (20nM) generated significant apoptosis in Ba/F3 cells however was associated with only approximately 40% inhibition of substrate release. This may also indicate that bortezomib may have targets other than the proteasome. Though not fully

characterised it has been demonstrated that bortezomib targets non-proteasomal cellular enzymes including the protease enzymes cathepsin A/G and chymase (200).

It has previously been shown by using FDCP-MIX cells transfected with a temperature sensitive BCR-ABL construct that BCR-ABL activity is associated with an increase in proteasome activity, as measure by release of fluorescent AMC-bound peptides. The BCR-ABL+ cells were also more susceptible than BCR-ABL- cells to apoptosis induced by PI (BzL-LLCOCHO) exposure (2). No clear pathway has been established linking the proteasome to BCR-ABL activity. However BCR-ABL activity has been associated with constitutive NFkB activity, reduced levels of CDKi and an altered balance of pro and antiapoptotic mediators – all of which involve potential proteasomal substrates. It is possible that the proteasome is activated by one or a number of the many molecular pathways activated by BCR-ABL kinase. We were interested to note that in K562 exposure to bortezomib for 48h was associated with a reduction in pCrkl in a dose-dependent manner, consistent with reduced BCR-ABL activity. This is consistent with results published by Soligo *et al.* where reduced BCR-ABL protein was detected at 48h with exposure of K562 to PSI (201). These results contrast with Yan *et al.* who failed to detect any difference in BCR-ABL protein in K562 with 48h exposure to 32nM bortezomib. We did not probe for BCR-ABL protein levels and so direct comparisons cannot be drawn. It is conceivable that the proteasome may be influencing stability and/or activity of proteins downstream of BCR-ABL modulating phosphorylation of Crkl though further characterisation of this was considered beyond the scope of this project.

4.3 Targeting the CML stem cell

We have demonstrated that CD34+ selected leukapheresis samples taken from patients with CP CML at diagnosis are susceptible to the antiproliferative and apoptotic effects of bortezomib. CML CD34+ cells were exposed to bortezomib and cultured in SFM+5GF. The LD_{50} was 8.8±0.7nM (n=5) at 24h, 7.6±0.4nM (n=3) at 48h and 5.7±1.6nM (n=7) at 72h. The different patient samples selected did not appear to vary in susceptibility to this drug and the absence of growth factors did not significantly affect responses. The expansion of CML CD34+ in SFM+5GF was impaired in the presence of the drug indicating an additional antiproliferative effect. These results are illustrated in **Figures 3.12A-C**. Evidence

for apoptosis was provided by the increase in detectable intracellular activated caspase-3 with bortezomib exposure (detected by flow cytometry, **Figure 3.13B**) and the cleavage of PARP (detected by Western blotting, **Figure 3.14**). The concentration of bortezomib required to achieve these results is similar to that inhibiting proliferation of human multiple myeloma cells (IC_{50} 2.5-30nM (5)) and CD34+ selected human AML samples (IC_{50} 5-10nM at 7d (6)).

We utilised Western blotting to detect the accumulation of polyubiquitinated proteins as a marker of proteasome inhibition. This was clearly demonstrated in CML CD34+ following 24h exposure to bortezomib though not with TKI therapy (**Figure 3.15A and 3.16**). This time point was chosen for consistency of analysis allowing correlation with experiments assessing apoptosis and proliferation – in turn based on drug wash-out experiments in cell lines. There is published evidence that a much shorter exposure of 1h is required to achieve maximum proteasomal inhibition *in vivo* (168) though the recovery of cells *in vitro* following short exposure may relate to the reversible inhibition associated with bortezomib.

We also demonstrate effects on the CDKi $p57^{kip2}$ (**Figure 3.16**). This is consistent with an inhibitory effect of PI on cell cycling through the prevention of the enhanced removal of CDKi seen in a number of malignancies including CML. PI treatment of CML has been associated with increased levels of $p27^{kip1}$ and $p21^{cip1}$ which are both members of the CIP/KIP family which also includes $p57^{kip2}$ (145, 147, 148). This is of particular interest as it has been shown that $p57^{kip2}$ but not $p27^{kip1}$ sensitises cancer cells to apoptosis by mitochondrial translocation resulting in loss of MMP and release of cytochrome *c* with consequent apoptosis (202).

In contrast to the results shown for the K562 cell line, we did not demonstrate significant effects on BCR-ABL activity with up to 20nM bortezomib exposure for up to 48h. There are a number of potential explanations for these differences. The comparison is between an immortalised BC cell line and a CP patient derived CD34+ selected product and so there is likely to be inherent differences in the balance of intracellular signalling pathways between these samples. It may be that longer exposure or higher concentrations of bortezomib are required to achieve the effect on BCR-ABL activity seen in K562. However we were interested to note significant BCR-ABL activity was detected in CD34+ CML samples at concentrations in excess of the LD_{50} and the derived area-under-the-curve drug

exposure *in vivo*. This would be consistent with the proteasome functioning either independently of BCR-ABL or downstream through activated signalling pathways. However there are caveats to both of these suggestions – BCR-ABL activity in cell lines is associated with increased proteasome activity and effective TKI exposure does not result in accumulation of polyubiquitinated proteins as detected by Western blot. It may be that BCR-ABL does mediate an increase in proteasome activity beyond basal levels. TKI therapy may ameliorate though not obliterate proteasome function which may continue at a sufficient rate to clear polyubiquitinated proteins. It is also speculated that the accumulation of ubiquitinated proteins may be minimised by stimulation of autophagy – a process related to proteasomal function which will be discussed. There may be additional interactions between BCR-ABL and the proteasome illustrated by work investigating molecular chaperones. It has been shown in BCR-ABL+ cell lines that BCR-ABL depends on an association with HSP90 to maintain stability. Targeting this association with HSP90 inhibitors (including geldanamycin and 17-AAG) results in increased ubiquitination and proteasomal degradation of BCR-ABL (p210 and mutated forms) (107, 109, 110). Proteasome inhibition may therefore protect cells against BCR-ABL breakdown.

We next used FACS to isolate the CD34+38- fraction from 3 CD34+ CML patient samples. It is within this population that primitive progenitor cells are enriched with evidence for this shown in **Table 1.1**. The LD_{50} at 24h was 8.93±1.42nM. This was similar to that of unsorted CML CD34+ cells and no significant difference was seen when comparing relatively primitive CD34+38- cells to more mature and proliferative CD34+38+ (**Figure 3.17B**).

To further assess the effect of bortezomib exposure on the different populations of cells we cultured CML CD34+ cells for 72h with CFSE. This provided insight into the number of divisions cell populations had undergone in different experimental conditions. As demonstrated previously dasatinib exposure was antiproliferative (**Figure 3.19** and (4)). Bortezomib treatment at concentrations >5nM showed a more marked effect and with 20nM exposure, of the remaining few cells surviving, the majority had failed to divide with the curve overlying that of the Colcemid® control. Furthermore as the cells divided in the presence of bortezomib they appeared to maintain a less mature phenotype as evident in the retention of CD34+ surface staining. This phenomenon has been noted by others culturing

CD34+ CML cells in the absence of exogenous growth factors and may reflect the reduced proliferative potential of cells exposed to bortezomib and it is speculated that this may reflect a tendency to undergo self-renewal divisions (60).

To determine the numbers of CD34+ viable cells for each division peak we performed recovery calculations based on the assumption that cells will divide in a balanced manner with 1 cell producing 2 progeny with equal potential for replication. We analysed cells exposed to 10nM bortezomib as this was close to the LD_{50} though it is accepted that the sustained drug exposure potentially achieved *in vivo* for this time period with conventional drug dosing is not known. We discovered differences between the 3 samples analysed in this way, however when assessing recovery from all division peaks with both dasatinib 150nM and bortezomib 10nM exposure there was impaired recovery of CD34+ cells – consistent with loss of cells presumably through apoptosis. When the undivided peak was assessed the differences were more marked, though only small numbers of cells contributed to these peaks. Here it was seen in 2 of the 3 samples examined there was an increase in recovery of undivided (quiescent) CD34+ cells with dasatinib (consistent with published data (4)) in contrast to a reduction in this cell population with bortezomib 10nM. This is significant as the quiescent Ph+CML is thought to contribute to MRD in TKI treated CML. Bortezomib appears to have the potential to reduce this population at concentrations which may be clinically relevant as demonstrated in an effect on FACS sorted CD34+38- cells and from the CFSE data in which cell division was tracked. However the cells are not eradicated and the concentration of bortezomib may be critical as higher levels appear to be ineffective in targeting the undivided cells and retention of CD34+ staining may reflect a stimulus to self-renewal and so maintenance of MRD.

4.4 Relative non-selectivity of bortezomib

The proteasome is found in all eukaryotic cells and plays a vital role in cellular functions – including those resulting in proliferation and apoptosis. Inhibition of the proteasome is therefore inherently a non-selective strategy to target cancer cells and relies on exploiting a difference in proteasome activity levels, a dependence on that activity and/or the ability to recover from disruption to protein turnover. We analysed 2 FACS sorted CD34+38- non-CML samples and demonstrated that at 24h drug exposure the LD_{50} was 10.18±1.85nM - not significantly different to the

results obtained for a similar population of CP CML cells (**Figure 3.17C**). To establish any true difference between CML and normal would clearly require more replicates, however a limited number of non-CML samples were available for analysis in our laboratory. It is interesting to note of the little published in this field there is marked variation in results obtained (**Table 4.2**). The variation may reflect a difference in techniques applied, time-points of analysis and cells used as representative of “normal” controls. There is no published data assessing the effects of bortezomib on the CD34+38- sorted population as shown here. However Servida *et al* have assessed the effects of a different PI on normal primitive HSC. They performed LT-CIC assays with 3 normal BM samples at a single concentration of PSI chosen as equivalent to the IC_{50} demonstrated in CML by CFU-GM assay. This concentration did not influence colony formation and was therefore considered selective for CML (8).

Table 4.2 Published effect of bortezomib on normal cells

Cells	Technique	IC_{50}/LD_{50}	Timepoint	Reference
PB MNC	Thymidine incorporation	>100nM	48h	(5)
	Annexin-V staining	50nM induced 48±22% apoptosis	48h	(9)
CD34+ BM	Annexin-V staining	50nM induced 5±5.2% apoptosis	18h	(9)
	CFU-GM	11.3nM	14d	(8)
	Thymidine incorporation	<20nM	7d	(6)
	MTT	260-780nM	48h	(203)

The technique applied and the timepoint for analysis is obtained from the relevant publication and the IC_{50} or LD_{50} quoted where available. Colony forming units granulocyte-macrophage (CFU-GM), MTT assay is a conventional proliferation assay measuring a colour change of 3-(4,5-Dimethylthiazol-2-yl)-2,5-diphenyltetrazolium bromide (MTT) by mitochondrial activity, Peripheral blood mononuclear cells (PB MNC) and CD34+ selected bone marrow cells (CD34+ BM).

4.5 Combination of bortezomib with dasatinib

Drug combinations are commonly utilised for cancer therapy and provide a mechanism for enhancing the effect of an agent without increased toxicity. Bortezomib is now commonly used in combination with other therapies in clinical trials and this is perhaps not a surprise when the myriad cellular processes potentially affected by this drug are considered. Bortezomib combinations also offer a mechanism to minimise the significant toxicity associated with this drug. In the APEX trial published in 2005 where patients were treated with the now established 1.3mg/m2 on days 1, 4, 8 and 11 in 3-week cycles, 37% discontinued treatment as a consequence of side-effects. Most common serious events (grade 3 or 4 by NCI common toxicity criteria) were thrombocytopaenia, anaemia and neutropaenia. Other more common toxicities included gastrointestinal upset (diarrhoea, nausea and vomiting in 57%, 57% and 35% of patients respectively) and peripheral neuropathy (in 36% of patients).

We combined bortezomib with dasatinib. Dasatinib was selected as the most potent TKI available in the clinic and therefore would enable maximal inhibition of BCR-ABL activity in combination with potent proteasomal inhibition by bortezomib. We did not investigate the molecular pathways which may link BCR-ABL activity and the proteasome, though we provide evidence that PI does not affect BCR-ABL activity and TKI does not significantly affect proteasome activity as evident by accumulation of polyubiquitinated proteins. It has been demonstrated previously by analysis of RNA transcripts that primitive Ph+HSC (CD34+38-) express relatively higher levels of BCR-ABL than more mature CML cells (4). These cells may have relatively higher proteasome activity if the association demonstrated in cell lines holds true (2). We hypothesised therefore that the proteasome and BCR-ABL may provide 2 targets and concomitant inhibiton of these would be synergistic. Our results in CD34+ cells are consistent with this demonstrating slight synergism to synergism seen at fixed ratio combinations of dasatinib and bortezomib at clinically relevant concentrations (**Table 3.3**). We did not assess CD34+38- cells or non-CML cells in this way.

Other groups have assessed TKI in combination with PI in CML cells. Gatto *et al.* exposed BC CML cell lines to IM and bortezomib simultaneously at a single concentration of bortezomib (11nM) and failed to demonstrate synergy (1). Aichberger *et al.* combined either IM or nilotinib with MG132 in BCR-ABL+ cell lines (including K562 and Ba/F3 cells) and assessed by ^{3}H-thymidine incorporation for cell proliferation. No data was presented in the paper though it was stated that no synergy was seen (155). We are the first to present data where dasatinib has been combined with bortezomib in CD34+ CML samples. Different factors may contribute to the more positive data generated in this project: dasatinib would be expected to induce more potent BCR-ABL inhibition than IM or nilotinib; and we assessed untreated CP CML CD34+ samples in contrast to the BC CML cell lines and transduced murine cells used by other groups.

4.6 Potential future work

There is scope to extend the work produced by this project from cell line, patient samples and stem cell data.

4.6.1 Extension of cell line data

We provided evidence that BCR-ABL+ cell lines have detectable proteasome activity and furthermore this activity may vary between BCR-ABL mutations. It would be important to establish whether this translates to a subtle difference in susceptibility to the apoptotic and antiproliferative effects and levels of detectable proteasome activity. This could be assessed with a series of dose-response experiments using bortezomib and the 4 BCR-ABL+ Ba/F3 mutants. Confirmed differences would imply a biological difference between the cell lines in line with current work in this field.

4.6.2 Extension of patient sample data

All CD34+ samples were taken at diagnosis from patients with CP CML. It would be of relevance clinically to establish whether BCR-ABL+ cells taken from patients who have failed IM therapy due to IM-resistance of intolerance demonstrate comparable sensitivity. Such cell samples are available through a collaborator (F. Niccolini) and testing of these forms the basis of a future project.

4.6.3 Extension of stem cell data

We did not perform functional analysis of the CD34+ CML cells to characterise the influence of bortezomib on the ability of cells to form colonies or to persist in long term culture. To confirm an effect on the most primitive quiescent population of Ph+HSC It is important to establish whether bortezomib (as monotherapy or in combination with TKI) influences LTC-IC potential. This could be performed as a 4-arm experiment comparing untreated CD34+ CML cells with dasatinib and bortezomib alone or in combination. Such an experiment would also yield additional CFU data, a further measure of proliferation and differentiation. A logical extension to LTC-IC would involve transplantation of treated and untreated Ph+HSC into immune compromised mice. Such work has been performed by Guzman *et al.* where normal (cord blood) and AML CD34+38- cells were treated with a combination of idarubicin and MG132 prior to transplantation into NOD/SCID mice. Engraftment was significantly impaired in the treated AML

population when compared to control indicating a selective effect of this combination on the disease HSC (7).

Functional HSC assays may also characterise any affect of bortezomib on the promyelocytic leukaemia (PML) gene. PML is a tumour suppressor that controls apoptosis, proliferation, senescence and is involved in neoangiogenesis. It is highly expressed in the normal human HSC and is required for HSC maintenance. In Ph+HSC PML is highly expressed and through experiments by which PML knockdown cells were transduced with BCR-ABL it is seen that PML is required for maintenance of LTC-IC. Furthermore downregulation of PML is effective for eradication of leukaemia initiating cells (204). PML is a target for proteasomal breakdown and PI exposure (MG132) of cell lines (HEK) increases PML levels (205). It may be speculated that the effect of bortezomib on the primitive population may involve an effect on PML.

4.6.4 Future clinical trials

The data generated from this project has potential clinical translation. As a front-line therapy bortezomib use may be difficult to support. IM is an effective well tolerated oral drug with 7y of clinical trial data supporting its use. Bortezomib would be a clinically unproven, is only available as an intra-venous infusion and though relatively well tolerated, has potential toxicities which may be considered unacceptable when compared to IM. It is likely that an appropriate role for bortezomib would be for those resistant to or intolerant of current treatment, or as a combination therapy with TKI. We have generated data that suggests that bortezomib targets the primitive Ph+HSC population and so would be expected *in vivo* to reduce MRD to undetectable levels – though clearly *in vivo* supportive data would be required prior to use in patients, for example through transplantation of NOD/SCID mice with treated cells. The combination data of dasatinib and bortezomib are of particular interest. These drugs used together as front-line therapy may enable a significant and rapid reduction of disease burden with a presumed associated improved outcome – as shown for those in the IRIS trial who had a relatively rapid response to IM. An alternative strategy would be to pursue the use of bortezomib in those with TKI-resistance, in particular those with the T315I mutation. A combination of bortezomib and dasatinib in this group may enable control of T315I and prevent selection for other TKI-sensitive mutations. New PI are under development with successful application in clinical trials

involving patients with mantle cell lymphoma or multiple myeloma. Of these Carfilzomib is of particular interest as it is reported to have similar CT-L inhibitory activity to bortezomib, though with fewer “off-target” effects and so reduced unwanted toxicity (200). It would therefore be of particular interest to assess this drug *in vitro* as bortezomib has been assessed here.

5 CONCLUSIONS

CML is treated effectively with TKI, however two key problems remain - the insensitivity of CM HSC to TKI and the emergence of TKI-resistant BCR-ABL mutations. BCR-ABL activity is associated with increased proteasome activity and PI are cytotoxic against CML cell lines. We demonstrate that bortezomib is antiproliferative and induces apoptosis in CD34+ cells taken at diagnosis from patients with CP CML cells, with an LD_{50} below concentrations achieved *in vivo*. We also demonstrate for the first time that CD34+38- CML cells, representing the TKI-insensitive primitive HSC, are similarly susceptible. Bortezomib is associated with inhibition of proteasome activity, however that of BCR-ABL appears unaffected. Significant synergy is seen when bortezomib and dasatinib are used in combination. We also demonstrate that bortezomib is effective in inhibiting proteasome activity and inducing apoptosis in cell lines expressing BCR-ABL mutations, including T315I. Therefore we believe that bortezomib offers a potential therapeutic option in CML by targeting both TKI-insensitive stem cells and TKI-resistant BCR-ABL mutations.

6 REFERENCES

1. Gatto S, Scappini B, Pham L, Onida F, Milella M, Ball G, et al. The proteasome inhibitor PS-341 inhibits growth and induces apoptosis in Bcr/Abl-positive cell lines sensitive and resistant to imatinib mesylate. Haematologica. 2003 Aug;88(8):853-63.
2. Magill L, Lynas J, Morris TC, Walker B, Irvine AE. Proteasome proteolytic activity in hematopoietic cells from patients with chronic myeloid leukemia and multiple myeloma. Haematologica. 2004 Dec;89(12):1428-33.
3. Yan H, Wang YC, Li D, Wang Y, Liu W, Wu YL, et al. Arsenic trioxide and proteasome inhibitor bortezomib synergistically induce apoptosis in leukemic cells: the role of protein kinase Cdelta. Leukemia. 2007 Jul;21(7):1488-95.
4. Copland M, Hamilton A, Elrick LJ, Baird JW, Allan EK, Jordanides N, et al. Dasatinib (BMS-354825) targets an earlier progenitor population than imatinib in primary CML but does not eliminate the quiescent fraction. Blood. 2006 Jun 1;107(11):4532-9.
5. Hideshima T, Richardson P, Chauhan D, Palombella VJ, Elliott PJ, Adams J, et al. The proteasome inhibitor PS-341 inhibits growth, induces apoptosis, and overcomes drug resistance in human multiple myeloma cells. Cancer Res. 2001 Apr 1;61(7):3071-6.
6. Stapnes C, Doskeland AP, Hatfield K, Ersvaer E, Ryningen A, Lorens JB, et al. The proteasome inhibitors bortezomib and PR-171 have antiproliferative and proapoptotic effects on primary human acute myeloid leukaemia cells. Br J Haematol. 2007 Mar;136(6):814-28.
7. Guzman ML, Neering SJ, Upchurch D, Grimes B, Howard DS, Rizzieri DA, et al. Nuclear factor-kappaB is constitutively activated in primitive human acute myelogenous leukemia cells. Blood. 2001 Oct 15;98(8):2301-7.
8. Servida F, Soligo D, Delia D, Henderson C, Brancolini C, Lombardi L, et al. Sensitivity of human multiple myelomas and myeloid leukemias to the proteasome inhibitor I. Leukemia. 2005 Dec;19(12):2324-31.
9. Colado E, Alvarez-Fernandez S, Maiso P, Martin-Sanchez J, Vidriales MB, Garayoa M, et al. The effect of the proteasome inhibitor bortezomib on acute myeloid leukemia cells and drug resistance associated with the CD34+ immature phenotype. Haematologica. 2008 Jan;93(1):57-66.
10. Dy GK, Thomas JP, Wilding G, Bruzek L, Mandrekar S, Erlichman C, et al. A phase I and pharmacologic trial of two schedules of the proteasome inhibitor, PS-

341 (bortezomib, velcade), in patients with advanced cancer. Clin Cancer Res. 2005 May 1;11(9):3410-6.

11. Hehlmann R, Hochhaus A, Baccarani M. Chronic myeloid leukaemia. Lancet. 2007 Jul 28;370(9584):342-50.
12. Daley GQ, Van Etten RA, Baltimore D. Induction of chronic myelogenous leukemia in mice by the P210bcr/abl gene of the Philadelphia chromosome. Science. 1990 Feb 16;247(4944):824-30.
13. Evans CA, Owen-Lynch PJ, Whetton AD, Dive C. Activation of the Abelson tyrosine kinase activity is associated with suppression of apoptosis in hemopoietic cells. Cancer Res. 1993 Apr 15;53(8):1735-8.
14. Biernaux C, Loos M, Sels A, Huez G, Stryckmans P. Detection of major bcr-abl gene expression at a very low level in blood cells of some healthy individuals. Blood. 1995 Oct 15;86(8):3118-22.
15. Bose S, Deininger M, Gora-Tybor J, Goldman JM, Melo JV. The presence of typical and atypical BCR-ABL fusion genes in leukocytes of normal individuals: biologic significance and implications for the assessment of minimal residual disease. Blood. 1998 Nov 1;92(9):3362-7.
16. Preston DL, Kusumi S, Tomonaga M, Izumi S, Ron E, Kuramoto A, et al. Cancer incidence in atomic bomb survivors. Part III. Leukemia, lymphoma and multiple myeloma, 1950-1987. Radiat Res. 1994 Feb;137(2 Suppl):S68-97.
17. Reuther JY, Reuther GW, Cortez D, Pendergast AM, Baldwin AS, Jr. A requirement for NF-kappaB activation in Bcr-Abl-mediated transformation. Genes Dev. 1998 Apr 1;12(7):968-81.
18. Mandanas RA, Leibowitz DS, Gharehbaghi K, Tauchi T, Burgess GS, Miyazawa K, et al. Role of p21 RAS in p210 bcr-abl transformation of murine myeloid cells. Blood. 1993 Sep 15;82(6):1838-47.
19. Skorski T, Nieborowska-Skorska M, Szczylik C, Kanakaraj P, Perrotti D, Zon G, et al. C-RAF-1 serine/threonine kinase is required in BCR/ABL-dependent and normal hematopoiesis. Cancer Res. 1995 Jun 1;55(11):2275-8.
20. Skorski T, Kanakaraj P, Nieborowska-Skorska M, Ratajczak MZ, Wen SC, Zon G, et al. Phosphatidylinositol-3 kinase activity is regulated by BCR/ABL and is required for the growth of Philadelphia chromosome-positive cells. Blood. 1995 Jul 15;86(2):726-36.
21. Skorski T, Bellacosa A, Nieborowska-Skorska M, Majewski M, Martinez R, Choi JK, et al. Transformation of hematopoietic cells by BCR/ABL requires activation of a PI-3k/Akt-dependent pathway. Embo J. 1997 Oct 15;16(20):6151-61.

22. Jain SK, Susa M, Keeler ML, Carlesso N, Druker B, Varticovski L. PI 3-kinase activation in BCR/abl-transformed hematopoietic cells does not require interaction of p85 SH2 domains with p210 BCR/abl. Blood. 1996 Sep 1;88(5):1542-50.
23. Coppo P, Dusanter-Fourt I, Millot G, Nogueira MM, Dugray A, Bonnet ML, et al. Constitutive and specific activation of STAT3 by BCR-ABL in embryonic stem cells. Oncogene. 2003 Jun 26;22(26):4102-10.
24. Nieborowska-Skorska M, Wasik MA, Slupianek A, Salomoni P, Kitamura T, Calabretta B, et al. Signal transducer and activator of transcription (STAT)5 activation by BCR/ABL is dependent on intact Src homology (SH)3 and SH2 domains of BCR/ABL and is required for leukemogenesis. J Exp Med. 1999 Apr 19;189(8):1229-42.
25. Coppo P, Flamant S, De Mas V, Jarrier P, Guillier M, Bonnet ML, et al. BCR-ABL activates STAT3 via JAK and MEK pathways in human cells. Br J Haematol. 2006 Jul;134(2):171-9.
26. Kindler T, Breitenbuecher F, Kasper S, Stevens T, Carius B, Gschaidmeier H, et al. In BCR-ABL-positive cells, STAT-5 tyrosine-phosphorylation integrates signals induced by imatinib mesylate and Ara-C. Leukemia. 2003 Jun;17(6):999-1009.
27. Whang J, Frei E, 3rd, Tjio JH, Carbone PP, Brecher G. The Distribution of the Philadelphia Chromosome in Patients with Chronic Myelogenous Leukemia. Blood. 1963 Dec;22:664-73.
28. Rastrick JM, Fitzgerald PH, Gunz FW. Direct evidence for presence of Ph-1 chromosome in erythroid cells. Br Med J. 1968 Jan 13;1(5584):96-8.
29. Martin PJ, Najfeld V, Hansen JA, Penfold GK, Jacobson RJ, Fialkow PJ. Involvement of the B-lymphoid system in chronic myelogenous leukaemia. Nature. 1980 Sep 4;287(5777):49-50.
30. Takahashi N, Miura I, Saitoh K, Miura AB. Lineage involvement of stem cells bearing the philadelphia chromosome in chronic myeloid leukemia in the chronic phase as shown by a combination of fluorescence-activated cell sorting and fluorescence in situ hybridization. Blood. 1998 Dec 15;92(12):4758-63.
31. Dean M, Fojo T, Bates S. Tumour stem cells and drug resistance. Nat Rev Cancer. 2005 Apr;5(4):275-84.
32. Jorgensen HG, Holyoake TL. A comparison of normal and leukemic stem cell biology in Chronic Myeloid Leukemia. Hematol Oncol. 2001 Sep;19(3):89-106.
33. Jiang X, Lopez A, Holyoake T, Eaves A, Eaves C. Autocrine production and action of IL-3 and granulocyte colony-stimulating factor in chronic myeloid leukemia. Proc Natl Acad Sci U S A. 1999 Oct 26;96(22):12804-9.

34. Holyoake T, Jiang X, Eaves C, Eaves A. Isolation of a highly quiescent subpopulation of primitive leukemic cells in chronic myeloid leukemia. Blood. 1999 Sep 15;94(6):2056-64.
35. Lapidot T, Sirard C, Vormoor J, Murdoch B, Hoang T, Caceres-Cortes J, et al. A cell initiating human acute myeloid leukaemia after transplantation into SCID mice. Nature. 1994 Feb 17;367(6464):645-8.
36. Cox CV, Evely RS, Oakhill A, Pamphilon DH, Goulden NJ, Blair A. Characterization of acute lymphoblastic leukemia progenitor cells. Blood. 2004 Nov 1;104(9):2919-25.
37. Terstappen LW, Huang S, Safford M, Lansdorp PM, Loken MR. Sequential generations of hematopoietic colonies derived from single nonlineage-committed CD34+CD38- progenitor cells. Blood. 1991 Mar 15;77(6):1218-27.
38. Liu H, Verfaillie CM. Myeloid-lymphoid initiating cells (ML-IC) are highly enriched in the rhodamine-c-kit(+)CD33(-)CD38(-) fraction of umbilical cord CD34(+) cells. Exp Hematol. 2002 Jun;30(6):582-9.
39. Blair A, Hogge DE, Sutherland HJ. Most acute myeloid leukemia progenitor cells with long-term proliferative ability in vitro and in vivo have the phenotype CD34(+)/CD71(-)/HLA-DR. Blood. 1998 Dec 1;92(11):4325-35.
40. Feuring-Buske M, Hogge DE. Hoechst 33342 efflux identifies a subpopulation of cytogenetically normal CD34(+)CD38(-) progenitor cells from patients with acute myeloid leukemia. Blood. 2001 Jun 15;97(12):3882-9.
41. Eisterer W, Jiang X, Christ O, Glimm H, Lee KH, Pang E, et al. Different subsets of primary chronic myeloid leukemia stem cells engraft immunodeficient mice and produce a model of the human disease. Leukemia. 2005 Mar;19(3):435-41.
42. Holyoake TL, Jiang X, Jorgensen HG, Graham S, Alcorn MJ, Laird C, et al. Primitive quiescent leukemic cells from patients with chronic myeloid leukemia spontaneously initiate factor-independent growth in vitro in association with up-regulation of expression of interleukin-3. Blood. 2001 Feb 1;97(3):720-8.
43. Melo JV, Barnes DJ. Chronic myeloid leukaemia as a model of disease evolution in human cancer. Nat Rev Cancer. 2007 Jun;7(6):441-53.
44. Jamieson CH, Ailles LE, Dylla SJ, Muijtjens M, Jones C, Zehnder JL, et al. Granulocyte-macrophage progenitors as candidate leukemic stem cells in blast-crisis CML. N Engl J Med. 2004 Aug 12;351(7):657-67.
45. Minami Y, Stuart SA, Ikawa T, Jiang Y, Banno A, Hunton IC, et al. BCR-ABL-transformed GMP as myeloid leukemic stem cells. Proc Natl Acad Sci U S A. 2008 Nov 18;105(46):17967-72.

46. Baccarani M, Saglio G, Goldman J, Hochhaus A, Simonsson B, Appelbaum F, et al. Evolving concepts in the management of chronic myeloid leukemia: recommendations from an expert panel on behalf of the European LeukemiaNet. Blood. 2006 Sep 15;108(6):1809-20.
47. Druker BJ, Sawyers CL, Kantarjian H, Resta DJ, Reese SF, Ford JM, et al. Activity of a specific inhibitor of the BCR-ABL tyrosine kinase in the blast crisis of chronic myeloid leukemia and acute lymphoblastic leukemia with the Philadelphia chromosome. N Engl J Med. 2001 Apr 5;344(14):1038-42.
48. Druker BJ, Talpaz M, Resta DJ, Peng B, Buchdunger E, Ford JM, et al. Efficacy and safety of a specific inhibitor of the BCR-ABL tyrosine kinase in chronic myeloid leukemia. N Engl J Med. 2001 Apr 5;344(14):1031-7.
49. Kantarjian H, Sawyers C, Hochhaus A, Guilhot F, Schiffer C, Gambacorti-Passerini C, et al. Hematologic and cytogenetic responses to imatinib mesylate in chronic myelogenous leukemia. N Engl J Med. 2002 Feb 28;346(9):645-52.
50. O'Brien SG, Guilhot F, Larson RA, Gathmann I, Baccarani M, Cervantes F, et al. Imatinib compared with interferon and low-dose cytarabine for newly diagnosed chronic-phase chronic myeloid leukemia. N Engl J Med. 2003 Mar 13;348(11):994-1004.
51. Druker BJ, Guilhot F, O'Brien SG, Gathmann I, Kantarjian H, Gattermann N, et al. Five-year follow-up of patients receiving imatinib for chronic myeloid leukemia. N Engl J Med. 2006 Dec 7;355(23):2408-17.
52. O'Brien SG, Guilhot F, Goldman J, Hochhaus A, Hughes T, Radich J, et al. International Randomized Study of Interferon Versus STI571 (IRIS) 7-Year Follow-up: Sustained Survival, Low Rate of Transformation and Increased Rate of Major Molecular Response (MMR) in Patients (pts) with Newly Diagnosed Chronic Myeloid Leukemia in Chronic Phase (CMLCP) Treated with Imatinib (IM). Blood. 2008 Nov 16;112(11):186.
53. de Lavallade H, Apperley JF, Khorashad JS, Milojkovic D, Reid AG, Bua M, et al. Imatinib for newly diagnosed patients with chronic myeloid leukemia: incidence of sustained responses in an intention-to-treat analysis. J Clin Oncol. 2008 Jul 10;26(20):3358-63.
54. Lucas CM, Wang L, Austin GM, Knight K, Watmough SJ, Shwe KH, et al. A population study of imatinib in chronic myeloid leukaemia demonstrates lower efficacy than in clinical trials. Leukemia. 2008 Oct;22(10):1963-6.
55. Hughes TP, Kaeda J, Branford S, Rudzki Z, Hochhaus A, Hensley ML, et al. Frequency of major molecular responses to imatinib or interferon alfa plus

cytarabine in newly diagnosed chronic myeloid leukemia. N Engl J Med. 2003 Oct 9;349(15):1423-32.

56. Mauro MJ, Druker BJ, Maziarz RT. Divergent clinical outcome in two CML patients who discontinued imatinib therapy after achieving a molecular remission. Leuk Res. 2004 May;28 Suppl 1:S71-3.

57. Rousselot P, Huguet F, Rea D, Legros L, Cayuela JM, Maarek O, et al. Imatinib mesylate discontinuation in patients with chronic myelogenous leukemia in complete molecular remission for more than 2 years. Blood. 2007 Jan 1;109(1):58-60.

58. Merante S, Orlandi E, Bernasconi P, Calatroni S, Boni M, Lazzarino M. Outcome of four patients with chronic myeloid leukemia after imatinib mesylate discontinuation. Haematologica. 2005 Jul;90(7):979-81.

59. Cortes J, O'Brien S, Kantarjian H. Discontinuation of imatinib therapy after achieving a molecular response. Blood. 2004 Oct 1;104(7):2204-5.

60. Graham SM, Jorgensen HG, Allan E, Pearson C, Alcorn MJ, Richmond L, et al. Primitive, quiescent, Philadelphia-positive stem cells from patients with chronic myeloid leukemia are insensitive to STI571 in vitro. Blood. 2002 Jan 1;99(1):319-25.

61. Holtz MS, Slovak ML, Zhang F, Sawyers CL, Forman SJ, Bhatia R. Imatinib mesylate (STI571) inhibits growth of primitive malignant progenitors in chronic myelogenous leukemia through reversal of abnormally increased proliferation. Blood. 2002 May 15;99(10):3792-800.

62. Jorgensen HG, Allan EK, Graham SM, Godden JL, Richmond L, Elliott MA, et al. Lonafarnib reduces the resistance of primitive quiescent CML cells to imatinib mesylate in vitro. Leukemia. 2005 Jul;19(7):1184-91.

63. Holtz MS, Forman SJ, Bhatia R. Nonproliferating CML CD34+ progenitors are resistant to apoptosis induced by a wide range of proapoptotic stimuli. Leukemia. 2005 Jun;19(6):1034-41.

64. Bhatia R, Holtz M, Niu N, Gray R, Snyder DS, Sawyers CL, et al. Persistence of malignant hematopoietic progenitors in chronic myelogenous leukemia patients in complete cytogenetic remission following imatinib mesylate treatment. Blood. 2003 Jun 15;101(12):4701-7.

65. Chu S, A. L, McDonald T, Snyder S, Forman SJ, Bhatia R. Persistence of Leukemia Stem Cells in Chronic Myelogenous Leukemia Patients in Complete Cytogenetic Remission on Imatinib Treatment for 5 Years Blood. 2008 November 16;112(11):194.

66. Wolff NC, Ilaria RL, Jr. Establishment of a murine model for therapy-treated chronic myelogenous leukemia using the tyrosine kinase inhibitor STI571. Blood. 2001 Nov 1;98(9):2808-16.
67. Hochhaus A, Kreil S, Corbin AS, La Rosee P, Muller MC, Lahaye T, et al. Molecular and chromosomal mechanisms of resistance to imatinib (STI571) therapy. Leukemia. 2002 Nov;16(11):2190-6.
68. Jabbour E, Kantarjian H, Jones D, Talpaz M, Bekele N, O'Brien S, et al. Frequency and clinical significance of BCR-ABL mutations in patients with chronic myeloid leukemia treated with imatinib mesylate. Leukemia. 2006 Oct;20(10):1767-73.
69. Lahaye T, Riehm B, Berger U, Paschka P, Muller MC, Kreil S, et al. Response and resistance in 300 patients with BCR-ABL-positive leukemias treated with imatinib in a single center: a 4.5-year follow-up. Cancer. 2005 Apr 15;103(8):1659-69.
70. Soverini S, Colarossi S, Gnani A, Rosti G, Castagnetti F, Poerio A, et al. Contribution of ABL kinase domain mutations to imatinib resistance in different subsets of Philadelphia-positive patients: by the GIMEMA Working Party on Chronic Myeloid Leukemia. Clin Cancer Res. 2006 Dec 15;12(24):7374-9.
71. Branford S, Rudzki Z, Walsh S, Parkinson I, Grigg A, Szer J, et al. Detection of BCR-ABL mutations in patients with CML treated with imatinib is virtually always accompanied by clinical resistance, and mutations in the ATP phosphate-binding loop (P-loop) are associated with a poor prognosis. Blood. 2003 Jul 1;102(1):276-83.
72. Ernst T, Erben P, Muller MC, Paschka P, Schenk T, Hoffmann J, et al. Dynamics of BCR-ABL mutated clones prior to hematologic or cytogenetic resistance to imatinib. Haematologica. 2008 Feb;93(2):186-92.
73. Jabbour E, Kantarjian H, Jones D, Breeden M, Garcia-Manero G, O'Brien S, et al. Characteristics and outcome of patients with chronic myeloid leukemia and T315I mutation following failure of imatinib mesylate therapy. Blood. 2008 Apr 10.
74. Nicolini FE, Hayette S, Corm S, Bachy E, Bories D, Tulliez M, et al. Clinical outcome of 27 imatinib mesylate-resistant chronic myelogenous leukemia patients harboring a T315I BCR-ABL mutation. Haematologica. 2007 Sep;92(9):1238-41.
75. O'Hare T, Walters DK, Stoffregen EP, Jia T, Manley PW, Mestan J, et al. In vitro activity of Bcr-Abl inhibitors AMN107 and BMS-354825 against clinically relevant imatinib-resistant Abl kinase domain mutants. Cancer Res. 2005 Jun 1;65(11):4500-5.

76. Leonard GD, Fojo T, Bates SE. The role of ABC transporters in clinical practice. Oncologist. 2003;8(5):411-24.
77. Mukai M, Che XF, Furukawa T, Sumizawa T, Aoki S, Ren XQ, et al. Reversal of the resistance to STI571 in human chronic myelogenous leukemia K562 cells. Cancer Sci. 2003 Jun;94(6):557-63.
78. Rousselot P, Huguet F, Rea D, Legros L, Cayuela JM, Maarek O, et al. Imatinib mesylate discontinuation in patients with chronic myelogenous leukemia in complete molecular remission for more than two years. Blood. 2006 Sep 14.
79. Mahon FX, Belloc F, Lagarde V, Chollet C, Moreau-Gaudry F, Reiffers J, et al. MDR1 gene overexpression confers resistance to imatinib mesylate in leukemia cell line models. Blood. 2003 Mar 15;101(6):2368-73.
80. Galimberti S, Cervetti G, Cecconi N, Fazzi R, Pacini S, Guerrini F, et al. Quantitative molecular evaluation of minimal residual disease in patients with chronic lymphocytic leukemia: efficacy of in vivo purging by alemtuzumab (Campath-1H). J Immunother. 2004 Sep-Oct;27(5):389-93.
81. Radujkovic A, Schad M, Topaly J, Veldwijk MR, Laufs S, Schultheis BS, et al. Synergistic activity of imatinib and 17-AAG in imatinib-resistant CML cells overexpressing BCR-ABL--Inhibition of P-glycoprotein function by 17-AAG. Leukemia. 2005 Jul;19(7):1198-206.
82. Burger H, van Tol H, Boersma AW, Brok M, Wiemer EA, Stoter G, et al. Imatinib mesylate (STI571) is a substrate for the breast cancer resistance protein (BCRP)/ABCG2 drug pump. Blood. 2004 Nov 1;104(9):2940-2.
83. Jordanides NE, Jorgensen HG, Holyoake TL, Mountford JC. Functional ABCG2 is overexpressed on primary CML CD34+ cells and is inhibited by imatinib mesylate. Blood. 2006 Aug 15;108(4):1370-3.
84. Carew JS, Nawrocki ST, Kahue CN, Zhang H, Yang C, Chung L, et al. Targeting autophagy augments the anticancer activity of the histone deacetylase inhibitor SAHA to overcome Bcr-Abl-mediated drug resistance. Blood. 2007 Jul 1;110(1):313-22.
85. Nakanishi T, Shiozawa K, Hassel BA, Ross DD. Complex interaction of BCRP/ABCG2 and imatinib in BCR-ABL-expressing cells: BCRP-mediated resistance to imatinib is attenuated by imatinib-induced reduction of BCRP expression. Blood. 2006 Jul 15;108(2):678-84.
86. White PL, Barton R, Guiver M, Linton CJ, Wilson S, Smith M, et al. A consensus on fungal polymerase chain reaction diagnosis?: a United Kingdom-Ireland

evaluation of polymerase chain reaction methods for detection of systemic fungal infections. J Mol Diagn. 2006 Jul;8(3):376-84.

87. White D, Saunders V, Lyons AB, Branford S, Grigg A, To LB, et al. In vitro sensitivity to imatinib-induced inhibition of ABL kinase activity is predictive of molecular response in patients with de novo CML. Blood. 2005 Oct 1;106(7):2520-6.

88. Wu J, Meng F, Kong LY, Peng Z, Ying Y, Bornmann WG, et al. Association between imatinib-resistant BCR-ABL mutation-negative leukemia and persistent activation of LYN kinase. J Natl Cancer Inst. 2008 Jul 2;100(13):926-39.

89. Nagar B, Bornmann WG, Pellicena P, Schindler T, Veach DR, Miller WT, et al. Crystal structures of the kinase domain of c-Abl in complex with the small molecule inhibitors PD173955 and imatinib (STI-571). Cancer Res. 2002 Aug 1;62(15):4236-43.

90. Shah NP, Tran C, Lee FY, Chen P, Norris D, Sawyers CL. Overriding imatinib resistance with a novel ABL kinase inhibitor. Science. 2004 Jul 16;305(5682):399-401.

91. Hochhaus A, Baccarani M, Deininger M, Apperley JF, Lipton JH, Goldberg SL, et al. Dasatinib induces durable cytogenetic responses in patients with chronic myelogenous leukemia in chronic phase with resistance or intolerance to imatinib. Leukemia. 2008 Apr 10.

92. Baccarani M, Rosti G, Saglio G, Cortes J, Stone R, Niederwieser DW, et al. Dasatinib Time to and Durability of Major and Complete Cytogenetic Response (MCyR and CCyR) in Patients with Chronic Myeloid Leukemia in Chronic Phase (CML-CP) Blood. 2008.

93. Hochhaus A, Muller C, Radich J, Branford S, Hanfstein B, Rousselot P, et al. Dasatinib-Associated Major Molecular Responses Are Rapidly Achieved in Patients with Chronic Myeloid Leukemia in Chronic Phase (CML-CP) Following Resistance, Suboptimal Response, or Intolerance on Imatinib Blood. 2008.

94. Guilhot F, Apperley J, Kim DW, Bullorsky EO, Baccarani M, Roboz GJ, et al. Dasatinib induces significant hematologic and cytogenetic responses in patients with imatinib-resistant or -intolerant chronic myeloid leukemia in accelerated phase. Blood. 2007 May 15;109(10):4143-50.

95. Weisberg E, Manley PW, Breitenstein W, Bruggen J, Cowan-Jacob SW, Ray A, et al. Characterization of AMN107, a selective inhibitor of native and mutant Bcr-Abl. Cancer Cell. 2005 Feb;7(2):129-41.

96. Kantarjian HM, Giles F, Gattermann N, Bhalla K, Alimena G, Palandri F, et al. Nilotinib (formerly AMN107), a highly selective BCR-ABL tyrosine kinase inhibitor, is effective in patients with Philadelphia chromosome-positive chronic myelogenous leukemia in chronic phase following imatinib resistance and intolerance. Blood. 2007 Nov 15;110(10):3540-6.

97. Kantarjian H, Giles F, Bhalla K, Larson R, Gattermann N, Ottmann O, et al. Nilotinib in Chronic Myeloid Leukemia Patients in Chronic Phase (CML-CP) with Imatinib Resistance or Intolerance: 2-Year Follow-up Results of a Phase 2 Study Blood. 2008.

98. le Coutre P, Ottmann OG, Giles F, Kim DW, Cortes J, Gattermann N, et al. Nilotinib (formerly AMN107), a highly selective BCR-ABL tyrosine kinase inhibitor, is active in patients with imatinib-resistant or -intolerant accelerated-phase chronic myelogenous leukemia. Blood. 2008 Feb 15;111(4):1834-9.

99. Cortes J, Khoury J, Corm S, Nicolini F, Lipton JH, Jones D, et al. Safety and Efficacy of Subcutaneous (SC) Omacetaxine Mepesuccinate in Imatinib(IM)-Resistant Chronic Myeloid Leukemia (CML) Patients (pts) with the T315I Mutation – Results of An Ongoing Multicenter Phase II Study. Blood. 2008 November 16;112(11):3239.

100. Rosti G, Castagnetti F, Poerio A, Breccia M, Levato L, Capucci A, et al. High and Early Rates of Cytogenetic and Molecular Response with Nilotinib 800 Mg Daily as First Line Treatment of Ph-Positive Chronic Myeloid Leukemia in Chronic Phase: Results of a Phase 2 Trial of the GIMEMA CML Working Party blood. 2008.

101. Quintas-Cardama A, Kantarjian H, Jones D, Nicaise C, O'Brien S, Giles F, et al. Dasatinib (BMS-354825) is active in Philadelphia chromosome-positive chronic myelogenous leukemia after imatinib and nilotinib (AMN107) therapy failure. Blood. 2007 Jan 15;109(2):497-9.

102. Bradeen HA, Eide CA, O'Hare T, Johnson KJ, Willis SG, Lee FY, et al. Comparison of imatinib mesylate, dasatinib (BMS-354825), and nilotinib (AMN107) in an N-ethyl-N-nitrosourea (ENU)-based mutagenesis screen: high efficacy of drug combinations. Blood. 2006 Oct 1;108(7):2332-8.

103. Catley L, Weisberg E, Kiziltepe T, Tai YT, Hideshima T, Neri P, et al. Aggresome induction by proteasome inhibitor bortezomib and alpha-tubulin hyperacetylation by tubulin deacetylase (TDAC) inhibitor LBH589 are synergistic in myeloma cells. Blood. 2006 Nov 15;108(10):3441-9.

104. Jorgensen HG, Allan EK, Jordanides NE, Mountford JC, Holyoake TL. Nilotinib exerts equipotent antiproliferative effects to imatinib and does not induce apoptosis in CD34+ CML cells. Blood. 2007 May 1;109(9):4016-9.
105. Gratwohl A, Brand R, Apperley J, Crawley C, Ruutu T, Corradini P, et al. Allogeneic hematopoietic stem cell transplantation for chronic myeloid leukemia in Europe 2006: transplant activity, long-term data and current results. An analysis by the Chronic Leukemia Working Party of the European Group for Blood and Marrow Transplantation (EBMT). Haematologica. 2006 Apr;91(4):513-21.
106. Heaney NB, Holyoake TL. Therapeutic targets in chronic myeloid leukaemia. Hematological Oncology. 2007;25:66-75.
107. George P, Bali P, Annavarapu S, Scuto A, Fiskus W, Guo F, et al. Combination of the histone deacetylase inhibitor LBH589 and the hsp90 inhibitor 17-AAG is highly active against human CML-BC cells and AML cells with activating mutation of FLT-3. Blood. 2005 Feb 15;105(4):1768-76.
108. Isaacs JS, Xu W, Neckers L. Heat shock protein 90 as a molecular target for cancer therapeutics. Cancer Cell. 2003 Mar;3(3):213-7.
109. Blagosklonny MV, Fojo T, Bhalla KN, Kim JS, Trepel JB, Figg WD, et al. The Hsp90 inhibitor geldanamycin selectively sensitizes Bcr-Abl-expressing leukemia cells to cytotoxic chemotherapy. Leukemia. 2001 Oct;15(10):1537-43.
110. Nimmanapalli R, O'Bryan E, Bhalla K. Geldanamycin and its analogue 17-allylamino-17-demethoxygeldanamycin lowers Bcr-Abl levels and induces apoptosis and differentiation of Bcr-Abl-positive human leukemic blasts. Cancer Res. 2001 Mar 1;61(5):1799-804.
111. Zonder JA, Pemberton P, Brandt H, Mohamed AN, Schiffer CA. The effect of dose increase of imatinib mesylate in patients with chronic or accelerated phase chronic myelogenous leukemia with inadequate hematologic or cytogenetic response to initial treatment. Clin Cancer Res. 2003 Jun;9(6):2092-7.
112. Rosti G, Martinelli G, Castagnetti F, Testoni N, Specchia G, Bassan R, et al. Imatinib 800 mg: Preliminary Results of a Phase 2 Trial of the GIMEMA CML Working Party in Intermediate Sokal risk Patients and Status-of-Art of an Ongoing Multinational, Prospective Randomized Trial of Imatinib Standard Dose (400mg Daily) vs. High Dose (800mg Daily) in High Sokal Risk Patients. Blood. 2005 November 16;106(11).
113. Guerci A, Nicolini F, Maloisel F, Corm S, Legros L, Rigal-Huguet F, et al. Randomized Comparison of Imatinib with Imatinib Combination Therapies in Newly Diagnosed Chronic Myelogenous Leukemia Patients in Chronic Phase:

Design and First Interim Analysis of a Phase 3 Trial from the French CML Group. Blood. 2005 November 16;106(11).

114. Faderl S, Hochhaus A, Hughes T. Monitoring of minimal residual disease in chronic myeloid leukemia. Hematol Oncol Clin North Am. 2004 Jun;18(3):657-70, ix-x.

115. Thiesing JT, Ohno-Jones S, Kolibaba KS, Druker BJ. Efficacy of STI571, an abl tyrosine kinase inhibitor, in conjunction with other antileukemic agents against bcr-abl-positive cells. Blood. 2000 Nov 1;96(9):3195-9.

116. Jorgensen HG, Copland M, Allan EK, Jiang X, Eaves A, Eaves C, et al. Intermittent exposure of primitive quiescent chronic myeloid leukemia cells to granulocyte-colony stimulating factor in vitro promotes their elimination by imatinib mesylate. Clin Cancer Res. 2006 Jan 15;12(2):626-33.

117. Illmer T, Schaich M, Platzbecker U, Freiberg-Richter J, Oelschlagel U, von Bonin M, et al. P-glycoprotein-mediated drug efflux is a resistance mechanism of chronic myelogenous leukemia cells to treatment with imatinib mesylate. Leukemia. 2004 Mar;18(3):401-8.

118. Galimberti S, Cervetti G, Guerrini F, Testi R, Pacini S, Fazzi R, et al. Quantitative molecular monitoring of BCR-ABL and MDR1 transcripts in patients with chronic myeloid leukemia during Imatinib treatment. Cancer Genet Cytogenet. 2005 Oct 1;162(1):57-62.

119. Vigneri P, Wang JY. Induction of apoptosis in chronic myelogenous leukemia cells through nuclear entrapment of BCR-ABL tyrosine kinase. Nat Med. 2001 Feb;7(2):228-34.

120. Aloisi A, Di Gregorio S, Stagno F, Guglielmo P, Mannino F, Sormani MP, et al. BCR-ABL nuclear entrapment kills human CML cells: ex vivo study on 35 patients with the combination of imatinib mesylate and leptomycin B. Blood. 2006 Feb 15;107(4):1591-8.

121. Borthakur G, Kantarjian H, Daley G, Talpaz M, O'Brien S, Garcia-Manero G, et al. Pilot study of lonafarnib, a farnesyl transferase inhibitor, in patients with chronic myeloid leukemia in the chronic or accelerated phase that is resistant or refractory to imatinib therapy. Cancer. 2006 Jan 15;106(2):346-52.

122. Jorgensen HG, Allan EK, Mountford JC, Richmond L, Harrison S, Elliott MA, et al. Enhanced CML stem cell elimination in vitro by bryostatin priming with imatinib mesylate. Exp Hematol. 2005 Oct;33(10):1140-6.

123. Dasmahapatra G, Nguyen TK, Dent P, Grant S. Adaphostin and bortezomib induce oxidative injury and apoptosis in imatinib mesylate-resistant hematopoietic cells expressing mutant forms of Bcr/Abl. Leuk Res. 2006 Oct;30(10):1263-72.
124. Dasmahapatra G, Rahmani M, Dent P, Grant S. The tyrphostin adaphostin interacts synergistically with proteasome inhibitors to induce apoptosis in human leukemia cells through a reactive oxygen species (ROS)-dependent mechanism. Blood. 2006 Jan 1;107(1):232-40.
125. Balabanov S, Gontarewicz A, Ziegler P, Hartmann U, Kammer W, Copland M, et al. Hypusination of eukaryotic initiation factor 5A (eIF5A): a novel therapeutic target in BCR-ABL-positive leukemias identified by a proteomics approach. Blood. 2007 Feb 15;109(4):1701-11.
126. Harrington EA, Bebbington D, Moore J, Rasmussen RK, Ajose-Adeogun AO, Nakayama T, et al. VX-680, a potent and selective small-molecule inhibitor of the Aurora kinases, suppresses tumor growth in vivo. Nat Med. 2004 Mar;10(3):262-7.
127. Giles FJ, Cortes J, Jones D, Bergstrom D, Kantarjian H, Freedman SJ. MK-0457, a novel kinase inhibitor, is active in patients with chronic myeloid leukemia or acute lymphocytic leukemia with the T315I BCR-ABL mutation. Blood. 2007 Jan 15;109(2):500-2.
128. Carter TA, Wodicka LM, Shah NP, Velasco AM, Fabian MA, Treiber DK, et al. Inhibition of drug-resistant mutants of ABL, KIT, and EGF receptor kinases. Proc Natl Acad Sci U S A. 2005 Aug 2;102(31):11011-6.
129. Sun Y. E3 ubiquitin ligases as cancer targets and biomarkers. Neoplasia. 2006 Aug;8(8):645-54.
130. Magill L, Walker B, Irvine AE. The proteasome: a novel therapeutic target in haematopoietic malignancy. Hematology. 2003 Oct;8(5):275-83.
131. Altun M, Galardy PJ, Shringarpure R, Hideshima T, LeBlanc R, Anderson KC, et al. Effects of PS-341 on the activity and composition of proteasomes in multiple myeloma cells. Cancer Res. 2005 Sep 1;65(17):7896-901.
132. Berkers CR, Verdoes M, Lichtman E, Fiebiger E, Kessler BM, Anderson KC, et al. Activity probe for in vivo profiling of the specificity of proteasome inhibitor bortezomib. Nat Methods. 2005 May;2(5):357-62.
133. Kumatori A, Tanaka K, Inamura N, Sone S, Ogura T, Matsumoto T, et al. Abnormally high expression of proteasomes in human leukemic cells. Proc Natl Acad Sci U S A. 1990 Sep;87(18):7071-5.

134. Adams J, Palombella VJ, Sausville EA, Johnson J, Destree A, Lazarus DD, et al. Proteasome inhibitors: a novel class of potent and effective antitumor agents. Cancer Res. 1999 Jun 1;59(11):2615-22.
135. Aggarwal BB. Nuclear factor-kappaB: the enemy within. Cancer Cell. 2004 Sep;6(3):203-8.
136. Kim HJ, Hawke N, Baldwin AS. NF-kappaB and IKK as therapeutic targets in cancer. Cell Death Differ. 2006 May;13(5):738-47.
137. Mihailovic T, Marx M, Auer A, Van Lint J, Schmid M, Weber C, et al. Protein kinase D2 mediates activation of nuclear factor kappaB by Bcr-Abl in Bcr-Abl+ human myeloid leukemia cells. Cancer Res. 2004 Dec 15;64(24):8939-44.
138. Kirchner D, Duyster J, Ottmann O, Schmid RM, Bergmann L, Munzert G. Mechanisms of Bcr-Abl-mediated NF-kappaB/Rel activation. Exp Hematol. 2003 Jun;31(6):504-11.
139. Nawata R, Yujiri T, Nakamura Y, Ariyoshi K, Takahashi T, Sato Y, et al. MEK kinase 1 mediates the antiapoptotic effect of the Bcr-Abl oncogene through NF-kappaB activation. Oncogene. 2003 Oct 30;22(49):7774-80.
140. Bueso-Ramos CE, Rocha FC, Shishodia S, Medeiros LJ, Kantarjian HM, Vadhan-Raj S, et al. Expression of constitutively active nuclear-kappa B RelA transcription factor in blasts of acute myeloid leukemia. Hum Pathol. 2004 Feb;35(2):246-53.
141. Besson A, Dowdy SF, Roberts JM. CDK inhibitors: cell cycle regulators and beyond. Dev Cell. 2008 Feb;14(2):159-69.
142. Kaldis P. Another piece of the p27Kip1 puzzle. Cell. 2007 Jan 26;128(2):241-4.
143. Alkarain A, Jordan R, Slingerland J. p27 deregulation in breast cancer: prognostic significance and implications for therapy. J Mammary Gland Biol Neoplasia. 2004 Jan;9(1):67-80.
144. Grimmler M, Wang Y, Mund T, Cilensek Z, Keidel EM, Waddell MB, et al. Cdk-inhibitory activity and stability of p27Kip1 are directly regulated by oncogenic tyrosine kinases. Cell. 2007 Jan 26;128(2):269-80.
145. Andreu EJ, Lledo E, Poch E, Ivorra C, Albero MP, Martinez-Climent JA, et al. BCR-ABL induces the expression of Skp2 through the PI3K pathway to promote p27Kip1 degradation and proliferation of chronic myelogenous leukemia cells. Cancer Res. 2005 Apr 15;65(8):3264-72.
146. Drexler HC, Pebler S. Inducible p27(Kip1) expression inhibits proliferation of K562 cells and protects against apoptosis induction by proteasome inhibitors. Cell Death Differ. 2003 Mar;10(3):290-301.

147. Yu C, Rahmani M, Conrad D, Subler M, Dent P, Grant S. The proteasome inhibitor bortezomib interacts synergistically with histone deacetylase inhibitors to induce apoptosis in Bcr/Abl+ cells sensitive and resistant to STI571. Blood. 2003 Nov 15;102(10):3765-74.
148. Ling YH, Liebes L, Jiang JD, Holland JF, Elliott PJ, Adams J, et al. Mechanisms of proteasome inhibitor PS-341-induced G(2)-M-phase arrest and apoptosis in human non-small cell lung cancer cell lines. Clin Cancer Res. 2003 Mar;9(3):1145-54.
149. Kamura T, Hara T, Kotoshiba S, Yada M, Ishida N, Imaki H, et al. Degradation of p57Kip2 mediated by SCFSkp2-dependent ubiquitylation. Proc Natl Acad Sci U S A. 2003 Sep 2;100(18):10231-6.
150. Ling YH, Liebes L, Ng B, Buckley M, Elliott PJ, Adams J, et al. PS-341, a novel proteasome inhibitor, induces Bcl-2 phosphorylation and cleavage in association with G2-M phase arrest and apoptosis. Mol Cancer Ther. 2002 Aug;1(10):841-9.
151. Kroemer G, Galluzzi L, Brenner C. Mitochondrial membrane permeabilization in cell death. Physiol Rev. 2007 Jan;87(1):99-163.
152. Kandasamy K, Srinivasula SM, Alnemri ES, Thompson CB, Korsmeyer SJ, Bryant JL, et al. Involvement of proapoptotic molecules Bax and Bak in tumor necrosis factor-related apoptosis-inducing ligand (TRAIL)-induced mitochondrial disruption and apoptosis: differential regulation of cytochrome c and Smac/DIABLO release. Cancer Res. 2003 Apr 1;63(7):1712-21.
153. Luciano F, Jacquel A, Colosetti P, Herrant M, Cagnol S, Pages G, et al. Phosphorylation of Bim-EL by Erk1/2 on serine 69 promotes its degradation via the proteasome pathway and regulates its proapoptotic function. Oncogene. 2003 Oct 2;22(43):6785-93.
154. Kuribara R, Honda H, Matsui H, Shinjyo T, Inukai T, Sugita K, et al. Roles of Bim in apoptosis of normal and Bcr-Abl-expressing hematopoietic progenitors. Mol Cell Biol. 2004 Jul;24(14):6172-83.
155. Aichberger KJ, Mayerhofer M, Krauth MT, Vales A, Kondo R, Derdak S, et al. Low-level expression of proapoptotic Bcl-2-interacting mediator in leukemic cells in patients with chronic myeloid leukemia: role of BCR/ABL, characterization of underlying signaling pathways, and reexpression by novel pharmacologic compounds. Cancer Res. 2005 Oct 15;65(20):9436-44.
156. Kuroda J, Puthalakath H, Cragg MS, Kelly PN, Bouillet P, Huang DC, et al. Bim and Bad mediate imatinib-induced killing of Bcr/Abl+ leukemic cells, and

resistance due to their loss is overcome by a BH3 mimetic. Proc Natl Acad Sci U S A. 2006 Oct 3;103(40):14907-12.

157. Fernandez Y, Verhaegen M, Miller TP, Rush JL, Steiner P, Opipari AW, Jr., et al. Differential regulation of noxa in normal melanocytes and melanoma cells by proteasome inhibition: therapeutic implications. Cancer Res. 2005 Jul 15;65(14):6294-304.

158. Perez-Galan P, Roue G, Villamor N, Montserrat E, Campo E, Colomer D. The proteasome inhibitor bortezomib induces apoptosis in mantle-cell lymphoma through generation of ROS and Noxa activation independent of p53 status. Blood. 2006 Jan 1;107(1):257-64.

159. Zhu H, Zhang L, Dong F, Guo W, Wu S, Teraishi F, et al. Bik/NBK accumulation correlates with apoptosis-induction by bortezomib (PS-341, Velcade) and other proteasome inhibitors. Oncogene. 2005 Jul 21;24(31):4993-9.

160. Qin JZ, Xin H, Sitailo LA, Denning MF, Nickoloff BJ. Enhanced killing of melanoma cells by simultaneously targeting Mcl-1 and NOXA. Cancer Res. 2006 Oct 1;66(19):9636-45.

161. Ling YH, Liebes L, Zou Y, Perez-Soler R. Reactive oxygen species generation and mitochondrial dysfunction in the apoptotic response to Bortezomib, a novel proteasome inhibitor, in human H460 non-small cell lung cancer cells. J Biol Chem. 2003 Sep 5;278(36):33714-23.

162. Hideshima T, Bradner JE, Wong J, Chauhan D, Richardson P, Schreiber SL, et al. Small-molecule inhibition of proteasome and aggresome function induces synergistic antitumor activity in multiple myeloma. Proc Natl Acad Sci U S A. 2005 Jun 14;102(24):8567-72.

163. Kamitsuji Y, Kuroda J, Kimura S, Toyokuni S, Watanabe K, Ashihara E, et al. The Bcr-Abl kinase inhibitor INNO-406 induces autophagy and different modes of cell death execution in Bcr-Abl-positive leukemias. Cell Death Differ. 2008 Nov;15(11):1712-22.

164. Ertmer A, Huber V, Gilch S, Yoshimori T, Erfle V, Duyster J, et al. The anticancer drug imatinib induces cellular autophagy. Leukemia. 2007 May;21(5):936-42.

165. Shao Y, Gao Z, Marks PA, Jiang X. Apoptotic and autophagic cell death induced by histone deacetylase inhibitors. Proc Natl Acad Sci U S A. 2004 Dec 28;101(52):18030-5.

166. Kawano M, Hirano T, Matsuda T, Taga T, Horii Y, Iwato K, et al. Autocrine generation and requirement of BSF-2/IL-6 for human multiple myelomas. Nature. 1988 Mar 3;332(6159):83-5.

167. Chauhan D, Uchiyama H, Akbarali Y, Urashima M, Yamamoto K, Libermann TA, et al. Multiple myeloma cell adhesion-induced interleukin-6 expression in bone marrow stromal cells involves activation of NF-kappa B. Blood. 1996 Feb 1;87(3):1104-12.
168. Orlowski RZ, Stinchcombe TE, Mitchell BS, Shea TC, Baldwin AS, Stahl S, et al. Phase I trial of the proteasome inhibitor PS-341 in patients with refractory hematologic malignancies. J Clin Oncol. 2002 Nov 15;20(22):4420-7.
169. Jagannath S, Barlogie B, Berenson J, Siegel D, Irwin D, Richardson PG, et al. A phase 2 study of two doses of bortezomib in relapsed or refractory myeloma. Br J Haematol. 2004 Oct;127(2):165-72.
170. Richardson PG, Barlogie B, Berenson J, Singhal S, Jagannath S, Irwin D, et al. A phase 2 study of bortezomib in relapsed, refractory myeloma. N Engl J Med. 2003 Jun 26;348(26):2609-17.
171. Richardson PG, Sonneveld P, Schuster MW, Irwin D, Stadtmauer EA, Facon T, et al. Bortezomib or high-dose dexamethasone for relapsed multiple myeloma. N Engl J Med. 2005 Jun 16;352(24):2487-98.
172. Fisher RI, Bernstein SH, Kahl BS, Djulbegovic B, Robertson MJ, de Vos S, et al. Multicenter phase II study of bortezomib in patients with relapsed or refractory mantle cell lymphoma. J Clin Oncol. 2006 Oct 20;24(30):4867-74.
173. Papandreou CN, Daliani DD, Nix D, Yang H, Madden T, Wang X, et al. Phase I trial of the proteasome inhibitor bortezomib in patients with advanced solid tumors with observations in androgen-independent prostate cancer. J Clin Oncol. 2004 Jun 1;22(11):2108-21.
174. Stewart AK, Sullivan D, Lonial S, Mohrbacher AF, Chatta G, Shustick C, et al. Pharmacokinetic (PK) and pharmacodynamics (PD) study of two doses of bortezomib (Btz) in patients with relapsed multiple myeloma (MM). Blood. 2006;108:3533.
175. Lightcap ES, McCormack TA, Pien CS, Chau V, Adams J, Elliott PJ. Proteasome inhibition measurements: clinical application. Clin Chem. 2000 May;46(5):673-83.
176. LeBlanc R, Catley LP, Hideshima T, Lentzsch S, Mitsiades CS, Mitsiades N, et al. Proteasome inhibitor PS-341 inhibits human myeloma cell growth in vivo and prolongs survival in a murine model. Cancer Res. 2002 Sep 1;62(17):4996-5000.
177. Adams J. Development of the proteasome inhibitor PS-341. Oncologist. 2002;7(1):9-16.

178. Cortes J, Thomas D, Koller C, Giles F, Estey E, Faderl S, et al. Phase I study of bortezomib in refractory or relapsed acute leukemias. Clin Cancer Res. 2004 May 15;10(10):3371-6.
179. Aghajanian C, Soignet S, Dizon DS, Pien CS, Adams J, Elliott PJ, et al. A phase I trial of the novel proteasome inhibitor PS341 in advanced solid tumor malignancies. Clin Cancer Res. 2002 Aug;8(8):2505-11.
180. Hamilton AL, Eder JP, Pavlick AC, Clark JW, Liebes L, Garcia-Carbonero R, et al. Proteasome inhibition with bortezomib (PS-341): a phase I study with pharmacodynamic end points using a day 1 and day 4 schedule in a 14-day cycle. J Clin Oncol. 2005 Sep 1;23(25):6107-16.
181. Cortes J, Giles F, O'Brien S, Miloslav B, McConkey D, Wright J, et al. Phase II study of Bortezomib (VELCADE, Formerly PS-341) for Patients with Imatinib-Refractory Chronic Myeloid Leukemia (CML) in Chronic (CP) or Accelerated Phase (AP). Blood. 2003 November 16;102(11):4971.
182. Lozzio CB, Lozzio BB. Human chronic myelogenous leukemia cell-line with positive Philadelphia chromosome. Blood. 1975 Mar;45(3):321-34.
183. Shtivelman E, Lifshitz B, Gale RP, Canaani E. Fused transcript of abl and bcr genes in chronic myelogenous leukaemia. Nature. 1985 Jun 13-19;315(6020):550-4.
184. Lyons AB, Parish CR. Determination of lymphocyte division by flow cytometry. J Immunol Methods. 1994 May 2;171(1):131-7.
185. Rea D, Legros L, Raffoux E, Thomas X, Turlure P, Maury S, et al. High-dose imatinib mesylate combined with vincristine and dexamethasone (DIV regimen) as induction therapy in patients with resistant Philadelphia-positive acute lymphoblastic leukemia and lymphoid blast crisis of chronic myeloid leukemia. Leukemia. 2006 Mar;20(3):400-3.
186. Crawford LJ, Walker B, Ovaa H, Chauhan D, Anderson KC, Morris TC, et al. Comparative selectivity and specificity of the proteasome inhibitors BzLLLCOCHO, PS-341, and MG-132. Cancer Res. 2006 Jun 15;66(12):6379-86.
187. Andre P, Cisternino S, Chiadmi F, Toledano A, Schlatter J, Fain O, et al. Stability of bortezomib 1-mg/mL solution in plastic syringe and glass vial. Ann Pharmacother. 2005 Sep;39(9):1462-6.
188. Liu S, Liu Z, Xie Z, Pang J, Yu J, Lehmann E, et al. Bortezomib induces DNA hypomethylation and silenced gene transcription by interfering with Sp1/NF-kappaB-dependent DNA methyltransferase activity in acute myeloid leukemia. Blood. 2008 Feb 15;111(4):2364-73.

189. Kisselev AF, Callard A, Goldberg AL. Importance of the different proteolytic sites of the proteasome and the efficacy of inhibitors varies with the protein substrate. J Biol Chem. 2006 Mar 31;281(13):8582-90.
190. Senechal K, Heaney C, Druker B, Sawyers CL. Structural requirements for function of the Crkl adapter protein in fibroblasts and hematopoietic cells. Mol Cell Biol. 1998 Sep;18(9):5082-90.
191. ten Hoeve J, Arlinghaus RB, Guo JQ, Heisterkamp N, Groffen J. Tyrosine phosphorylation of CRKL in Philadelphia+ leukemia. Blood. 1994 Sep 15;84(6):1731-6.
192. Hamilton A, Elrick L, Myssina S, Copland M, Jorgensen H, Melo JV, et al. BCR-ABL activity and its response to drugs can be determined in CD34+ CML stem cells by CrkL phosphorylation status using flow cytometry. Leukemia. 2006 Jun;20(6):1035-9.
193. Yinjun L, Jie J, Weilai X, Xiangming T. Homoharringtonine mediates myeloid cell apoptosis via upregulation of pro-apoptotic bax and inducing caspase-3-mediated cleavage of poly(ADP-ribose) polymerase (PARP). Am J Hematol. 2004 Jul;76(3):199-204.
194. O'Brien S, Kantarjian H, Keating M, Beran M, Koller C, Robertson LE, et al. Homoharringtonine therapy induces responses in patients with chronic myelogenous leukemia in late chronic phase. Blood. 1995 Nov 1;86(9):3322-6.
195. Quintas-Cardama A, Kantarjian H, Garcia-Manero G, O'Brien S, Faderl S, Estrov Z, et al. Phase I/II study of subcutaneous homoharringtonine in patients with chronic myeloid leukemia who have failed prior therapy. Cancer. 2007 Jan 15;109(2):248-55.
196. Nicolini F, Legros L, Roy L, Chomel JC, Chabane K, Ducastelle S, et al. Homo-Harringtonine (Omacetaxine mepesuccinate) Induces a Dramatic and Sustained Reduction of BCR-ABL T315I mutated Transcripts in Chronic Phase Chronic Myelogenous Leukemia Patients Resistant to Tyrosine Kinase Inhibitors Blood. 2008 November 16;112(11):1103.
197. Roche-Lestienne C, Soenen-Cornu V, Grardel-Duflos N, Lai JL, Philippe N, Facon T, et al. Several types of mutations of the Abl gene can be found in chronic myeloid leukemia patients resistant to STI571, and they can pre-exist to the onset of treatment. Blood. 2002 Aug 1;100(3):1014-8.
198. Griswold IJ, MacPartlin M, Bumm T, Goss VL, O'Hare T, Lee KA, et al. Kinase domain mutants of Bcr-Abl exhibit altered transformation potency, kinase activity,

and substrate utilization, irrespective of sensitivity to imatinib. Mol Cell Biol. 2006 Aug;26(16):6082-93.

199. Skaggs BJ, Gorre ME, Ryvkin A, Burgess MR, Xie Y, Han Y, et al. Phosphorylation of the ATP-binding loop directs oncogenicity of drug-resistant BCR-ABL mutants. Proc Natl Acad Sci U S A. 2006 Dec 19;103(51):19466-71.

200. Arastu-Kapur S, Shenk K, Parlati F, Bennett MK. Non-Proteasomal Targets of Proteasome Inhibitors Bortezomib and Carfilzomib. Blood. 2008 Nov 2008;112(11):2657.

201. Soligo D, Servida F, Delia D, Fontanella E, Lamorte G, Caneva L, et al. The apoptogenic response of human myeloid leukaemia cell lines and of normal and malignant haematopoietic progenitor cells to the proteasome inhibitor PSI. Br J Haematol. 2001 Apr;113(1):126-35.

202. Vlachos P, Nyman U, Hajji N, Joseph B. The cell cycle inhibitor p57(Kip2) promotes cell death via the mitochondrial apoptotic pathway. Cell Death Differ. 2007 Aug;14(8):1497-507.

203. Ma MH, Yang HH, Parker K, Manyak S, Friedman JM, Altamirano C, et al. The proteasome inhibitor PS-341 markedly enhances sensitivity of multiple myeloma tumor cells to chemotherapeutic agents. Clin Cancer Res. 2003 Mar;9(3):1136-44.

204. Ito K, Bernardi R, Morotti A, Matsuoka S, Saglio G, Ikeda Y, et al. PML targeting eradicates quiescent leukaemia-initiating cells. Nature. 2008 Jun 19;453(7198):1072-8.

205. Scaglioni PP, Yung TM, Choi SC, Baldini C, Konstantinidou G, Pandolfi PP. CK2 mediates phosphorylation and ubiquitin-mediated degradation of the PML tumor suppressor. Mol Cell Biochem. 2008 Sep;316(1-2):149-54.